AN ABSTRACT OF THE THESIS OF

Sean G. Brosig for the degree of Master of Science in Electrical and Computer Engineering presented on June 13, 2013.
Title: A Methodology to Reduce the Strain on Hydro Turbines Using Advanced Life Extending Control of Multiple Energy Storage Systems.

Abstract approved:

_____

Ted K.A. Brekken

Over the last 20 years, there has been rapid growth in the amount of installed wind power in the Pacific Northwest, specifically in the Columbia River Gorge. The variable and non-dispatchable nature of this resource requires that it be balanced in some form by other sources on the grid. In the Northwest specifically, the most relied upon generation sources have been hydropower units. However, it is thought that heavy reliance upon hydropower units to rapidly change their output to provide balancing increases the wear and tear on different components of these machines. This research aims to quantify damage incurred on these units in real time through a Real-time Damage Incurrence (RDI) model and minimize this damage and its associated cost through integration of Energy Storage using Advanced Life Extending Control (LEC). First, the relationship between wind power and hydroelectric power generation is investigated. The RDI model for hydropower units as well as multiple Energy Storage System (ESS) technologies is then developed, and LEC is implemented and simulated, resulting in significant reduction of damage incurrence and total cost of damage incurrence up to 10% in some cases.

A Methodology to Reduce the Strain on Hydro Turbines Using Advanced Life Extending Control of Multiple Energy Storage Systems

by
Sean G. Brosig

A THESIS

submitted to

Oregon State University

in partial fulfillment of
the requirements for the
degree of

Master of Science

Presented June 13, 2013
Commencement June 2013

Master of Science thesis of Sean G. Brosig presented on June 13, 2013.

APPROVED:

Major Professor, representing Electrical and Computer Engineering

Director of the School of Electrical Engineering and Computer Science

Dean of the Graduate School

I understand that my thesis will become part of the permanent collection of Oregon State University libraries. My signature below authorizes release of my thesis to any reader upon request.

Sean G. Brosig, Author

ACKNOWLEDGEMENTS

I would first like to thank my advisor, Dr. Brekken, for all of his valuable insight and assistance with this work, as well as for the excellent courses that he has always taught so well. I consider myself very fortunate to have had the opportunity to learn from Dr. Brekken. I would also like to thank all of the professors and instructors that I have had the opportunity to take classes from, as every one of these classes and individuals has taught me extremely valuable lessons. Thank you also to Marty Stoddard and Jiajia Song for your extremely helpful assistance and guidance in this work.

Thank you to the Hydro Research Foundation and the Department of Energy for the opportunity to conduct this research, and for providing such a rewarding fellowship experience. The knowledge gained from attending conferences and interacting with other fellows and industry members has been invaluable.

Thank you to BPA, Beacon Power, ZBB, and the USACE, especially those at the Hydroelectric Design Center, for all of the valuable information that was critical to this work.

Thank you as well to my fellow graduate students for being such an integral part of what has been an amazing graduate school experience. Thank you especially to Dr. Douglas Halamay, Kelcey Lajoie, and Arne Bostrom for your assistance and input, it has been greatly appreciated.

And finally, thank you to my family and friends for all of your support and encouragement. Your contribution is immeasurable.

TABLE OF CONTENTS

TABLE OF CONTENTS (Continued)

LIST OF FIGURES

Figure Page

LIST OF FIGURES (Continued)

Figure Page

LIST OF FIGURES (Continued)

Figure Page

LIST OF TABLES

A Methodology to Reduce the Strain on Hydro Turbines Using Advanced Life Extending Control of Multiple Energy Storage Systems

1 Introduction

1.1 Background

It has become increasingly clear over the last 40 years that the existing level of dependency upon fossil fuels, such as oil and coal, will not be feasible in the future. There are many problems that have been discussed with regards to the widespread use of fossil fuels, including the effect on the environment and climate change, as well as the inevitability of reaching peak oil and peak coal. The terms “peak oil” and “peak coal” refer to the points at which the oil and coal being produced reach a maximum and begin continually declining (Maggio & Cacciola, 2012). Due to ever-increasing energy demand, reaching peak oil and peak coal will have a significant impact on the prices for gas and transportation, as well as electricity. The effects that extracting and burning fossil fuels have on the environment have been debated, but research indicates that these actions have a significant impact on global carbon dioxide levels and thereby global temperature and climate (Höök & Tang, 2013) (Judkins, Fulkerson, & Sanghvi, 1993).

In response to the concerns about utilizing fossil fuels as the overwhelmingly dominant source of energy, the focus on renewable energy has increased dramatically. There are many different types of renewable energy technologies that are being developed, including wind, solar, and wave power, among many others. All renewable energy sources have advantages and disadvantages, and it has been discussed by some that a merging of renewable energy sources, to form a large

"portfolio" of different resources, could be an ideal way to cover the needs of a dynamic power system (Atwa, El-Saadany, Salama, & Seethapathy, 2010) (Halamay, Brekken, Simmons, & McArthur, 2011).

Wind power has grown to become one of the most preferred and heavily developed forms of renewable energy on the market, accounting for approximately 62% of the generation from renewable sources (not including hydroelectric power). In contrast, solar energy only makes up approximately 1% of this energy generation (U.S. Energy Information Administration, 2013). The challenge inherent to wind power, along with other forms of naturally occurring renewable energy sources, is that the power that is generated is not completely controllable. These types of sources are therefore considered to be non-dispatchable sources.

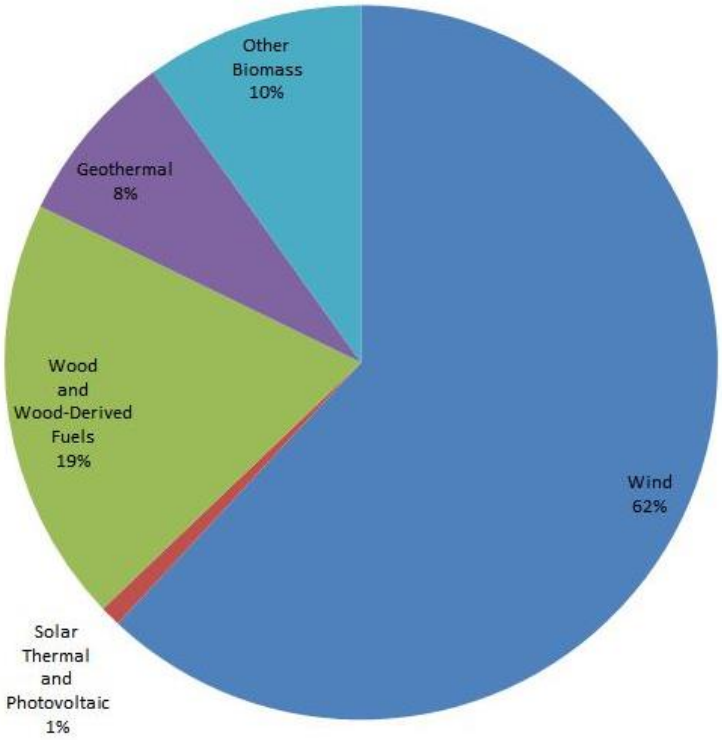

Fig. 1.1. Net generation of renewable energy sources (generated based on data from U.S. Energy Information Administration, 2013)

Not only is wind power non-dispatchable, it is also highly variable. The generation of wind power can swing rapidly and somewhat unpredictably, leading to error in wind forecasting (difference between the forecasted wind power and the actual wind power). Observe Fig. 1.2 for an example of what this variability looks like over a seven day period.

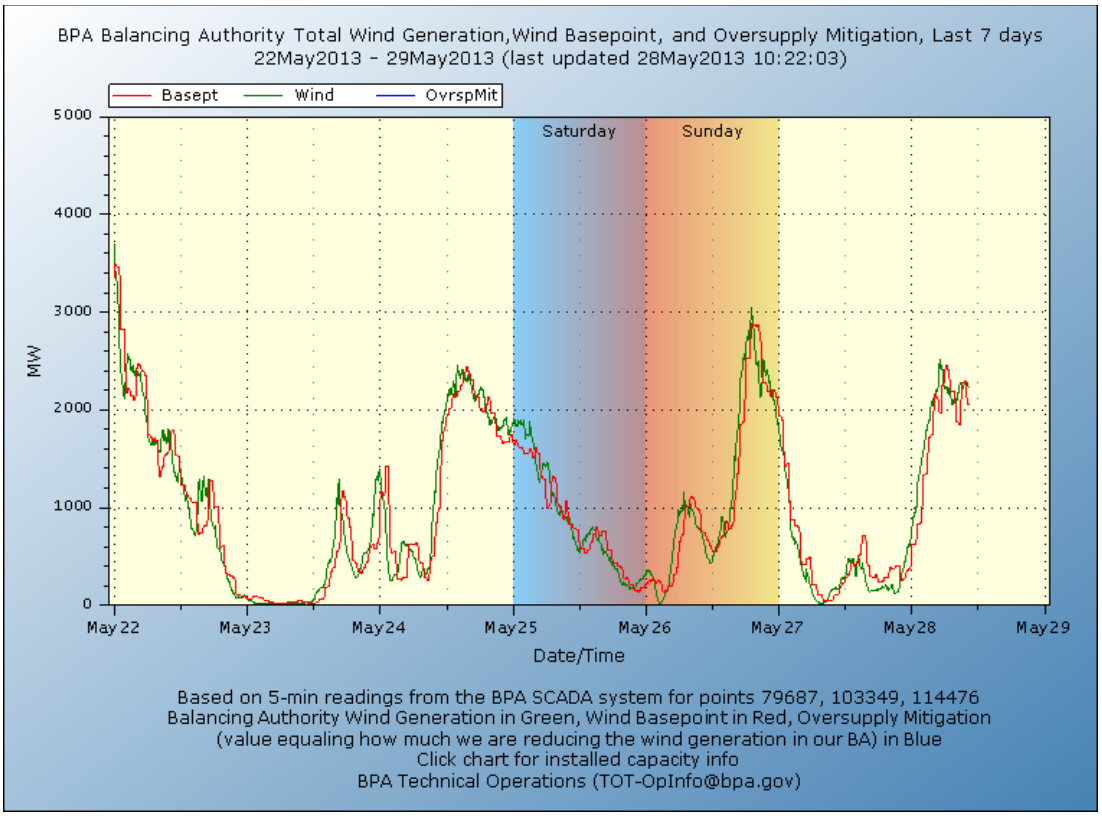

Fig. 1.2. Wind Generation – Forecast and actual wind generation over seven days (plot from BPA Balancing Authority Total Wind Generation, Near-Real-Time, 2013)

The figure above clearly shows how quickly and unexpectedly wind power can change, and the amount of power that can come onto the grid or be taken off of the grid in a short amount of time. Note the power spike on May 24th near the middle of the day, when approximately 1500 MW of generation came online rapidly.

In order to be able to integrate large quantities of non-dispatchable wind generation on to the grid, it is necessary to prevent wind power from threatening the stability of the power grid. At any moment, the power that is consumed from the grid (the "load") must be essentially equal to the power being generated onto the grid (the "generation"). If this condition is not met, it can quickly lead to stability concerns that can black out entire regions. One method of providing stability support is through the use of generation reserves, which are dispatchable forms of generation that may rapidly change their output in order to ensure that the power on the grid remains balanced.

In the northwestern United States, one of the most convenient and versatile sources of generation reserves is hydropower. In fact, hydropower accounted for approximately 77% of the energy generation in Washington and Oregon during 2011 (U.S. Energy Information Administration, 2013). Hydropower has many benefits, one of which is that it is very easy to change the power output rapidly to meet demand on the grid. Through the use of Automatic Generation Control (AGC), some units are able to automatically adjust their output based on the measured grid frequency. If the grid frequency drops, that is an indication that the generation may not be able to meet the load, and thus the AGC unit increases power output. An increase in grid frequency corresponds to a surplus of generation on the system, and the AGC unit responds by decreasing power output. By applying this to many generating units, this method can be effective in maintaining the balance of load and generation for small disturbances.

The significant increase of wind power in the Northwest has led to an increase in variability on the system. In fact, one of the largest concentrations of wind power in the United States is in the Columbia River Gorge, which produced more wind energy than all states with the exception of Texas and Iowa in 2011 (U.S. Energy Information Administration, 2013). This is leading to more dependency on the hydropower infrastructure in the region to provide the balancing and stability support for the system. Based upon forecasted wind power, and the error between the wind power forecast and the actual wind power, it has been theorized that some hydro units may be changing their output more than was required in previous years.

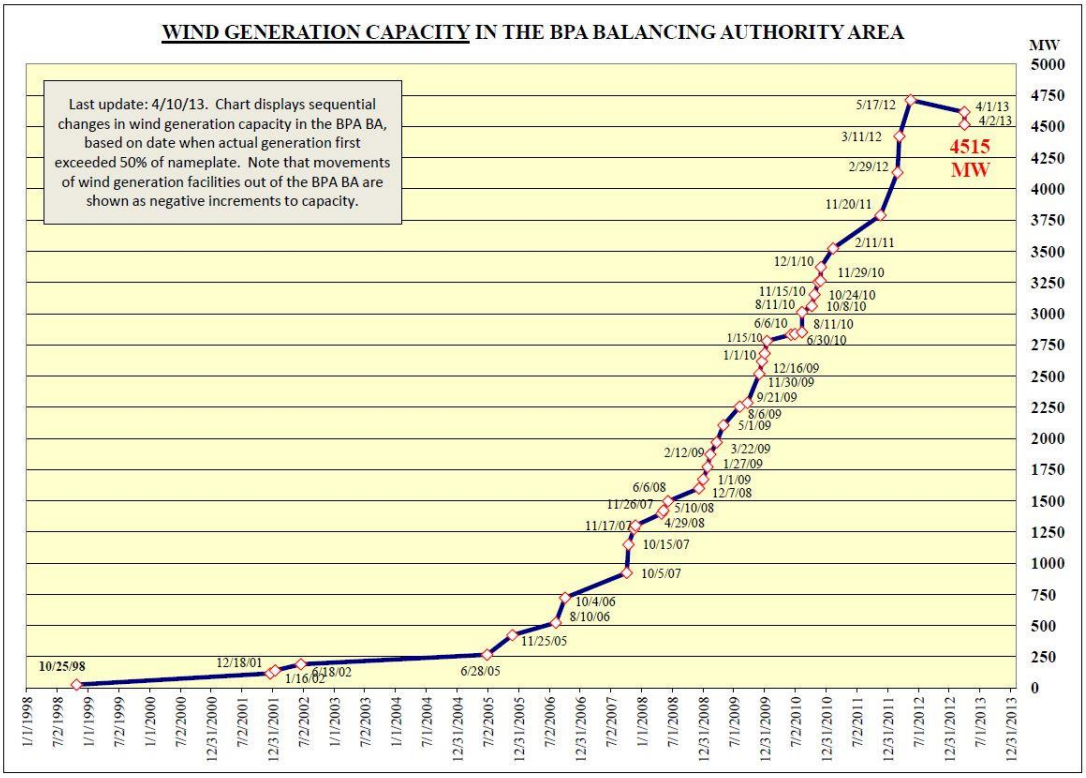

Fig. 1.3. Installed wind capacity in BPA balancing authority area (plot from Wind Generation Capacity in the BPA Balancing Authority Area, 2013)

When hydropower generating units are required to change their output, many subsystems and components are called into action in order to elicit the desired response. With the large change in power that results from this action, many of these components are put under strain - more strain than they would experience under steady operating conditions. Therefore, there is concern that the additional wind power being added to the grid may be leading to increased dependency on the hydropower units, and in turn more damage being accrued by those units.

A major benefit of energy storage systems is to provide a dispatchable power source or load in order to best complement the system in which it is installed. In the context of energy storage for the grid, it is desirable to allow both rapid charging and discharging of the energy source in order to provide maximum power sourcing and sinking capability. For this work, energy storage is integrated into the developed Life Extending Control (LEC) system to utilize its ability to rapidly charge and discharge in order to decrease the variation that hydroelectric units experience.

1.2 Scope of Thesis

The main focus of this research is to model the damage that is incurred by hydropower units due to different operating conditions and to develop a LEC system in order to minimize damage through the use of integrated energy storage. Before doing so, it is desirable to establish if there is a connection between wind generation and hydroelectric generation. It should be determined if hydroelectric generation units are indeed being affected by wind generation and if the error in wind

forecasting is also having an effect (as this is the case most likely to lead to AGC-related action).

After determining the degree of this relationship, the Real-time Damage Incurrence (RDI) model for the various components of a hydropower generating unit must be developed. There are many components which are affected differently by various operating conditions that the unit experiences. It is necessary to look into the characteristics of damage incurrence for each one and develop the damage model accordingly. Similarly, damage models for the Energy Storage System (ESS) technologies to be considered must be developed, in order to account for the damaging effects of their utilization as well.

Upon developing an RDI model for hydroelectric generators as well as ESS technologies, it is then possible to develop a LEC algorithm in order to reduce wear and tear on hydro units and ultimately reduce the effective operating costs of all equipment due to incurred damage.

Before beginning with the discussion of the research that was conducted, it is helpful to show the general layout of a hydropower dam to understand the system on a high level.

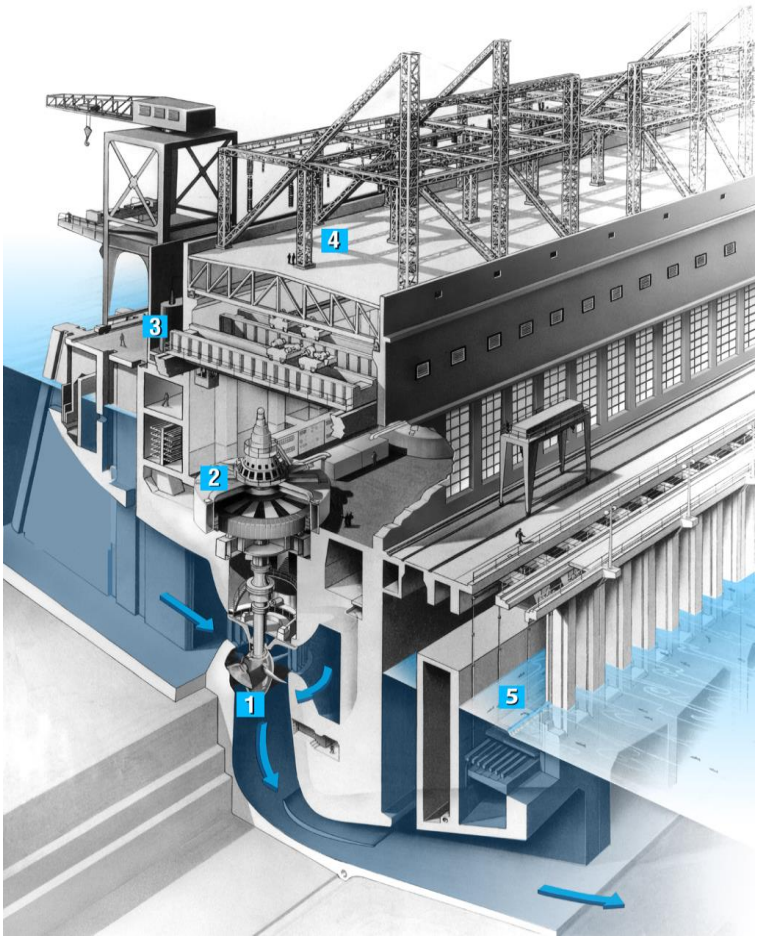

Fig. 1.4. Hydropower dam diagram showing various components (from About hydropower generation, 2013)

The components labeled in Fig. 1.4 are described below:

1.) Turbine – Water motion converted to rotational mechanical power

2.) Generator – Mechanical power converted to electrical power

3.) Transformer – Boosts voltage to transmission levels

4.) Switch Yard – Directs power to different transmission lines

5.) Fish Ladder – Provides safe upstream passage for fish

Note that while in the previous figure there is only one generator unit shown, large hydroelectric generating facilities have far more than one generator. Grand Coulee Dam, for example, has 33 generating units. The basic operation of any generating plant is that it is given a required amount of power to output and it meets that power output by whatever means chosen. In the case of hydroelectric dams this means that individual generating units may be controlled to generate various power output levels which combine to meet the required generation.

2 Wind Generation/Error and Hydro Generation Relationship

The main purpose for investigating the effect that wind generation and error in wind forecasting have on hydropower, in the context of this research, is to establish basis for the concern that the variability in wind power is affecting hydroelectric units. If this is established to some degree, it also indicates that adding more variable resources to the grid without providing some additional form of balancing would only add to this impact on hydroelectric units.

Due to the complexity of the system, it is challenging to get a definitive demonstration of the effect, as units are having their output adjusted regularly for a variety of reasons. Therefore, seeing the power output of one unit go down just as wind power increases does not necessarily mean that this change was directly caused by the change in wind power. The unit could have been decreasing power in order to compensate for another unit coming online, a rapid change in load, or many other scenarios. Expanding this uncertainty to all of the different hydroelectric dams, units, and all of the different generating sources, as well as the dynamic nature of the load, it becomes clear that looking for specific instances of wind impacting hydroelectric units is not the most feasible method of addressing this issue. However, it is possible to get an idea of the effect through a number of different approaches, and there were two methods that were performed in this work.

2.1 Correlation Analysis

The first method for analyzing the relationship between wind power and hydropower involved finding the correlation between wind power, as well as wind forecast error, and hydropower. This was investigated by looking at each hydroelectric dam individually, as well as each hydroelectric generating unit individually. Generating units' output power data was acquired at five minute resolution from August 2009 to December 2011 for all of the hydroelectric facilities in BPA's balancing authority area. Wind forecast and wind generation data was also acquired at a five minute resolution for the same time period. Using these data sets, the desired correlations were then calculated using MATLAB. The concept in this approach is that while individual unit power ramps may be hard to associate to wind power, if an overall trend is present it will be evident in the correlation data.

The correlations were calculated using built in MATLAB functions which utilize the Pearson product–moment correlation coefficient, or simple correlation coefficient. This correlation coefficient is utilized by dividing the sample covariance by the product of the sample standard deviations, according to (1) (Shieh, 2010).

$$r = \frac{S_{XY}}{S_X S_Y} \tag{1}$$

It is anticipated that there should be a negative correlation between change in hydropower output and change in wind generation, as an increase in wind generation should lead to a decrease in hydropower generation in order to keep the system balanced. Note, however, that this generalization is neglecting the impact of other variables of the system. These include load, thermal generation, and power

transported out of the local balancing area via interchanges. These effects may act to lessen the correlation, but the negative correlation trend should remain.

Similarly, if error between the forecast and actual generated wind power is defined as $P_{error} = P_{gen} - P_{forecast}$, then positive error corresponds to the system having more wind power than expected. This would in turn lead to an expectation that having an increase in the error should result in a decrease in hydropower output, and thus a negative correlation between these terms.

Table 2.1 shows the labels that are used for the various dams in the results as well as the names of the dams that they represent, for ease of presenting the results.

Table 2.1. Labels used for dams and actual names of dams

Label of Dam	**Name of Dam**
BONNE	Bonneville
CHIEF	Chief Joseph
GRANDC	Grand Coulee
ICEHAR	Ice Harbor
JD	John Day
LILGOOS	Little Goose
LWRMON	Lower Monumental
MCNARY	McNary
LWRGRAN	Lower Granite
TDALLES	The Dalles

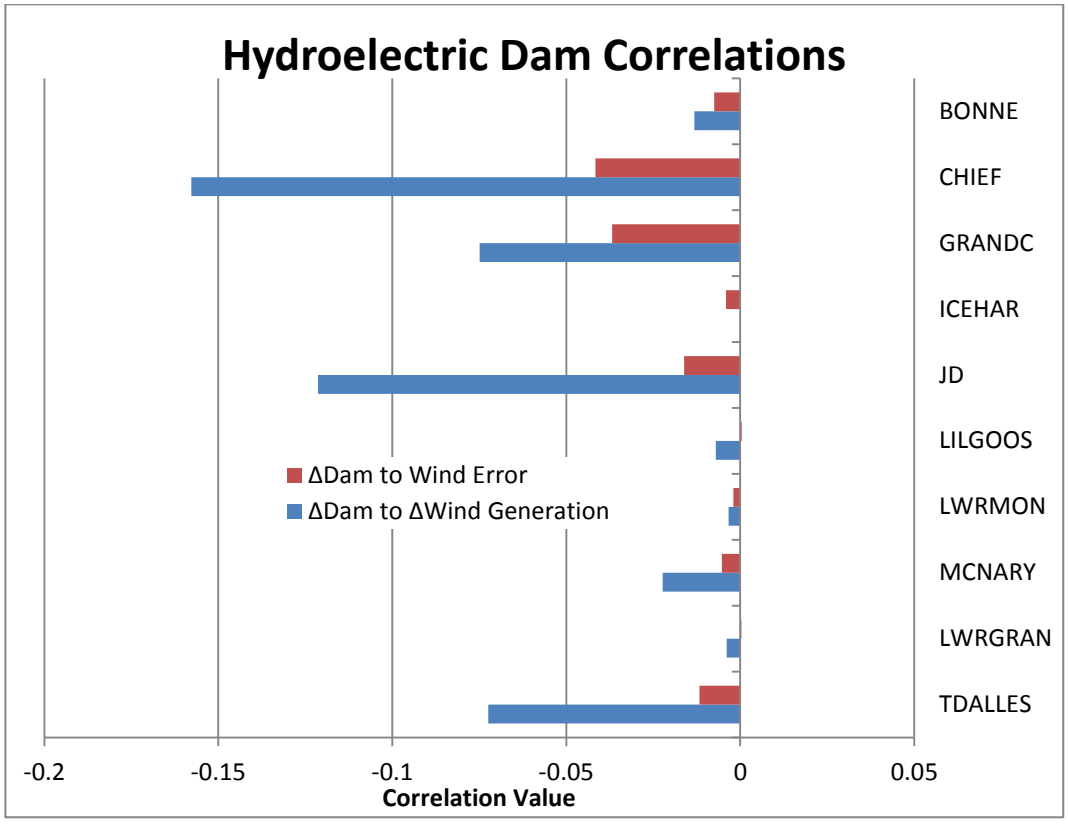

Fig. 2.1. Correlation values for analysis of hydroelectric dam output to change in wind generation and to wind error.

In Fig. 2.1, it appears quite evident that some dams are far more affected by characteristics of wind power than other projects. This implies that wind power is certainly having an impact, although the precise extent of that impact is difficult to determine. However, the fact that there is a clear delineation between the correlation values for the dams shows that there is some reason for concern when it comes to increasing the amount of wind power in the region, especially pertaining to the plants that are most significantly impacted by wind power.

Running the same correlation analysis at the unit level, as shown in Fig. 2.2, shows a similar trend, as the projects that were most affected by wind also have the units that are most affected by wind, which makes intuitive sense. The values of the correlations are all quite small, which implies that individual units are less likely to see consistent impact from wind power than entire hydroelectric dams are. Although they are small, there is a significant enough trend in the locations of the most heavily influenced units to gather some insight. It is interesting to note that no unit outside of the top four most affected dams (Chief Joseph, Grand Coulee, John Day, and The Dalles) was determined to be in the top fourty of the most affected units. This gives further evidence of the relationship that was seen at the dam level.

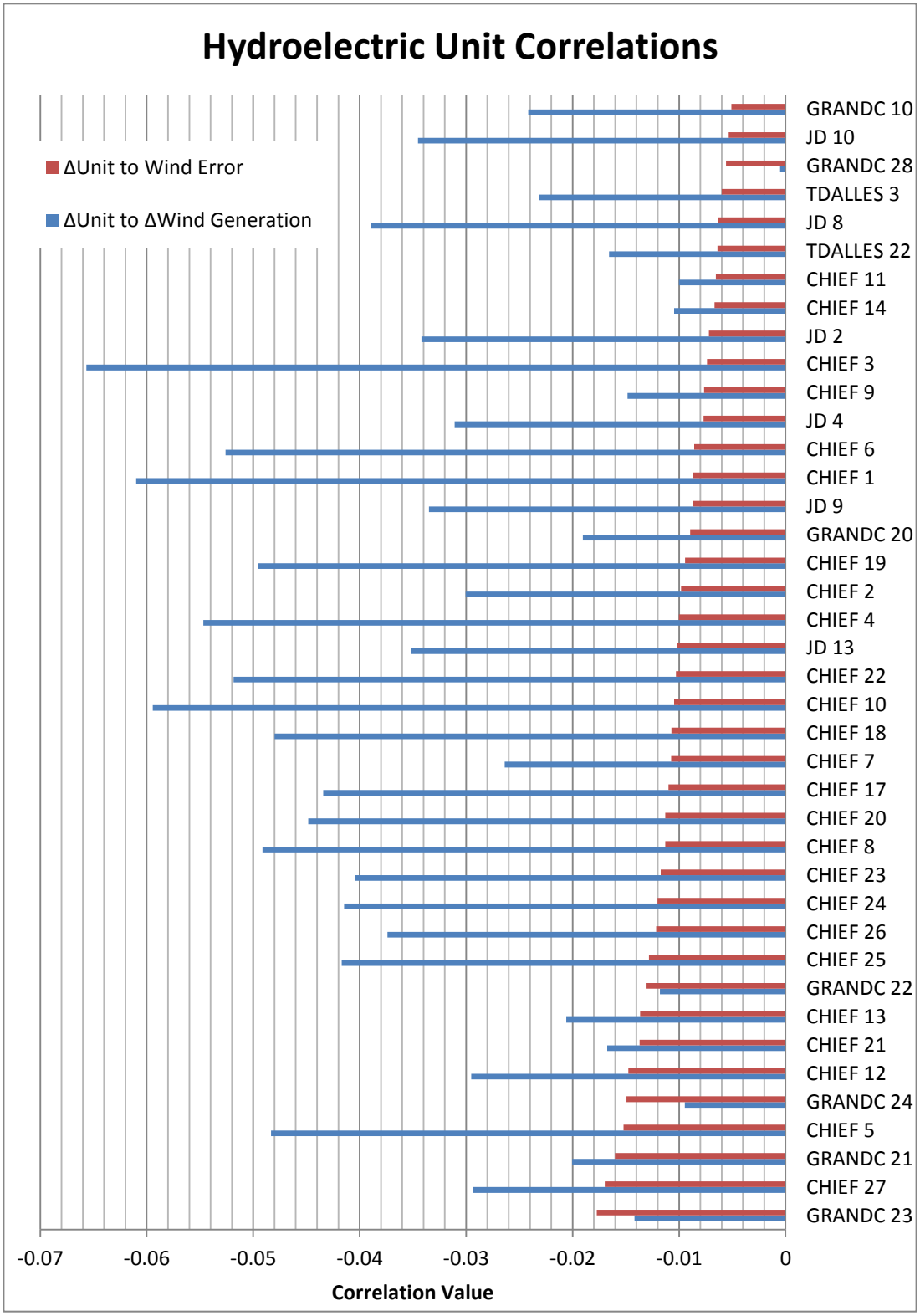

Fig. 2.2. Correlation values for analysis of hydroelectric unit output to change in wind generation and wind error.

2.2 Linear Least Squares Analysis

A second method of analyzing the relationship between wind power and hydroelectric power was utilized which entailed modeling the entire power grid in a Linear Least Squares model. The goal with this approach was to determine to what extent wind power (forecast and error) affected the output of the different hydroelectric dams.

This idea was based upon the concept that, at any point, the generation of power onto the grid must match the load on the grid, within some small tolerance. Based on this concept, the entire summation of all of the components on the grid should behave in the following way at each moment, assuming steady state conditions:

$$Load + Interchange = Hydro + Thermal + Wind\_Forecast + Wind\_Error \quad (2)$$

Each term of (2) represents the entirety of the generation or load under its respective category. Interchange power is defined as positive for power being delivered over the interchange, and wind error is again defined as generation minus forecast (thus it is also a positive generation quantity in this formulation). This means that the sum of the wind forecast term and the wind error term equals the total wind generation. Representing each quantity by a variable, this becomes the following expression:

$$L + I = H + T + W_F + W_E \quad (3)$$

Rearranging this equation then gives:

$$H = L + I - T - W_F - W_E \quad (4)$$

This expression holds for each moment, and represents the bulk sum of all of the hydropower equaling the net load left over after other forms of generation are subtracted.

At this point, instead of using the entire sum of the hydroelectric generation it is possible to use the generation of only one hydroelectric dam, and model it as a linear combination of coefficients and their respective generation/load components as follows:

$$H_1 = K_{L1}L + K_{I1}I - K_{T1}T - K_{F1}W_F - K_{E1}W_E \quad (5)$$

In (5), H_1 represents the power output from a single dam, and the various K_{x1} terms represent a coefficient which, when multiplied by its respective component, gives the amount of that component which is accounted for by the dam H_1. However, it is also important to consider the fact that not all hydroelectric dams have the same power generation capability. Because of this, the analysis of the relationship between the different components of the system and the output of each dam may become skewed in favor of larger dams, simply because they are capable of generating more power. It is therefore necessary to change the different values in the system equation above to "per unit" type values, where each is divided by the rating or maximum value of that component. For the power output from each dam, this means that the power output must be divided by the nameplate rating of the dam. For the rest of the data, the values should be divided by the maximum value that they take over the entirety of the data, such that they range from 0 to 1. This results in coefficients that are (1) of reasonable magnitude for comparison, and (2) are not biased by the generation capacity of the dams. Therefore, the equation may now be described as follows:

$$\frac{H_1}{\max(H_1)} = K_{L1}\frac{L}{\max(L)} + K_{I1}\frac{I}{\max(I)} - K_{T1}\frac{T}{\max(T)} - K_{F1}\frac{W_F}{\max(W_F)} - K_{E1}\frac{W_E}{\max(W_E)} \quad (6)$$

For brevity, in future equations H_1 represents $H_1/\max(H_1)$, and so on.

This expression then allows for a determination of how much each type of generation or load on the grid contributes to that single dam's output, by calculating the values of the coefficients. Considering different numerical methods, Least Squares analysis was very promising in this situation in order to determine the coefficients.

In a least squares problem, the general form of a model is as follows (Kariya & Kurata, 2004):

$$Y = X * \beta + n \quad (7)$$

Where:

$$Y = \begin{bmatrix} y_1 \\ y_2 \\ \vdots \\ y_n \end{bmatrix} \qquad X = \begin{bmatrix} x_{11} & x_{12} & \dots & x_{1m} \\ x_{21} & x_{22} & \dots & x_{2m} \\ \vdots & \vdots & \ddots & \vdots \\ x_{n1} & x_{n2} & \dots & x_{nm} \end{bmatrix} \qquad \beta = \begin{bmatrix} \beta_1 \\ \beta_2 \\ \vdots \\ \beta_m \end{bmatrix} \qquad \varepsilon = \begin{bmatrix} \varepsilon_1 \\ \varepsilon_2 \\ \vdots \\ \varepsilon_n \end{bmatrix}$$

In this representation, the *Y* matrix may be thought of as the output at each time step (1 through n), the *X* matrix may be thought of as the different system values (1 through m) at each time step, and β may be considered the parameters that multiply each system value (1 through m). The ε matrix is essentially an error or noise matrix which represents the error in the approximation at each time step. Note also that there is no offset term included in this formulation, as there is no offset in the system that is being represented.

The goal of Least Squares estimation is to minimize the sum of the squared errors, which is achieved through the following calculation (Kariya & Kurata, 2004):

$$\beta = (X^T X)^{-1} X^T y \tag{8}$$

It is now evident that for the system that was described previously, the *Y* matrix is the power output from each hydroelectric dam, the *X* matrix contains the values of each system component at each time step, and the β matrix represents the coefficients that must be found to describe the system. With this format, the system may be cast into least squares form as follows:

$$Y = \begin{bmatrix} H_1(1) \\ H_1(2) \\ \vdots \\ H_1(n) \end{bmatrix} \qquad X = \begin{bmatrix} L(1) & I(1) & T(1) & W_F(1) & W_E(1) \\ L(2) & I(2) & T(2) & W_F(2) & W_E(2) \\ \vdots & \vdots & \vdots & \vdots & \vdots \\ L(n) & I(n) & T(n) & W_F(n) & W_E(n) \end{bmatrix} \qquad \beta = \begin{bmatrix} K_{L1} \\ K_{I1} \\ K_{T1} \\ K_{F1} \\ K_{E1} \end{bmatrix}$$

With the system now represented in Least Squares form, the parameters β may be determined by using (8).

It is important to realize that the power grid is a highly dynamic system, comprised of highly dynamic subsystems. That is, the power grid has a vast variety of devices, generators, loads, and interconnections, which themselves are constantly changing due to various contingencies. Hydroelectric generators are also highly dynamic as they are affected by numerous external factors besides power requirements. These can include environmental concerns (water flow, reservoir levels, dissolved gasses, and fish passage), navigation concerns, and recreation requirements, among others. This implies that the coefficients of this modeled system can vary significantly from day to day. Because of this fact, it is not

appropriate to simply run a single Least Squares approximation for the entirety of the data and consider it sufficient.

A more reasonable and applicable way to run this Least Squares Analysis is to use a sliding window approach, where only a certain window of data is considered for modeling the system. This allows the parameters to vary freely over different periods of time, based on the window width. This type of analysis was described by Zhao, Ling, Lev-Ari, and Proakis (1994):

> To facilitate tracking of time-varying parameters, it is desirable to discard old data as new data are collected…. In some applications, it is preferable to use a true finite memory algorithm, i.e., a sliding-window algorithm, in order to avoid undesired effects from data in the remote past. A typical case is where parameters that generate the signal are subject to occasional jump type variations of random amplitude.

This sort of technique fits with the system that is being modeled.

As a simple way of implementing this Linear Least Squares approximation, using a sliding window framework, it was decided that the Least Squares estimation would be computed for one data window, and again for the next window, and so on. In this case, the window simply advances by one data point each time step, to allow for smooth transition and consideration of each combination of data for each time window. This analysis gives many different values for the parameters (one for each Least Squares calculation), and all of the estimates can then be plotted in histogram form to observe their frequency of occurrence and general trends for each dam.

In Fig. 2.3, mean values for the wind error and wind forecast coefficients are plotted for each of the dams, in order to get a comparison with the previous correlation results.

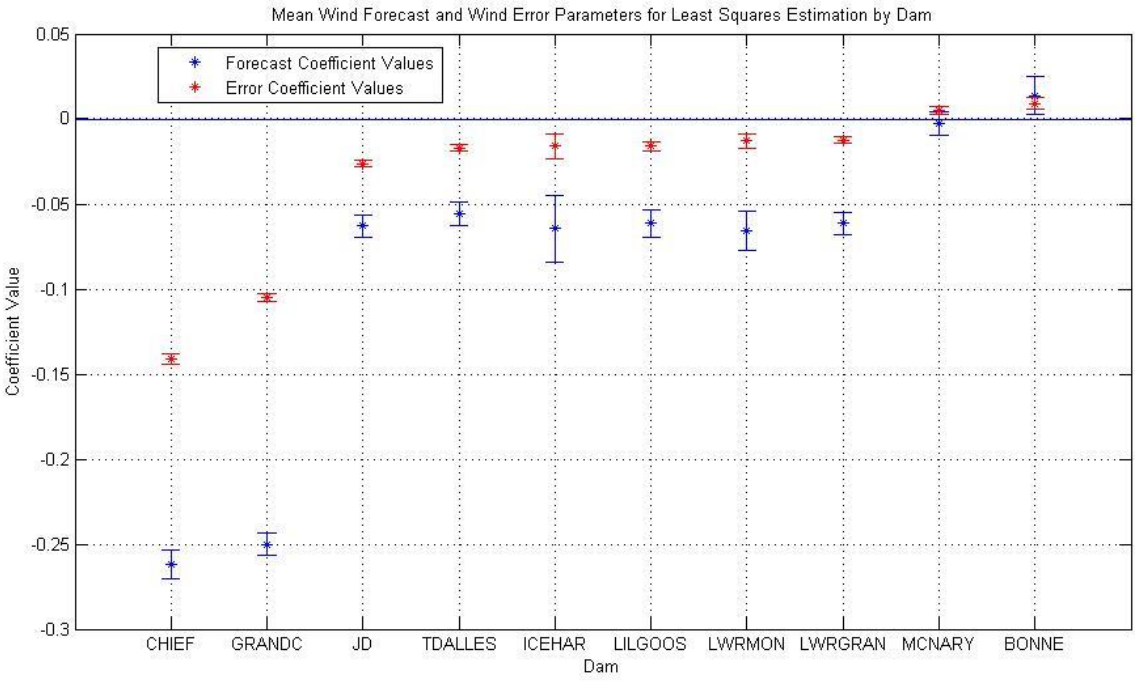

Fig. 2.3. Wind forecast (K_F) and wind error (K_E) coefficients from Least Squares analysis for each dam

Note that in this figure, the coefficients are largely negative. This is because the sign of both the wind forecast and wind error terms in the original expression are negative as well. Also, it is evident in these results that Chief Joseph and Grand Coulee are once again highly impacted by error in the wind forecast (denoted by the red points). John Day and The Dalles appear to be much less affected based on these results, but are slightly more impacted than the other plants.

In order to get a visual perspective of the results that came out of the Least Squares analysis for each of the windows where the calculations were made, it is very useful to view them in histogram form. Histograms of occurrences of parameter value estimations are given for numerous dams of interest in Fig. 2.4 through Fig. 2.7.

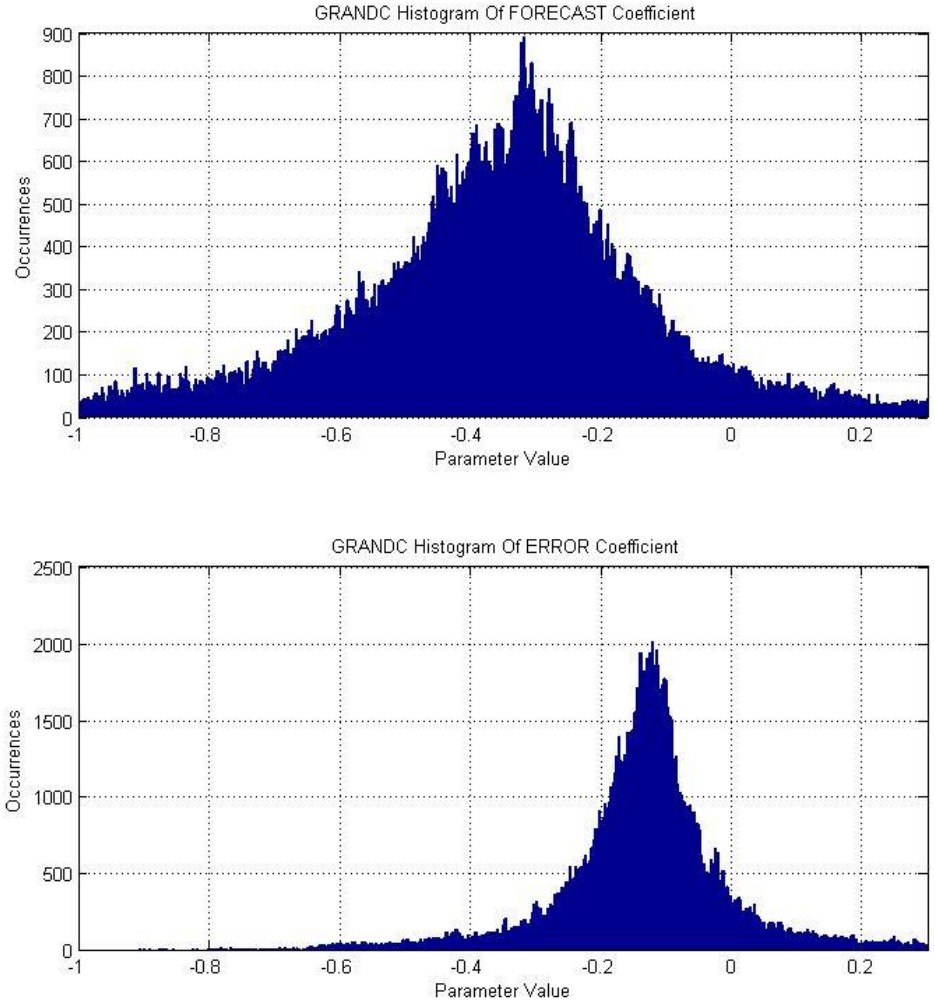

Fig. 2.4. Grand Coulee wind forecast (K_F) and wind error (K_E) coefficient histograms

For Grand Coulee, the histogram of parameters for the wind forecast and wind error coefficients indicates a strong negative correlation between unit output and both wind forecast and wind error. Because the centers of the distributions of the two parameters are not at zero, in the least squares analysis wind forecast and wind error both played significant roles in Grand Coulee's power generation.

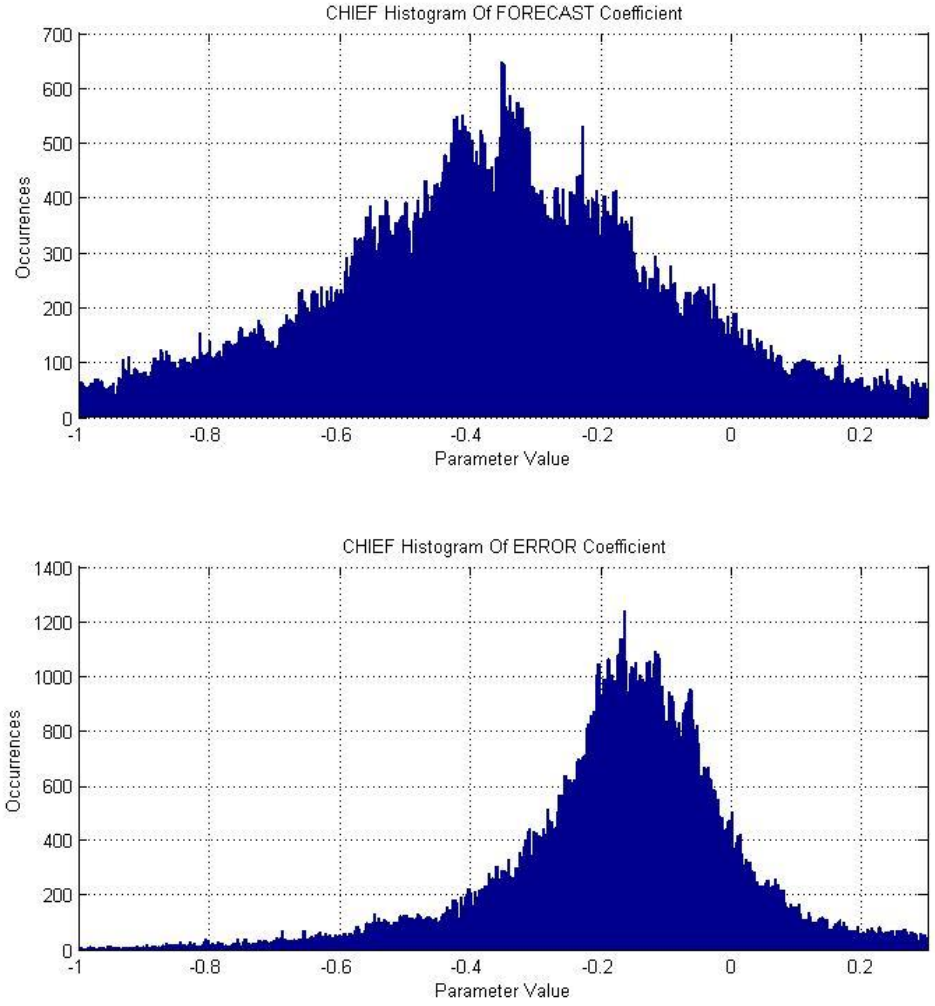

Fig. 2.5. Chief Joseph wind forecast (K_F) and wind error (K_E) coefficient histograms

Again, the center of the distribution for both wind error and wind forecast coefficients is not at zero, and therefore it is again apparent that wind error and wind forecast have an effect on power generation at Chief Joseph Dam. These histograms are very similar in shape as those determined for Grand Coulee.

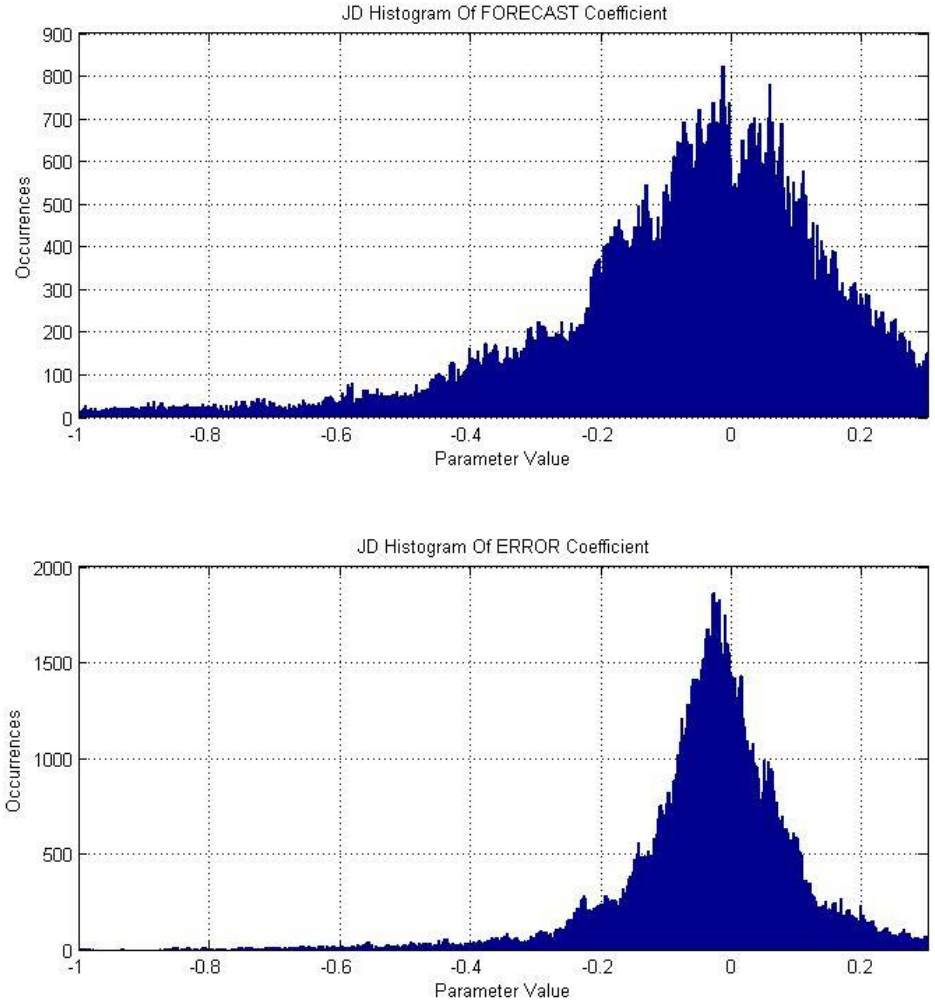

Fig. 2.6. John Day wind forecast (K_F) and wind error (K_E) coefficient histograms

John Day dam shows a similar trend, with a noticeable peak in the error coefficient histogram at a value less than zero. However, this peak is much closer to zero than before, as well as the peak in the forecast coefficient histogram. This indicates that it may not be as heavily influenced by wind forecast or error as Grand Coulee or Chief Joseph, but there still does appear to be an influence.

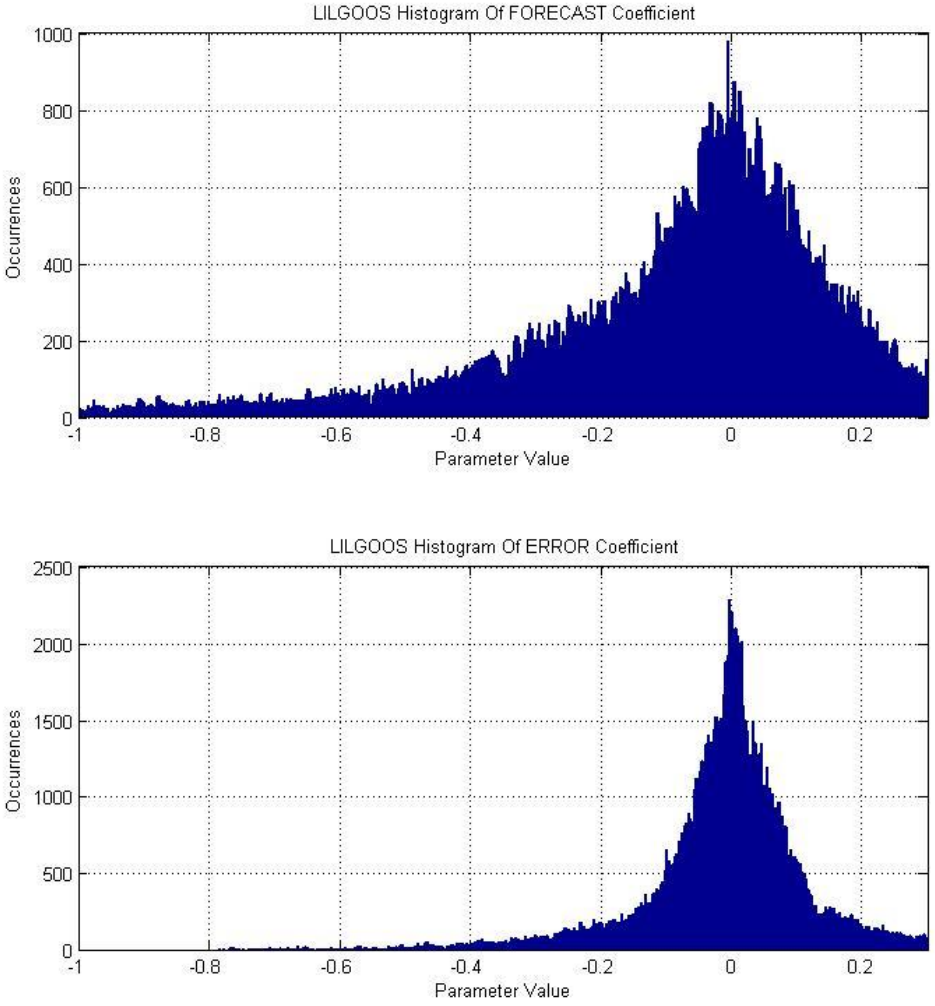

Fig. 2.7. Little Goose wind forecast (K_F) and wind error (K_E) coefficient histograms

As a contrast, the histograms of coefficients for Little Goose are quite clearly centered on zero, and therefore show a trend of not being heavily affected by wind forecast and wind error. This result seems to agree with the results from the correlation analysis for Little Goose.

2.3 Discussion of Results

The analysis conducted gives an indication as to the relative impacts of wind generation and error in wind forecasting on different hydroelectric dams. Multiple methods of analysis indicate that some dams are being more greatly affected by wind power than others, and it seems to be consistent and significant enough in both methods to conclude that wind generation is having an effect on hydroelectric generators. This also implies that the addition of more variable and non-dispatchable generation, with the same characteristics, is likely to have an impact on hydroelectric units. However, it should also be noted that the absolute impact that wind generation has on hydroelectric generation units is either not clearly evident or not quite as significant as originally anticipated, based upon the values of the correlations that were found.

3 Development of RDI Models

3.1 Hydroelectric Generation Unit RDI model

In order to design a Real-time Damage Incurrence model for a system as complex as a hydroelectric generating unit, it is important to consider the effect of each individual subcomponent. In this way, damage accruement of each subcomponent may be tracked and estimated independently, as it is neither feasible nor accurate to attempt to quantify damage accruement of the entire system as a whole. This method of determining RDI for each individual subcomponent is also important because if any of the subcomponents fail or are in need of repair, the entire unit may need to be brought out of operation. Shown below is a table of all of the considered components for the hydroelectric unit, and a brief description of each.

Table 3.1. Table of components considered for hydroelectric unit RDI

Component	Function
Wicket Bushings	Allow smooth movement of wicket gates
Wicket Seals	Prevent leaking through wicket gates
Wicket Ring Servo	Motor to control wicket gate opening/closing
Turbine Thrust Bearing	Bearing supporting turbine vertically
Turbine Guide Bearing	Bearing supporting turbine radially
Turbine Blade Seals (Kaplan)	Prevent leaking past turbine blades
Turbine Blade Servos (Kaplan)	Motors to control blade position
Turbine Runner	Physical rotating turbine shaft/blades
Governor System	Controls wicket gates and power output
Generator Windings (Insulation)	Stator windings of the generator
Generator Brakes	Stop the rotational motion when shut down
Rotor Windings	Windings around the rotor
Excitation System	Controls current applied to rotor
Breaker	Operates when unit is tripped offline
Transformer	Increases voltage from the generator

The basic framework of the RDI model utilized for a hydroelectric generator is rather straightforward. The damage accrued by each component of the hydroelectric generator is to be calculated based on a combination of the power level at each instant, and the change in power that the unit is generating. A block diagram of this methodology is shown in Fig. 3.1.

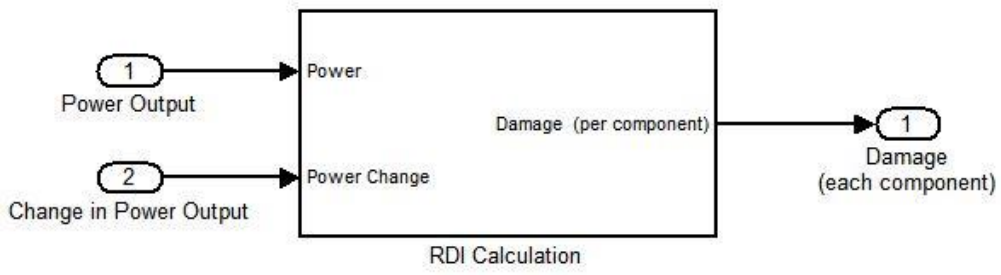

Fig. 3.1. Basic hydroelectric generation unit RDI calculation diagram

The complexity of this model arises from the fact that various components are affected differently by different operating conditions, and therefore the damage rates for each component under every operating condition must be determined individually. This led to a drastic increase in the complexity of the model, but was necessary to have a more reasonable representation of the physical processes at work. Ideally, in order to determine what these specific damage rates are, one would be able to acquire analysis of wear and tear of different components and damage that is experienced under different operating conditions.

One option for attaining such data would be through careful tracking of component condition while in operation on a yearly, if not monthly, basis and then analyzing the results along with usage records. A second possibility is by conducting extensive laboratory testing involving expensive equipment and running tests of

component wear under different conditions. As a note, in this laboratory testing it would still be challenging to fully represent the entire system, and even if it were possible it is not guaranteed that the results would be scalable to a much larger system. For these reasons, the only reasonable way to extremely accurately determine damage rates for different components of a hydroelectric generating unit is to track the usage records of actual hydro units in operation as well as the wear of each subcomponent. Unfortunately, this data was not available at the time of research, and a large amount of data was not releasable due to security and privacy concerns of various operating plants.

Given the difficulty in acquiring the ideal data, a new approach had to be formulated. The data that was available consisted of the usage records for all hydro units in the BPA balancing authority area, as well as industry estimated component lifespans and repair/replacement costs. From this data, it was possible to derive a method of estimating damage coefficients for each component. The concept of the use of these damage coefficients is that at any data point, the amount of damage incurred by the component may be estimated as either damage due to a start or stop condition or, under normal operation, the sum of the damage due to power output plus the damage due to the change in power output. Below, (9) and (10) also serve to describe this method.

$$if\,(Start\ or\ Stop):\quad Damage = D_{Start/Stop}\Delta P \tag{9}$$

$$if\,(Normal\ Operation):\quad Damage = D_{\Delta P}\Delta P + D_P P \tag{10}$$

The first step of implementing this method was to derive the damage coefficients for each component. In order to do so, it was necessary to determine the

average operating conditions for hydroelectric generation units. After finding this, the relative amount of damage that each operating condition causes on each component was estimated. This information, combined with the predicted lifespan of each unit, led to the following derivation for each damage incurrence term for each component, in units of % of Life per PU power at each time step. Table 3.2 and Table 3.3 describe the variables and coefficients used in this derivation.

Table 3.2. Damage coefficient derivation – variable meanings

L_T	Total Life – Considered to be 1 (100%) for full life of component
D	Damage rate – Amount of damage incurred per PU operating condition
N	Number of operating condition occurrences in one lifespan
n	Average number of operating condition occurrences in one day
T	Typical life of component in days
ΔP	Change in power output
P	Power Output
L_x	Amount of life lost due to operating condition x.

Table 3.3. Damage coefficient derivation – subscript meanings

S	Small Ramp ($0 < \Delta P \leq 10\%$)
M	Medium Ramp ($10\% < \Delta P \leq 20\%$)
L	Large Ramp ($\Delta P > 20\%$)
SS	Start or Stop condition
P	Power output
DP	Damaging power output ($30\% < P < 50\%$)

First, the total amount of life lost may be thought of as a summation of the life lost due to different damage terms.

$$L_T = D_S \sum_{i=1}^{N_S} |\Delta P_S(i)| + D_M \sum_{i=1}^{N_M} |\Delta P_M(i)| + D_L \sum_{i=1}^{N_L} |\Delta P_L(i)| + D_{SS} \sum_{i=1}^{N_{SS}} |\Delta P_{SS}(i)| + D_P \sum_{i=1}^{N_P} P(i) + D_{DP} \sum_{i=1}^{N_{DP}} P_{DP}(i) \quad (11)$$

Note the relationship between the sum and average of the terms:

$$\frac{\sum_{i=1}^{N_S} |\Delta P_S(i)|}{N_S} = \overline{|\Delta P_S|} \quad \text{therefore,} \quad \sum_{i=1}^{N_S} |\Delta P_S(i)| = N_S \overline{|\Delta P_S|}$$

This result is used for all summed quantities.

Also, total life is considered to be 100%, therefore $L_T = 1$.

$$1 = D_S N_S \overline{|\Delta P_S|} + D_M N_M \overline{|\Delta P_M|} + D_L N_L \overline{|\Delta P_L|} + D_{SS} N_{SS} \overline{|\Delta P_{SS}|} + D_P N_P \bar{P} + D_{DP} N_{DP} \overline{P_{DP}}$$

This formulation is useful if it is known how many occurrences of each operating condition occur in one lifespan. However, all that is known is the average expected lifespan of a component. To include the lifespan of the component, include T.

$$N_S = T n_S$$

This result is used for all total occurrence terms.

$$1 = D_S T n_S \overline{|\Delta P_S|} + D_M T n_M \overline{|\Delta P_M|} + D_L T n_L \overline{|\Delta P_L|} + D_{SS} T n_{SS} \overline{|\Delta P_{SS}|} + D_P T n_P \bar{P} + D_{DP} T n_{DP} \overline{P_{DP}} \quad (12)$$

Now, consider the different amount of life that is lost due to each of these terms, and that over an entire lifespan for that component they must sum to 100%.

$$L_T = 1 = L_S + L_M + L_L + L_{SS} + L_P + L_{DP}$$

$$L_S = D_S T n_S \overline{|\Delta P_S|} \quad \text{therefore,} \quad \boldsymbol{D_S = \frac{L_S}{T n_S \overline{|\Delta P_S|}}} \quad (13)$$

This result is used to calculate all of the damage coefficients.

Based on this result, the damage coefficients that are to be utilized for the Real-time Damage Incurrence model may be calculated through knowing the typical lifespan for each component in days (T), the average number of occurrences per day for each condition $\boldsymbol{x}$ (n_x), the average power or change in power for each condition $\boldsymbol{x}$ ($\overline{|P_x|}$ or $\overline{|\Delta P_x|}$), as well as an estimation for how much of the lifespan of each component was lost due to condition $\boldsymbol{x}$ (L_x). Through information acquired from industry contacts, all of the required information was obtained.

The average number of starts (going from zero power output to positive power output), stops (positive power output to zero power output), small ramps ($\Delta\boldsymbol{P}$ less than 10% per unit [PU] power), medium ramps ($\Delta\boldsymbol{P}$ between 10% and 20% PU), and large ramps ($\Delta\boldsymbol{P}$ greater than 20% PU) were determined on a per-day basis. The ranges of each ramp category were determined based on both industry contacts and analysis of typical unit operation. The average number of 5 minute periods per day during which the units were generating power in the damaging and non-damaging range, and the average amount of power being generated during these times, were also determined. Using this data, as well as estimations of life lost due to the different operating conditions for each component, the damage coefficients were calculated and are given in Table 3.4.

Table 3.4. Damage coefficients derived for hydropower unit components

Component	D_S	D_M	D_L	D_{SS}	D_P	D_{DP}
Wicket Bushings	3.88E-06	1.77E-05	8.31E-05	1.13E-04	0	0
Wicket Seals	3.88E-06	1.77E-05	8.31E-05	1.13E-04	0	0
Wicket Ring Servo	4.65E-06	1.42E-05	3.74E-05	6.75E-05	0	0
Thrust Bearing	4.63E-06	7.06E-06	3.71E-05	8.44E-05	3.98E-10	3.86E-07
Guide Bearing	4.65E-06	1.42E-05	3.74E-05	6.75E-05	0	0
Turbine Blade Seals	3.26E-06	9.23E-06	3.74E-05	8.44E-05	0	0
Turbine Blade Servos	4.65E-06	1.42E-05	3.74E-05	6.75E-05	0	0
Turbine Runner	1.86E-06	4.26E-06	3.73E-05	1.01E-04	3.98E-10	7.72E-07
Governor System	3.1E-06	7.1E-06	1.04E-04	1.13E-04	0	0
Generator Windings	9.31E-07	5.68E-06	6.23E-05	2.35E-04	1.59E-09	7.72E-07
Generator Brakes	0	0	0	2.11E-04	0	0
Rotor Windings	2.91E-06	1.33E-05	3.12E-05	1.25E-04	9.95E-10	9.65E-07
Excitation System	5.82E-06	2.66E-05	1.25E-04	1.69E-04	0	0
Breaker	0	0	0	1.69E-03	0	0
Transformer	0	0	4.66E-05	1.47E-04	4.98E-10	4.83E-07

3.1.1 Fuzzy RDI Model

At this point, it was noted that the methodology used to determine the damage coefficients was well suited for a fuzzy logic type of approach. Fuzzy logic allows states that variables can take to blend together at the boundaries, essentially making the distinction between states “fuzzy.” In this case, this type of system allows for a much more smooth transition between different damage conditions, as well as a way of merging the different power output and change in power output damage terms into a single fuzzy logic style calculation.

The ability to smooth transitions in damage levels is well described by Kasabov (1996) who described that “the truth values for fuzzy propositions are not TRUE/FALSE only, as is the case in propositional Boolean logic, but include all the

grayness between two extreme values." For example, consider the case where the change in power generation is barely above the threshold for being considered a medium change in power damage rate. The amount of damage that is estimated to be incurred may be significantly higher than if the change in power were to be only slightly under the medium change in power damage threshold, which intuitively does not make sense. By instead blending together the small and medium change in power damage rate zones, it prevents this type of immediate jump in damage to occur.

In order to design a fuzzy logic system, it is first necessary to define the membership functions for each physical quantity. A membership function defines how well a quantity fits into that membership function's state. In this case, the two quantities to be determined were change in power and power output. For change in power, the states considered were small, medium, and large. The membership functions for the change in power variable represent these three zones as determined by the thresholds that were given in Table 3.3. The membership function should return a value of one if the quantity is completely within that membership functions state. The membership function should return a value of between zero and one if the quantity is on the boundary of the state, and a zero if it lies outside of the state. The resulting fuzzy logic membership function for change in power is shown in Fig. 3.2. Note that the membership function for "Small" is higher than all other membership functions until 10%, which is the highest change in power that is considered small. At this point the membership function for "Medium" becomes equal, and this process continues until the "Large" membership function becomes one.

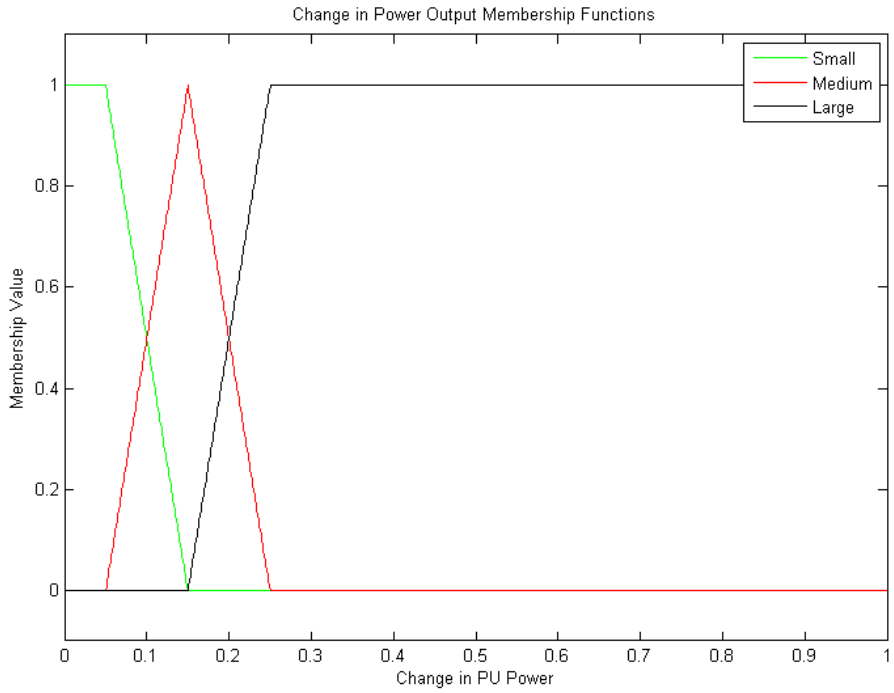

Fig. 3.2. Fuzzy membership function for change in output power

For power output, the zones considered were low, damaging, and safe power output. ‘Low’ is qualified as anything below 30% PU output, ‘damaging’ is between 30% and 50% of PU output, and ‘safe’ is anything above 50% PU output. The reason for the ‘damaging’ category is that hydroelectric turbines can experience harmonic vibrations when they are operating near 40% of their output power, which can be more damaging to equipment than operating at other power levels (Harano, Tani, & Nomoto, 2006). As was expected, analyzing unit utilization data show it to be very rare for equipment to be operated within this power range. The resulting membership function for power output is shown in Fig. 3.3.

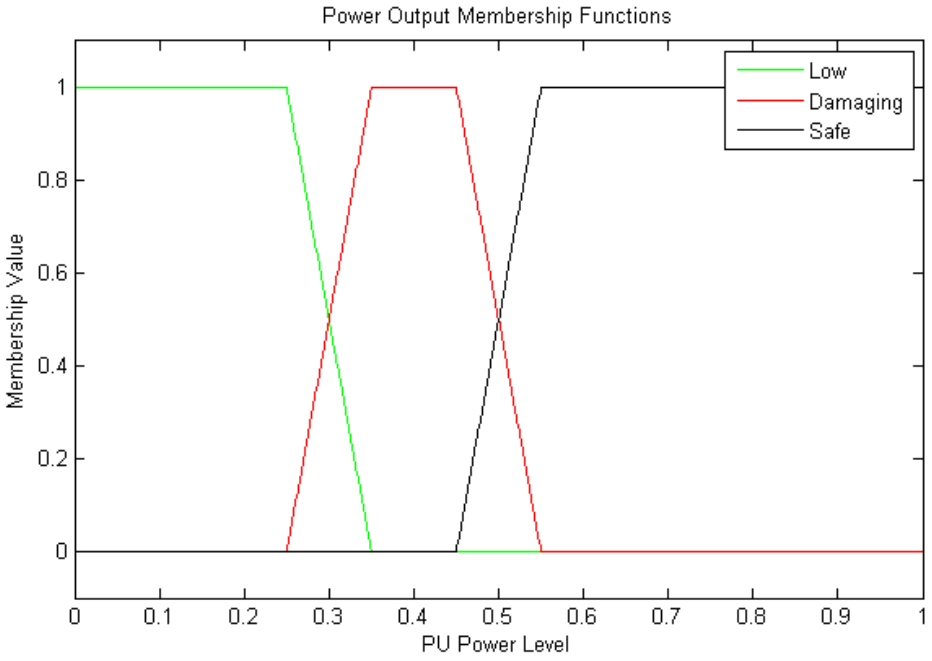

Fig. 3.3. Fuzzy membership function for power output

Note that in both of the previous fuzzy membership functions it is possible for a quantity to be considered partially two categories. For example, if the change in power is at precisely 20% PU, it would be considered half medium and half large in terms of membership. This capability is what allows the fuzzy system to blend together different variable states in order to create a smooth transition between different damage conditions.

At this point it is now possible, given a power and change in power condition, to determine the fuzzy memberships for each quantity. The "rules" for generating the output damage given the fuzzy memberships must be defined at this point. For example, one rule may be described as, "If ΔP is small AND P is safe, damage rate is calculated as $f(\Delta P, P, \Delta Ps_{memb}, Ps_{memb})$," where P and ΔP represent power output and change in power output respectively, the subscript '$_S$' represents

both small and safe, and the subscript ‘memb’ represents the membership function value. This same way of defining rules is continued until each possible combination is described, as in Table 3.5.

Table 3.5. Table of rules used for defining damage calculations based on fuzzy memberships

Rule 1	*If ΔP is*	Small	*AND P is*	Low	*then D =*	$\Delta P * D_S + P * D_P$
Rule 2	*If ΔP is*	Small	*AND P is*	Damaging	*then D =*	$\Delta P * D_S + P * D_{DP}$
Rule 3	*If ΔP is*	Small	*AND P is*	Safe	*then D =*	$\Delta P * D_S + P * D_P$
Rule 4	*If ΔP is*	Medium	*AND P is*	Low	*then D =*	$\Delta P * D_M + P * D_P$
Rule 5	*If ΔP is*	Medium	*AND P is*	Damaging	*then D =*	$\Delta P * D_M + P * D_{DP}$
Rule 6	*If ΔP is*	Medium	*AND P is*	Safe	*then D =*	$\Delta P * D_M + P * D_P$
Rule 7	*If ΔP is*	Large	*AND P is*	Low	*then D =*	$\Delta P * D_L + P * D_P$
Rule 8	*If ΔP is*	Large	*AND P is*	Damaging	*then D =*	$\Delta P * D_L + P * D_{DP}$
Rule 9	*If ΔP is*	Large	*AND P is*	Safe	*then D =*	$\Delta P * D_L + P * D_P$

This set of rules allow not only for specific damage coefficients to be applied depending upon the conditions, but also for the combination of rules if a condition is to fall between two or more rule sets. For example, in the case where ΔP is between small and medium and P is safe, rules 3 and 6 would be combined. They would be applied in such a way that the contribution of rule 3 would be weighted according to the membership of ΔP in the small fuzzy set, and rule 6 would be weighted based on the membership of ΔP in the medium fuzzy set. The way in which this combination is achieved is through a method known as defuzzification. An expression for the defuzzification of a fuzzy system with two variables (in this case, ΔP and P) and one output variable (damage incurred, D) can be written in the following way (Saade & Diab, 2000):

$$D = \sum_{i=1}^{n} \sum_{j=1}^{p} \left[A_i(x_0) \text{ x } B_j(y_0) \right] f_{ij}(D_{A_i}, D_{B_j}) \qquad (14)$$

In this expression, $A_1, A_2 \ldots A_n$ are the fuzzy sets for the first input variable (which yield a membership for that variable in that fuzzy set), $B_1, B_2 \ldots B_p$ are fuzzy sets for the second input variable, and x_0 and y_0 are the values of the input variables. The $f_{ij}(D_{A_i}, D_{B_j})$ term represents the rule that is to be applied, based upon the damage due to the first variable and the second variable. Note also that there is no need to divide by the sum of the membership values, because the sum is always one (Saade & Diab, 2000). This is because, with the membership functions chosen, the summation of memberships of a single variable at any value is always one. This may be verified in Fig. 3.2 and Fig. 3.3.

Applying this formulation to the damage system as designed, and referring to Table 3.5, the equation may be rewritten with variable names for RDI modeling in the following way:

$$D = \sum_{i=1}^{3} \sum_{j=1}^{3} \left[M_{\Delta P\, i}(\Delta P) \text{ x } M_{P\, j}(P) \right] f_{ij}(D_{M_{\Delta P i}}, D_{M_{P\, j}}) \qquad (15)$$

Where:

$M_{\Delta P_1} =$ membership of ΔP in "small" $\qquad M_{P_1} =$ membership of P in "low"

$M_{\Delta P_2} =$ membership of ΔP in "medium" $\qquad M_{P_2} =$ membership of P in "damaging"

$M_{\Delta P_3} =$ membership of ΔP in "large" $\qquad M_{P_3} =$ membership of P in "safe"

$$D_{M_{\Delta P_1}} = \Delta P * D_S \qquad D_{M_{P_1}} = P * D_P$$

$$D_{M_{\Delta P_2}} = \Delta P * D_M \qquad D_{M_{P_2}} = P * D_{DP}$$

$$D_{M_{\Delta P_3}} = \Delta P * D_L \qquad D_{M_{P_3}} = P * D_P$$

$$f_{ij}\left(D_{M_{\Delta P i}}, D_{M_{P\, j}}\right) = D_{M_{\Delta P i}} + D_{M_{P\, j}}$$

This calculation then determines the amount of damage that is incurred by each component based upon change in power output and power output. However, note that this formulation does not include starts and stops. This is because starts and stops are not well suited for the fuzzy framework, as they are very distinct and discrete events that are well defined. Because of this, a very simple linear model for start/stop damage incurrence may be given in the following form, separate from the fuzzy framework, assuming that the change in power was during a start or stop event:

Fig. 3.4. Start/Stop damage incurrence model

At this point, damage incurrence models for both start/stop and regular operation conditions have been developed. For start/stop situations, a simple linear model is given that determines damage incurred based upon the damage coefficients as derived before as well as the severity of the start/stop, as indicated by the change in power. The regular operation damage model, which is a function of change in power output and power output, is defined in a fuzzy framework in order to smoothly blend different regions of damage severity together to determine the damage incurrence under any operating conditions.

These two models may then be merged together into a single RDI model for the hydroelectric generation unit in such a way that the damage incurred is dependent

upon the operating condition (start/stop or normal). This overall model is given in the following figure, along with an explanation of its operation.

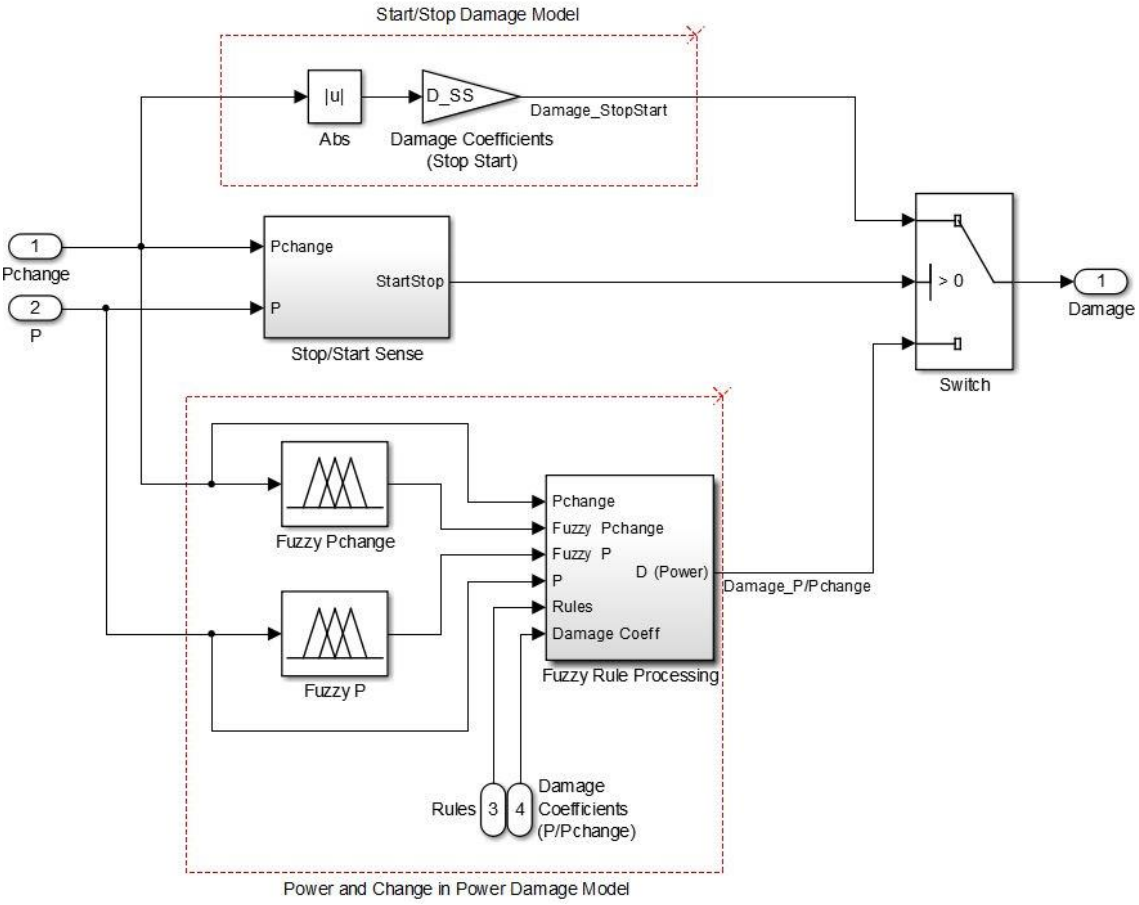

Fig. 3.5. Block diagram of hydropower unit RDI model

In this block diagram, the way in which the damage is calculated depending upon the state of the system is able to be seen. At each time, it is determined if a start or stop situation has occurred. If a start or stop has occurred, the damage output is calculated through the start/stop damage model. If there has not been a start or stop, the damage is instead calculated by the fuzzy system that has been developed. This involves first determining the fuzzy memberships for both power and change in

power, and then calculating the damage incurred based on the defuzzification rules and the damage coefficients.

Note that to this point, each block diagram and determination of damage incurrence has been considered for each individual component of the system. This same process would then be applied to each component in order to determine the RDI for all components. These may be done individually for each component, but it is far more efficient to calculate them all simultaneously through the use of matrices.

Recall that in Table 3.4 damage coefficients for each component were given, and were termed D_S, D_M, D_L, and so on. These values were later used in (15) in order to calculate the damage incurred by each component. In this form, D_S, D_M, D_L were considered to be scalar value damage coefficients for each component. Instead, consider $\mathbf{D_S}$ to be a vector containing the damage coefficients due to a small change in power for all of the components. Using this same method with all of the D terms, $\mathbf{D_M}$, $\mathbf{D_L}$, $\mathbf{D_{SS}}$, $\mathbf{D_P}$, and $\mathbf{D_{DP}}$ vectors may then be formed as well for the other damage coefficients in the following way for all m components:

$$\mathbf{D_S} = \begin{bmatrix} \mathrm{D_{S_1}} \\ \mathrm{D_{S_2}} \\ \vdots \\ \mathrm{D_{S}}_m \end{bmatrix} \mathbf{D_M} = \begin{bmatrix} \mathrm{D_{M_1}} \\ \mathrm{D_{M_2}} \\ \vdots \\ \mathrm{D_{M}}_m \end{bmatrix} \mathbf{D_L} = \begin{bmatrix} \mathrm{D_{L_1}} \\ \mathrm{D_{L_2}} \\ \vdots \\ \mathrm{D_{L}}_m \end{bmatrix} \mathbf{D_{SS}} = \begin{bmatrix} \mathrm{D_{SS_1}} \\ \mathrm{D_{SS_2}} \\ \vdots \\ \mathrm{D_{SS}}_m \end{bmatrix} \mathbf{D_P} = \begin{bmatrix} \mathrm{D_{P_1}} \\ \mathrm{D_{P_2}} \\ \vdots \\ \mathrm{D_{P}}_m \end{bmatrix} \mathbf{D_{DP}} = \begin{bmatrix} \mathrm{D_{DP_1}} \\ \mathrm{D_{DP_2}} \\ \vdots \\ \mathrm{D_{DP}}_m \end{bmatrix}$$

In this way the damage for all components may be determined simultaneously through (16).

$$\mathbf{D} = \begin{bmatrix} D_1 \\ D_2 \\ \vdots \\ D_m \end{bmatrix} = \sum_{i=1}^{3} \sum_{j=1}^{3} \left[M_{\Delta P_i}(\Delta P) \times M_{P_j}(P) \right] f_{ij}(\mathbf{D_{M_{\Delta P_i}}}, \mathbf{D_{M_{P_j}}}) \qquad (16)$$

Where:

$$\mathbf{D_{M_{\Delta P_1}}} = \Delta P * \mathbf{D_S}\,, \qquad \mathbf{D_{M_{\Delta P_2}}} = \Delta P * \mathbf{D_M}\,, \quad \mathbf{D_{M_{\Delta P_3}}} = \Delta P * \mathbf{D_L}, \cdots$$

And **D** is a vector of the total damage incurred by each component at that time step.

In order to translate the damage incurred at each time into a cost, recall that the damage incurrence values are given as amount of life lost. In this way, the cost associated with an amount of life being lost may be determined by simply multiplying the cost to replace or repair the component by the amount of life that was lost. This can be shown in the following equation:

$$C_{5min} = D * C$$

Where *D* is the damage incurred as calculated from the RDI modeling function and *C* is the component cost. This cost can be calculated for all components at once in matrix form in the following way, where the $.*$ operator represents element-wise multiplication:

$$\mathbf{C} = \begin{bmatrix} C_1 \\ C_2 \\ \vdots \\ C_m \end{bmatrix}, \ \mathbf{D} = \begin{bmatrix} D_1 \\ D_2 \\ \vdots \\ D_m \end{bmatrix} \text{and } \mathbf{C_{5min}} = \mathbf{C} .* \mathbf{D} = \begin{bmatrix} C_{5\text{min}\_1} \\ C_{5\text{min}\_2} \\ \vdots \\ C_{5\text{min}\_m} \end{bmatrix} \tag{17}$$

The total amount of cost due to damage accrued at each time step may then be found as simply the summation of all of the elements of $\mathbf{C_{5min}}$.

3.2 Zinc/Bromine Flow-cell Battery RDI Model

The Zinc/Bromine flow-cell battery was one of the considered technologies for this control system because it has higher energy density, a longer expected lifespan, offers higher performance, and is more cost efficient than many other advanced battery technologies that are currently in development (Lex & Jonshagen, 1999). There are very low operating hazards involved with a Zinc/Bromine battery, and it also has a very low self-discharge rate combined with the capability for extended standby time without degradation. It also is less intensive in terms of both labor and costs to repair the battery after it has reached the end of its life as only the battery stack and pumps must be replaced, which only equate to approximately 20% of the initial battery installation cost (Lex & Jonshagen, 1999). In addition, as it is a flow-cell battery technology, it is possible to scale the power and energy capacity of the system independently, allowing for many possible configurations. The configuration of the flow-cell battery system may also be changed after installation without disrupting the rest of the system due to its modularity (Lex & Jonshagen, 1999).

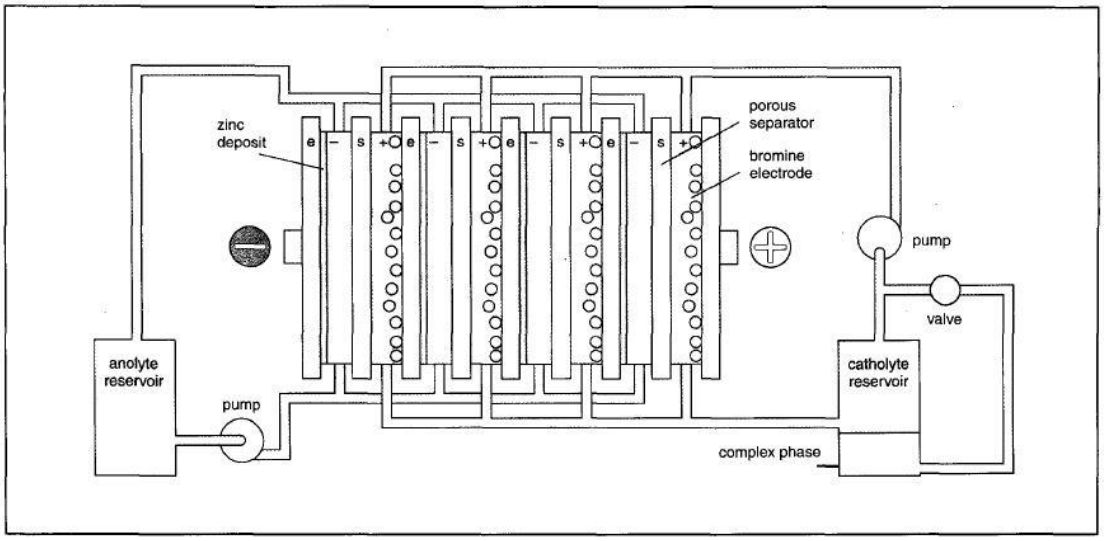

Fig. 3.6. Zinc/Bromine flow-cell battery schematic (from Lex & Jonshagen, 1999)

A Zinc/Bromine battery consists of a number of components, namely battery stacks, electrolyte storage reservoirs, and an electrolyte circulation system used to ensure uniform electrolyte distribution as well as improve thermal management for the battery. A diagram of the overall system may be seen in Fig. 3.6. Note that there are four cells (two electrodes with a microporous separator in between) in the system shown. The electrodes used are bipolar which makes it possible for the cells to be stacked together, allowing for current flow directly through the battery stack. In this way the entire battery may be thought of as multiple smaller battery cells in series (Lex & Jonshagen, 1999).

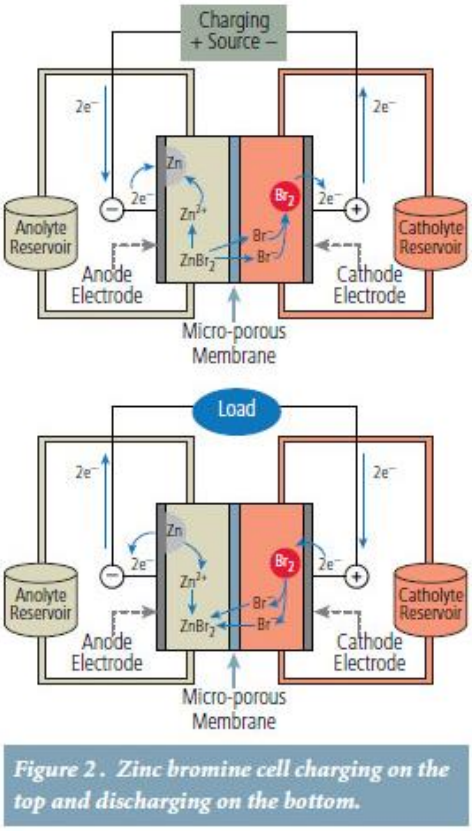

Fig. 3.7. Charging and discharging reactions for Zinc/Bromine flow-cell battery (from Faries, 2012)

While the battery is charging, zinc is deposited on the anode of each electrode and bromine is evolved at the cathode. During discharge, zinc is oxidized into zinc ions at the anodes and bromine is reduced to bromide ions at the cathodes (Faries, 2012). The electron flow during these reactions is visually shown in Fig. 3.7.

In order to determine a damage incurrence model for a Zinc/Bromine flow-cell battery, it is necessary to understand the conditions that lead to damage and to quantify the amount of damage incurred in terms of discharging and charging power, as well as to determine the effect that changing the power output may have on the system. First, it is noted that a Zinc/Bromine flow-cell battery is a chemical system which does not use mechanical means to generate energy and thus does not have

mechanical wear components. Therefore its primary cause of degradation will not be based upon changing the power level, but rather upon the amount of current (and thus power) that the system is sinking or sourcing, through charging or discharging respectively. Furthermore, it was discovered by Bistrika (2013) that "battery charging was quantitatively shown to be the primary degradation mechanism in bromine based batteries and is predicted to be the mechanism by which the reactor stack will fail."

Based upon the quantitative experimental results done in in this prior research, the estimated number of cycles that the zinc/bromine system could endure was calculated based upon the operating power as well as the rated power (Bistrika, 2013).

$$n_{cyc} = \exp\left(\frac{P_{rated}(1-k_{\lim})}{0.03*P_{op}}\right) \tag{18}$$

In the previous equation, $k_{\lim}$ describes the theoretical capacity at which the flow-cell battery is determined to fail. This is considered to be 80% for all calculations. The cost of operation ($/kWh) may then be calculated as follows (Bistrika, 2013):

$$Cost = \frac{C_{sys}}{E_{sys}*n_{cyc}} = \frac{C_{sys}}{E_{sys}} * \exp\left(\frac{-P_{rated}(1-k_{\lim})}{0.03*P_{op}}\right) \tag{19}$$

Where C_{sys} and E_{sys} are the cost and energy rating of the flow-cell battery, respectively. This determination is very useful for estimating the cost of operation based upon a power output. If a pure cost is desired, it is necessary to multiply this by the amount of energy that the system has experienced during a time period. Thus the cost for any five minute period may be calculated in the following way.

$$C_{5min} = \frac{C_{sys}}{E_{sys}} * \exp\left(\frac{-P_{rated}(1-k_{\lim})}{0.03*P_{5min}}\right) * \frac{P_{5min}}{12} \quad (20)$$

In order to translate this cost function model into a damage model, it may simply be divided by the cost, giving instead an estimate of the percentage of life lost per five minute period.

$$D_{5min} = \frac{P_{5min}}{12*E_{sys}} * \exp\left(\frac{-P_{rated}(1-k_{\lim})}{0.03*P_{5min}}\right) \quad (21)$$

It should also be noted that this calculation applies to the charging of the battery only. Based upon the qualitative analysis that was conducted by previous research, it was evident that discharging of the battery within the power rating did not result in damage of relative significance (Bistrika, 2013). Based upon this observation, the damage model may be visualized by the following block diagram. This type of damage model for the Zinc/Bromine battery system may then be integrated into the LEC system.

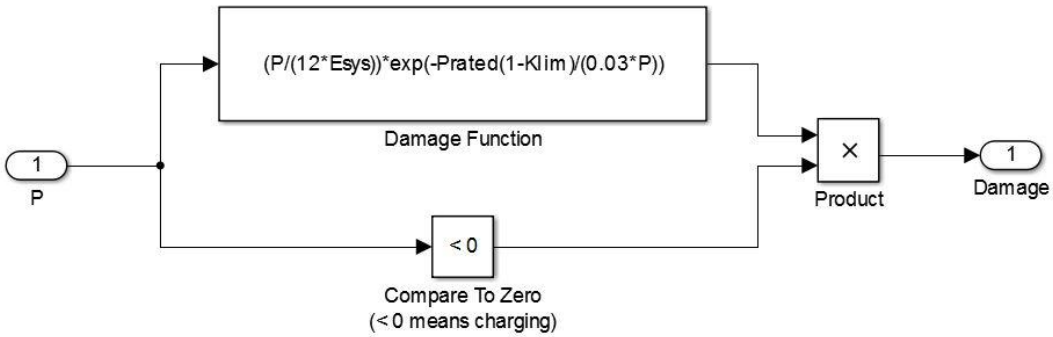

Fig. 3.8. Flow-cell battery damage model

3.3 Flywheel RDI Model

Flywheel energy storage is a means to store electrical energy in the kinetic energy of a rotating mass. Essentially, by using electrical energy it is possible to drive a large mass to rotate at high speeds, converting the electrical energy into rotating kinetic energy. This energy may later be extracted and converted back into electrical energy through the use of a motor-generator. This is the method by which flywheel energy storage devices operate.

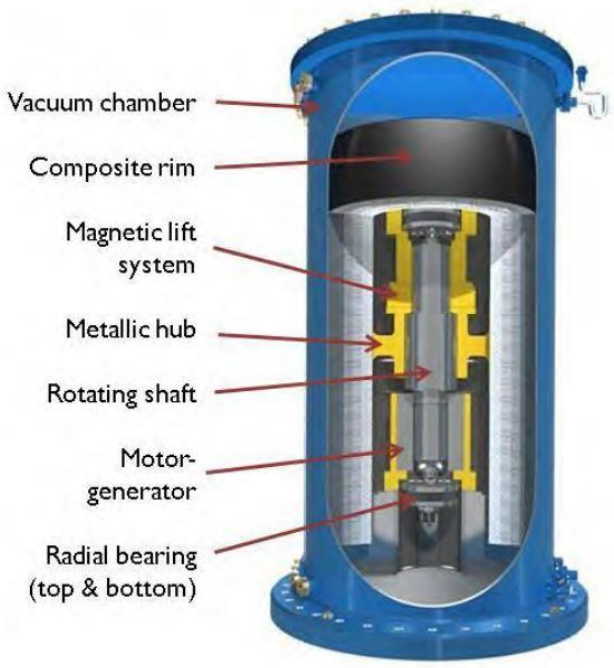

Fig. 3.9. Diagram of Flywheel energy storage device (from Flywheel Energy Storage System, 2013)

This technology is considered to be very power-dense because it is able to supply a large amount of power relative to its energy rating. The considered flywheel system is able to supply power up to four times the energy rating of the device. This corresponds to a “C” rating of 4, which is simply the ratio of how much power may

be output from a device to the energy which may be stored in a device. This type of system works well with a flow-cell battery type of storage, such as the Zinc/Bromine flow-cell battery, because it has a relatively low "C" rating of ½. This means that the flywheel may be better in fast operation and rapid response, whereas the flow-cell battery may be better at storing energy for longer periods.

A flywheel energy storage system is suitable for this application because it is modular, and thus able to be sized depending upon the needs of the specific area or plant. Flywheels are also extremely fast responding, as they are able to increase power output (or input) from zero to 100% rated power within one second (Flywheel Energy Storage System, 2013). With magnetic lift systems operating in a vacuum chamber, they are also extremely reliable with a very high cycle life of over 150,000 effective charge/discharge cycles over a 20 year design lifespan (FACT SHEET - Frequency Regulation and Flywheels, 2003).

The energy that is stored in a rotating mass is determined by the following expression (Bolund, Bernhoff, & Leijon, 2007):

$$E = \frac{1}{2}\boldsymbol{I}\omega^2 \tag{22}$$

Where the variable $\boldsymbol{I}$ represents the moment of inertia of the rotating mass and ω represents its angular velocity. The flywheels considered for this research are designed and manufactured by Beacon Power, and have a composite rim attached to a rotating shaft, which yields the following expression for the moment of inertia (Bolund, Bernhoff, & Leijon, 2007):

$$\boldsymbol{I} = \frac{1}{4}m({r_o}^2 + {r_i}^2) \tag{23}$$

Where m represents the mass of the rotating body, r_o represents the outer radius of the rim, and r_i represents the inner radius of the rim.

From (22) and (23), it is clear that the amount of energy that is stored in a flywheel is a proportional to the mass of the rotating body as well as the square of its angular velocity. A result of this simple method of calculating the energy stored in a flywheel is that it is relatively simple to accurately determine the state of charge (SOC) of the device, which here is defined as the ratio of the energy stored to the energy capacity of the device. Because the mass is constant, simply tracking the rotating speed of the device gives an accurate measure of how much energy it is currently storing.

Due to the relatively recent installations of flywheel energy storage systems in grid application and the lack of significant prior research into the wear and tear of flywheel systems in vacuum chambers with magnetic lift systems of this size, RDI model development is difficult for this technology. Because of the lack of prior analysis and data, an RDI model may be approximated by utilizing the rated lifespan of the device in terms of the numbers of effective charge and discharge cycles. In order to develop this model it is necessary to determine the approximate number of charge/discharge cycles that the flywheel energy storage system can experience in one lifespan and calculate the damage based upon the change in SOC. This calculation may be made by using the following equation:

$$D = \frac{|\Delta SOC|/2}{Cycles_{Life}} \tag{24}$$

Here $|\Delta SOC|$ represents the absolute value of the change in state of charge from the previous data point, and $Cycles_{Life}$ represents the amount of charge/discharge cycles expected in one lifespan. Note that the $|\Delta SOC|$ term is divided by two because the amount of cycles are given in terms of charge/discharge cycles, meaning that effectively a total of $\sum|\Delta SOC| = 2$ is needed in order to complete an entire equivalent charge and discharge. (24) essentially calculates an estimated amount of life lost given the change in SOC that the system experienced.

In order to estimate the SOC of the flywheel energy storage system, it is necessary to know the power delivered by the system over a time period and the length of time over which the power was delivered. The change in state of charge may be calculated as follows:

$$\Delta SOC = \frac{-P_{out\_5min} * \frac{1}{12}}{E_{rated}} \tag{25}$$

Power is defined to be positive for power supplied and negative for power absorbed. The power over five minutes must then be divided by twelve in order to convert it into units of MWh energy terms to match the unit of the bottom term, which is the energy rating of the system. From these methods and calculations, the damage for the flywheel energy storage system at any time step may be represented by the diagram in Fig. 3.10.

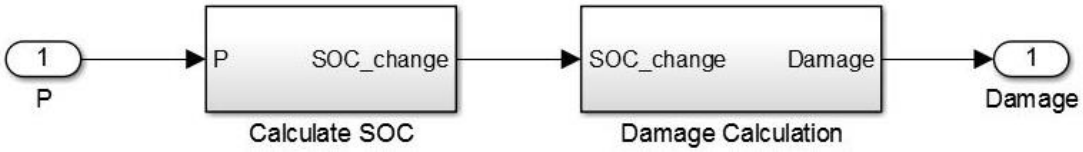

Fig. 3.10. Flywheel damage modeling

As with the other models, it is desirable to also have an estimate for cost accruement based upon the amount of damage incurred for a flywheel energy storage system. A simple way to do this is to multiply the damage by the cost that is considered for the repair/replacement cost of the system, as this is the cost that will be incurred at end of life of the system. Therefore, at each time step the cost may be calculated in the following way:

$$C_{5min} = C * D = C * \frac{|\Delta SOC|/_2}{Cycles_{Life}} \quad (26)$$

Where C is considered the estimated cost of replacement or repair for the system.

3.4 Discussion

To this point, RDI models have been developed for all systems under consideration. Due to differing availability in data and prior research, these models have been developed in slightly different ways. However, the end model that has been developed is fundamentally of the same form in each case. All of the models utilize the amount of power generated or absorbed by the system at each time, and/or the change in power, and calculate the amount of damage that is incurred due to those conditions.

4 RDI Model Simulation

4.1 Hydroelectric Generation Unit RDI Simulation

From section 3.1, recall the form of the damage model for a hydroelectric generation unit:

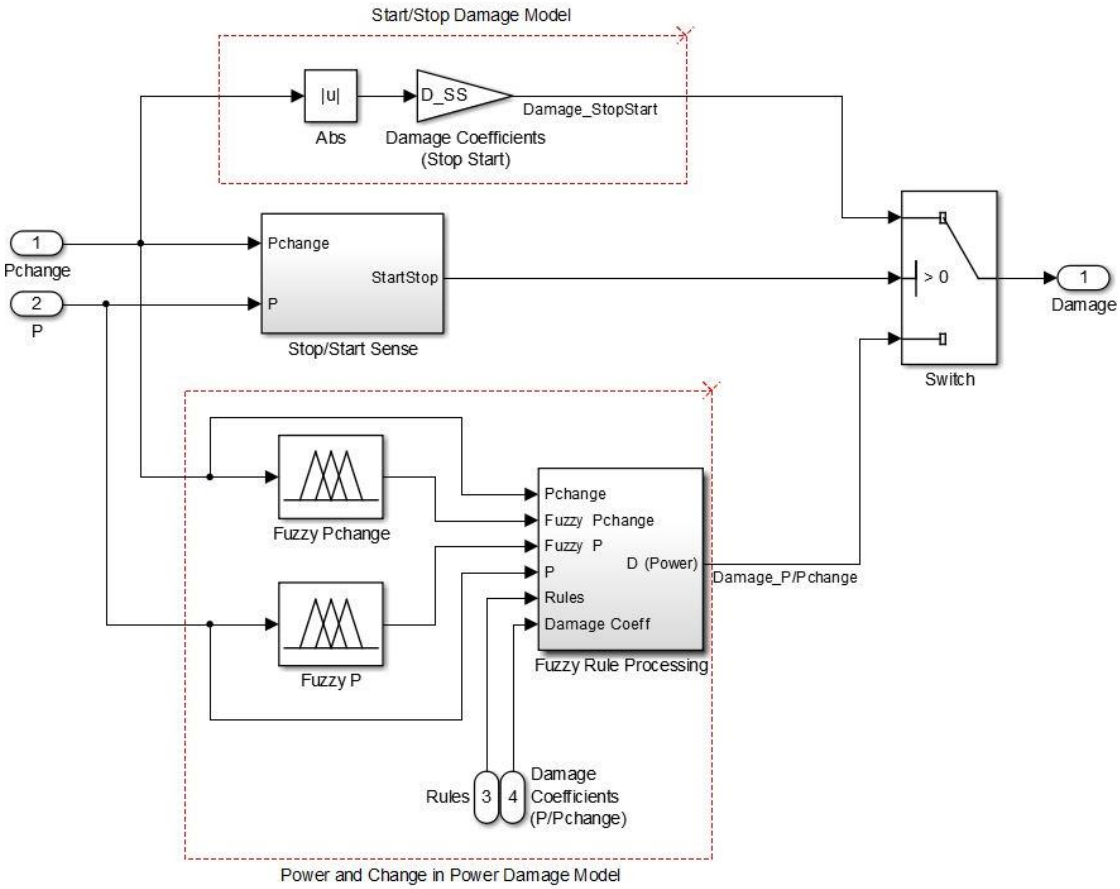

Fig. 4.1. Hydroelectric generation unit RDI model diagram

In order to run a simulation of damage incurrence for a hydroelectric generation unit, power data from an actual unit has been utilized, allowing for simulation of damage incurrence based upon real world data. The damage model was implemented in a MATLAB script, where this hydroelectric unit's generation data was used as input to the damage modeling.

Shown in Fig. 4.2 is the result of the simulation showing the power output of the unit, as well as the instantaneous damage incurred by each component of the unit, over a time window of approximately four hours.

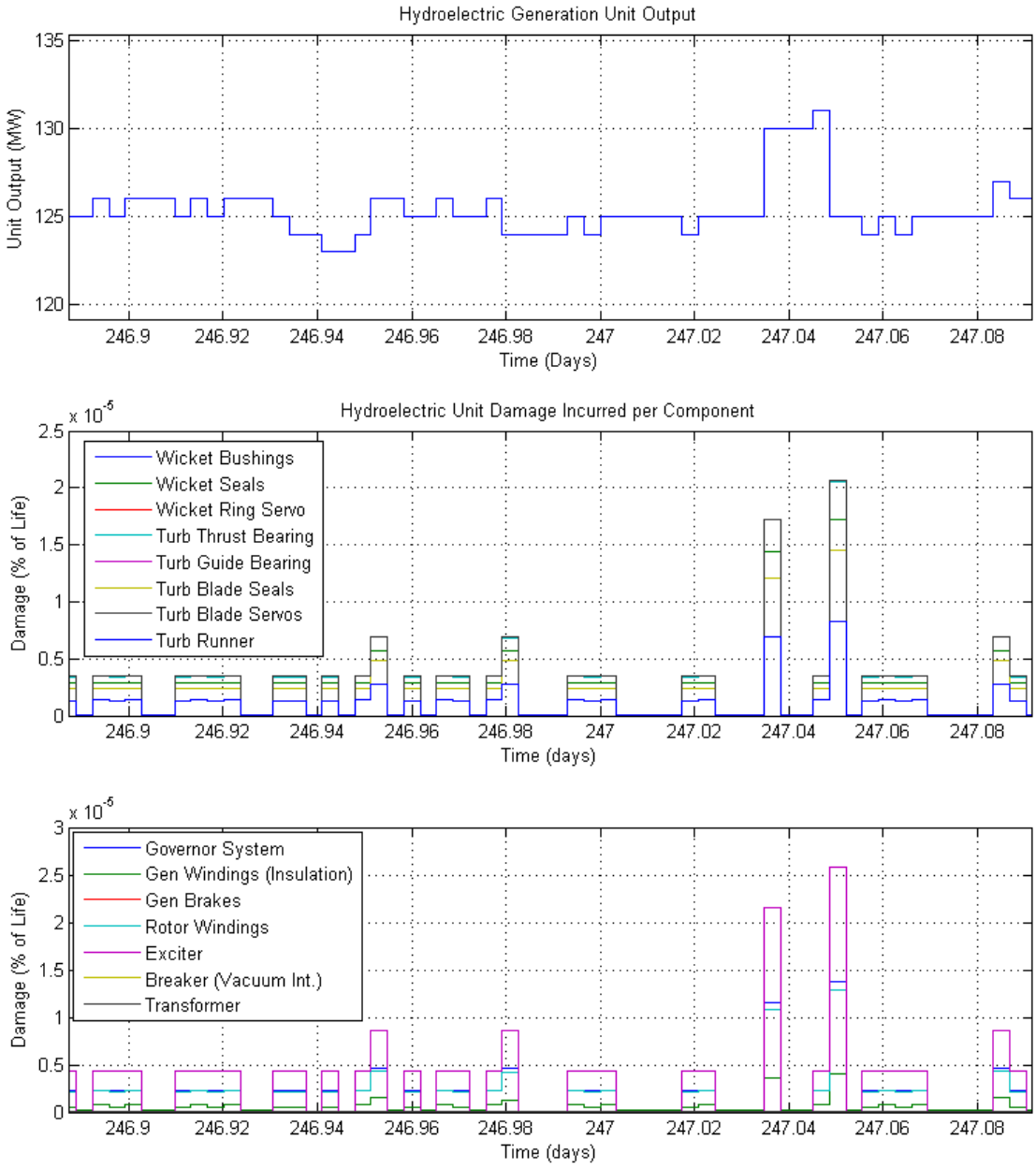

Fig. 4.2. Hydroelectric unit RDI simulation result – Normal Operation

Note that in the previous case the power output is between ~123 MW and ~132 MW, with ramping occurring occasionally. As is expected based on the damage incurrence model, there are larger spikes in the incurred damage when the power output changes most significantly. For comparison, another type of damage incurrence instance is shown in Fig. 4.3, where a unit is dropped offline.

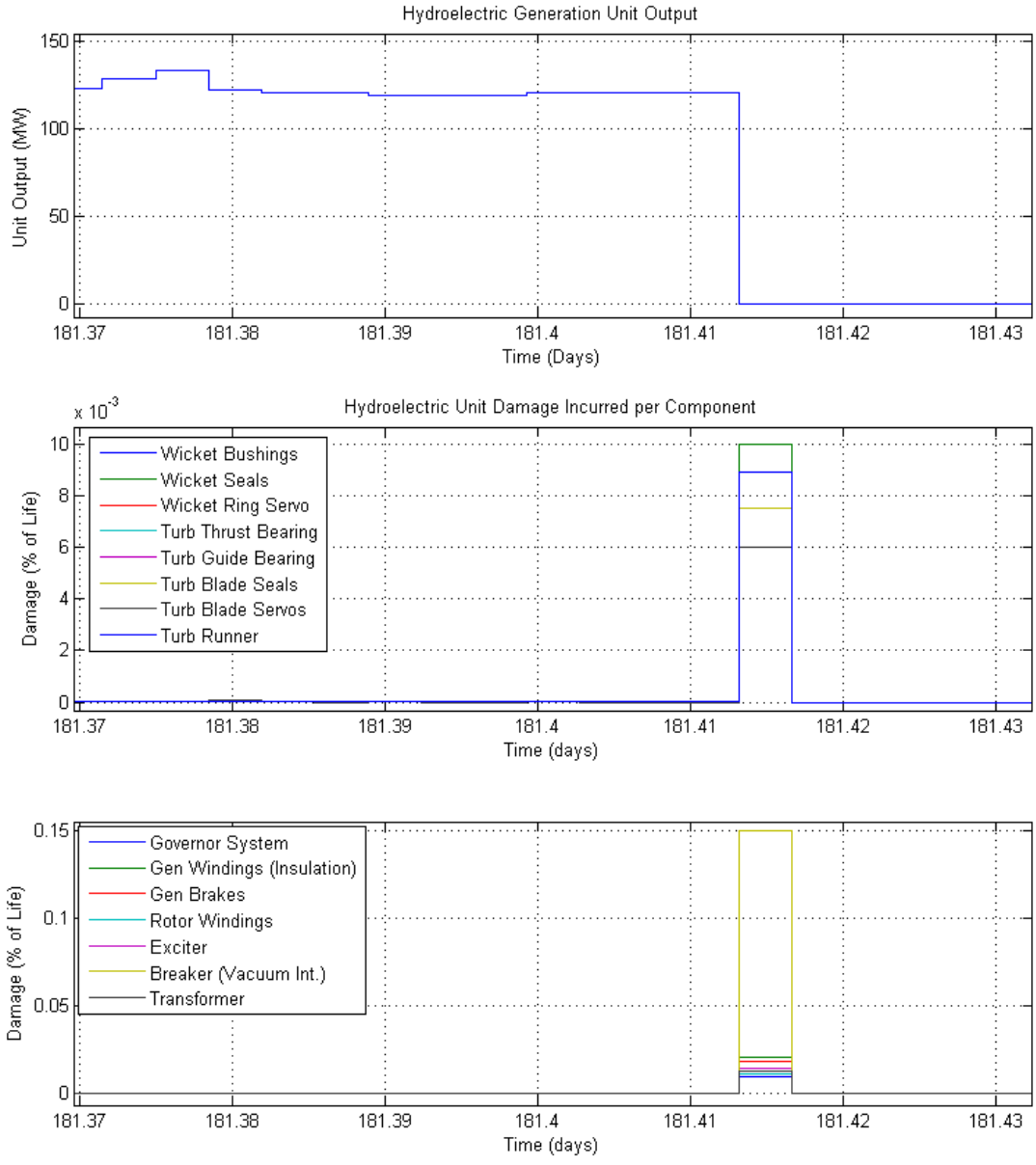

Fig. 4.3. Hydroelectric unit RDI simulation result – Unit Drop

In this case, the unit was quickly taken out of operation after previously generating over 110 MW of power. The damage incurred from this operation is clearly larger in magnitude than smaller ramping of unit output power.

This RDI simulation was run for over two years of actual unit power output data to make it possible to track the amount of damage accrued over this time frame. Each component's damage accruement was determined and plotted in Fig. 4.4.

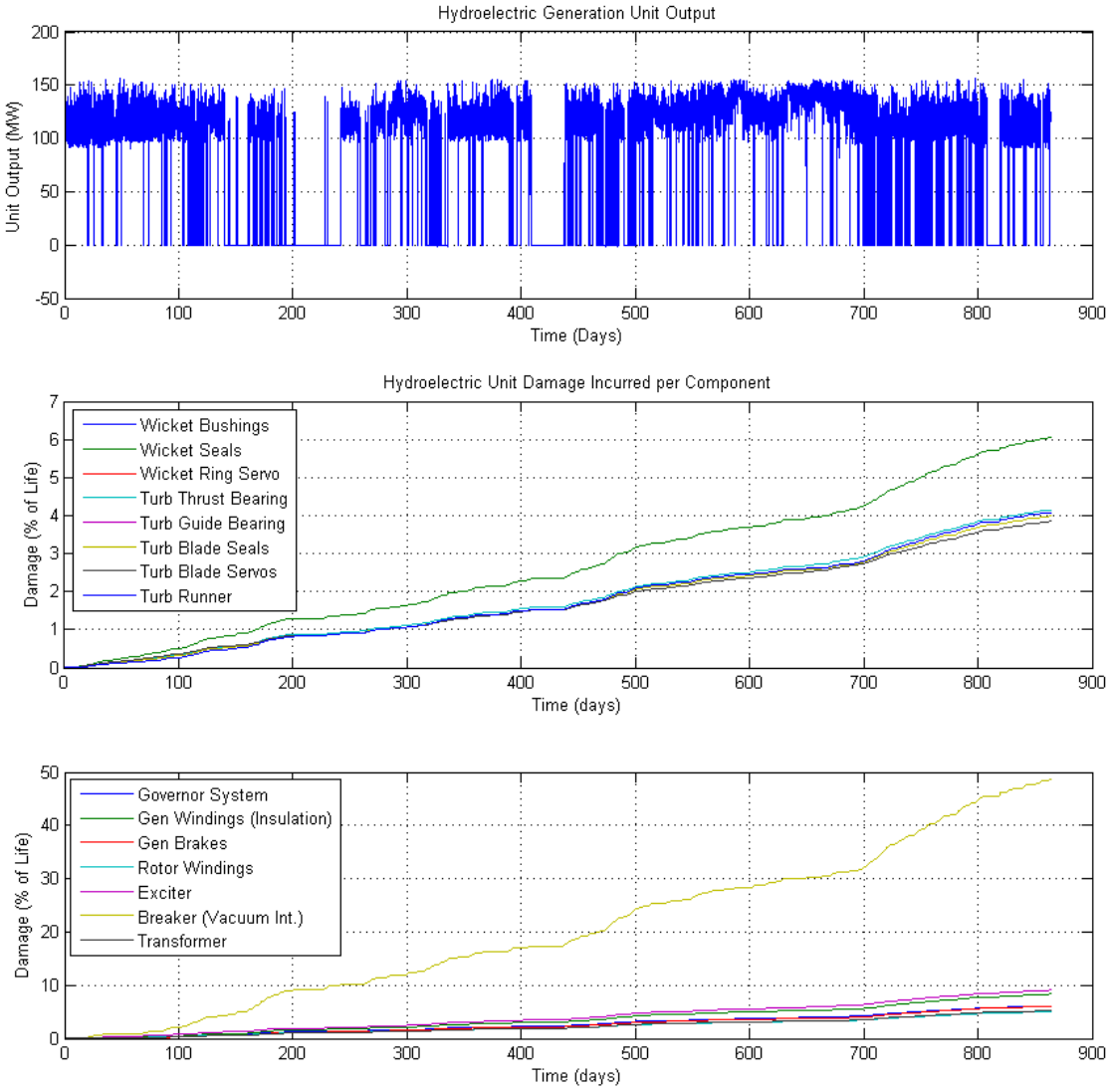

Fig. 4.4. Hydroelectric unit RDI Simulation – Extended Duration Simulation

Observing the results of this simulation, it is apparent that the unit breaker is the component that most rapidly approaches the end of its projected lifespan. This is because of a couple of reasons. First, the expected lifespan of this component is by far the lowest of the components (five years). Also, the data for the simulation was from a unit at John Day dam, which is a project that has been found to be more affected by wind generation than many other dams and thus is more likely to experience frequent ramping and starts/stops when compared to many other projects. Fig. 4.5 shows the accumulation over time of the cost due to damage for all of the components of the hydroelectric generation unit. Observing this plot and comparing it with the first plot of Fig. 4.4 reveals that periods of time when the unit is started and stopped more frequently result in the largest increase in cost, as would be expected.

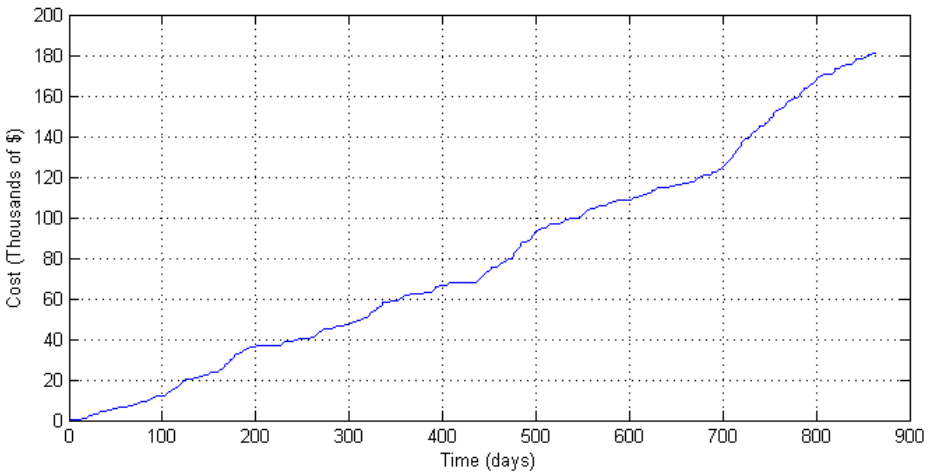

Fig. 4.5. Hydroelectric unit RDI Simulation – Cost Accumulation

4.2 Zinc/Bromine Flow-Cell Battery RDI Simulation

For a Zinc/Bromine flow-cell battery system, the damage that is incurred is modeled by the damage model as given in Section 3.2:

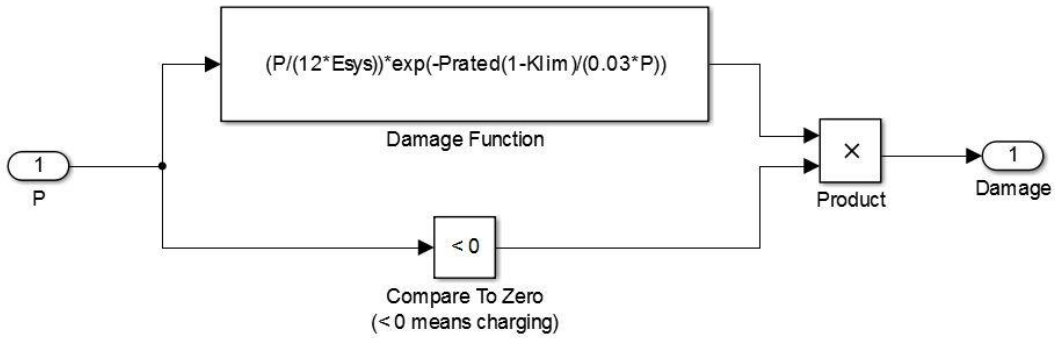

Fig. 4.6. Zinc/Bromine flow-cell battery damage incurrence model

In order to run this simulation, the flow-cell battery system must be given flow-cell power output data that is within the ratings of the system and also similar in form to what the system would be expected to provide in actual application. For this reason, the change in power data from the hydroelectric power data used in the LEC system was utilized. This data was then scaled such that it fit within the rated power for the flow-cell battery model. The charging/discharging power for the flow-cell battery system was then taken to be this scaled change in power data, with consideration for SOC taken into account as well. In this way, the power output for the flow-cell battery system is both within the ratings of the unit and similar in form to actual power change data that the system would be expected to balance.

Note that for this simulation, the goal was neither to extend the life of the flow-cell battery nor to minimize cost. The goal is only to see how damage is incurred by the system based upon charging/discharging power, while operating it within reasonable constraints based upon the damage model for flow-cell batteries. The power rating for this system is 6 MW and therefore the maximum discharging power was set to 6 MW. However, the maximum charging power was limited to 4 MW. This is because the damage model for the Zinc/Bromine flow-cell system is highly sensitive to high levels of charging current due to its exponential form, so to get a more realistic look at how damage would be incurred under typical use the charging power was limited.

Fig. 4.7 shows power output, the SOC, and the instantaneous damage incurred by the flow-cell battery system for a time period of approximately two days. Note that in this figure, large charging power led to very large amounts of instantaneous damage incurred. It is evident that during periods of charging (when SOC is increasing), there is significant damage incurred.

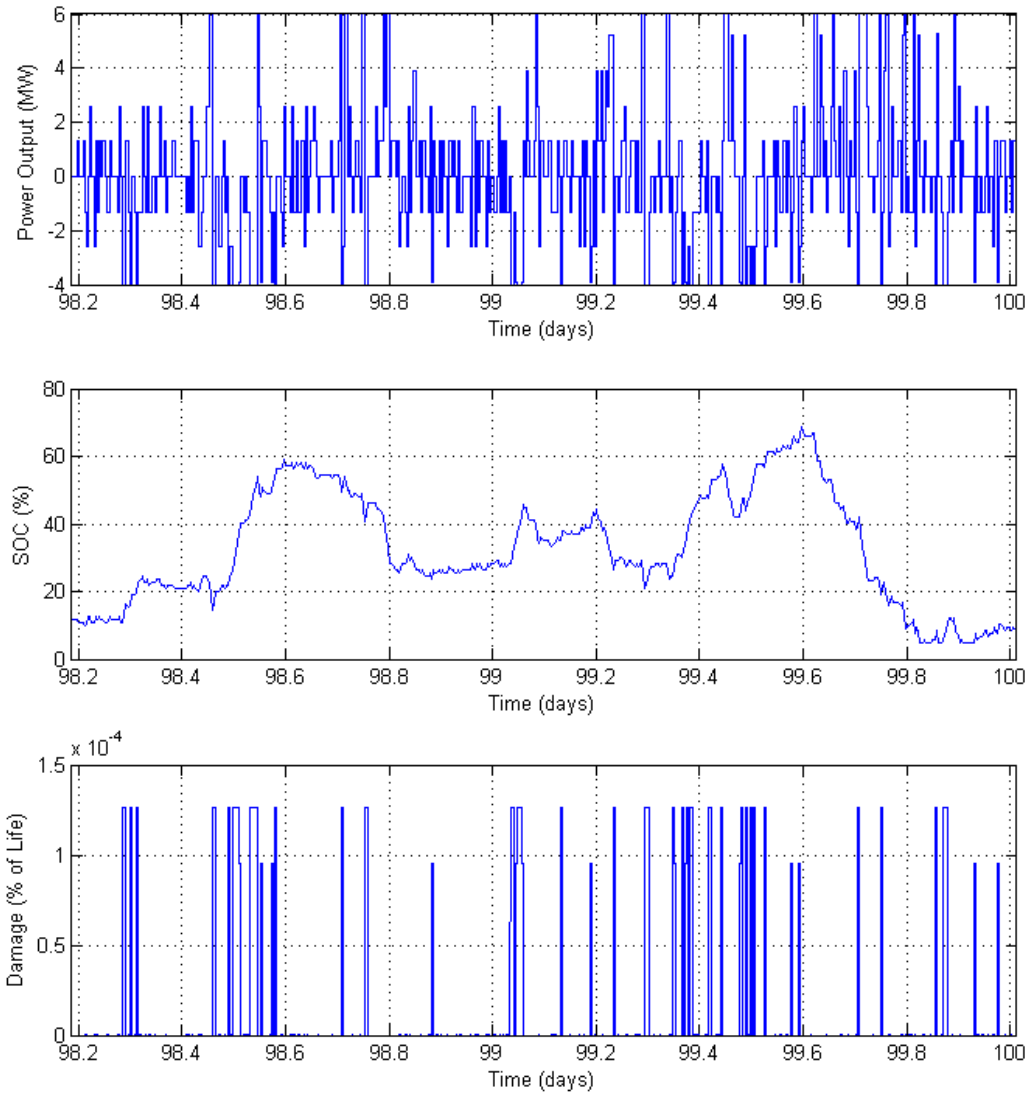

Fig. 4.7. Flow-cell RDI simulation – Two days

In order to get a closer look at this effect, this figure was observed over a much smaller time window. The resulting figure is given in Fig. 4.8.

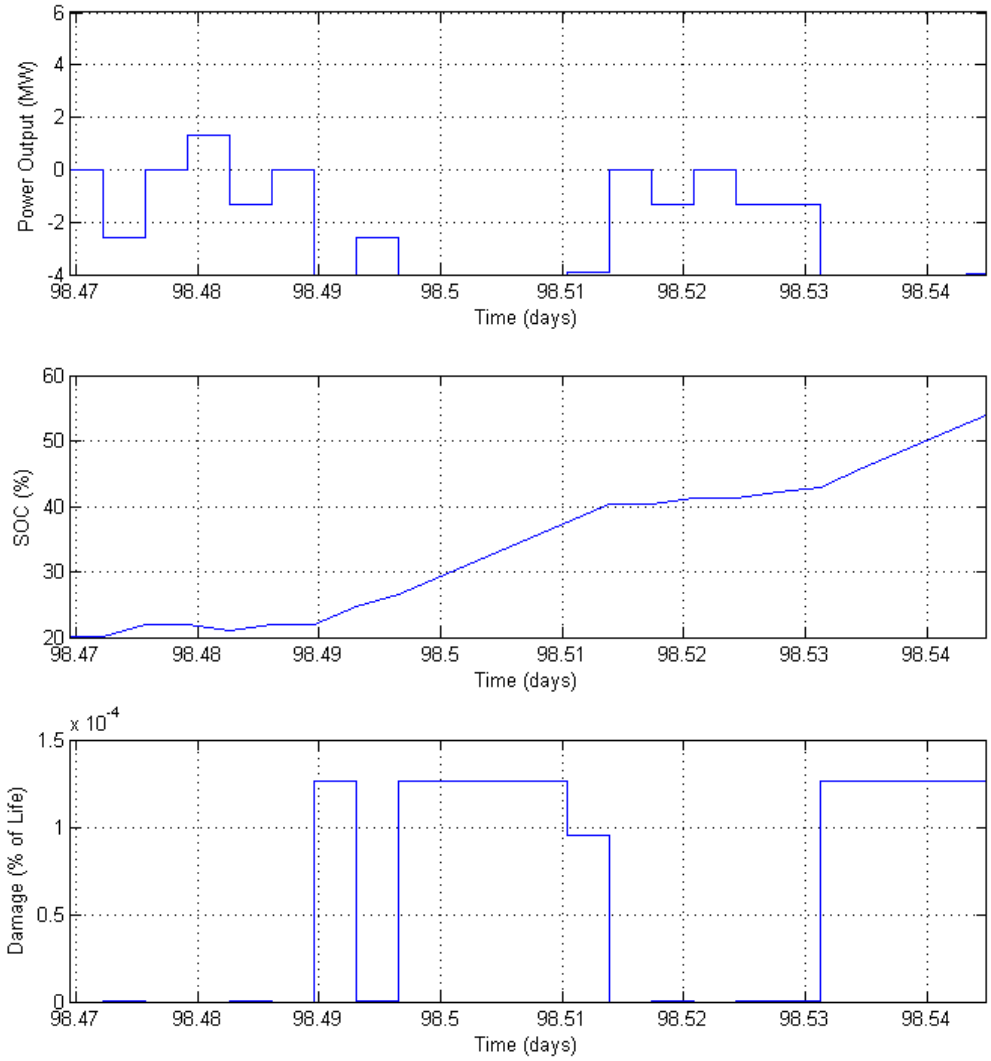

Fig. 4.8. Flow-cell RDI simulation – Three hours

In this figure, notice that relative to the damage that is incurred when the system is charging at 4 MW, the damage at any power less than 2 MW is extremely small. Due to the exponential form of the damage incurrence model, there is an order of magnitude difference between the two cases. This is useful to know when developing the LEC system, as charging power can be limited to reduce damage and cost incurrence.

A long term view of the damage and cost accrued by the flow-cell system over a two year simulation time is given in the following figure.

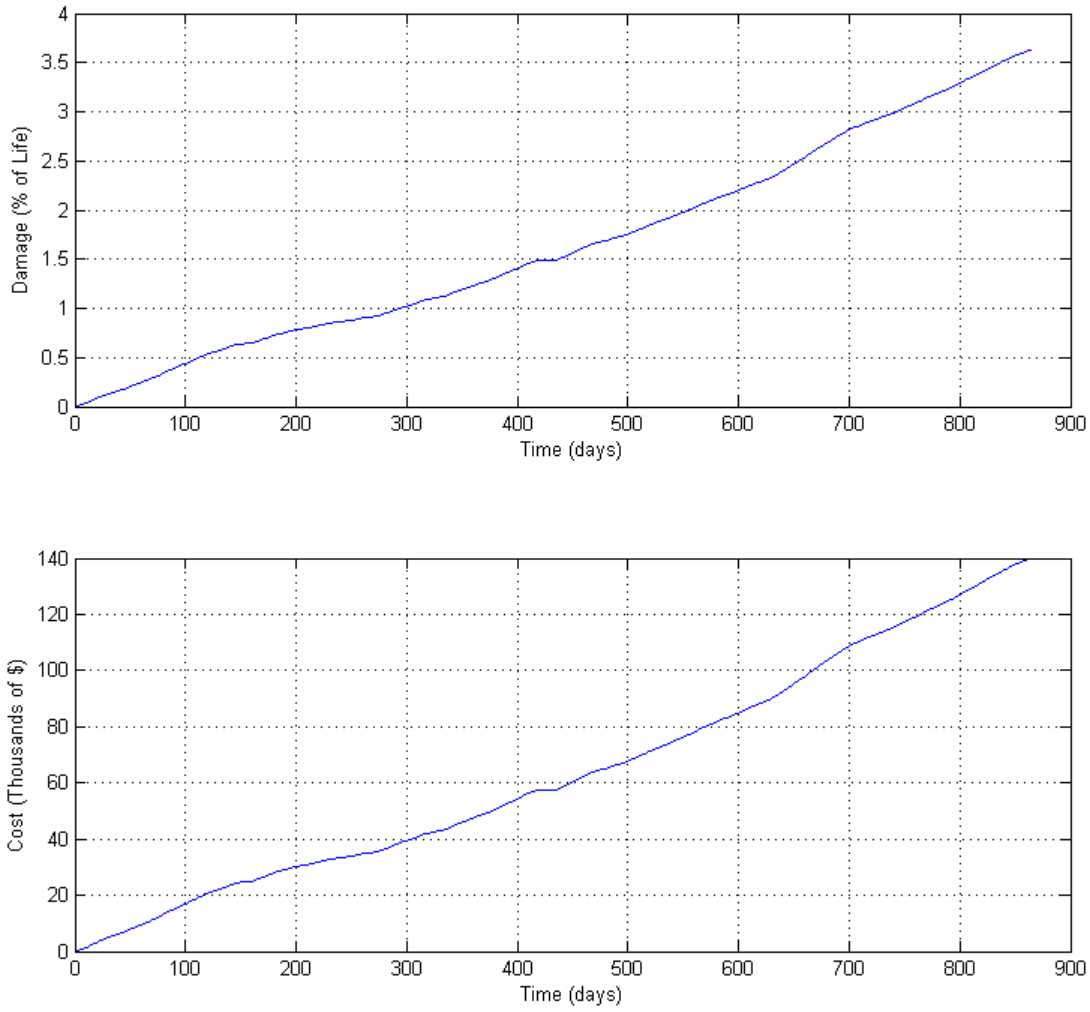

Fig. 4.9. Flow-cell RDI simulation – Extended Simulation

Because of the charging power limit placed on this system, similar to how it would be in actual implementation, the damage and cost accrued by the flow cell battery are much lower than they would be without any limits placed.

4.3 Flywheel RDI Simulation

As described in section 3.3, the damage incurrence model for the flywheel energy storage system was modeled in the following way.

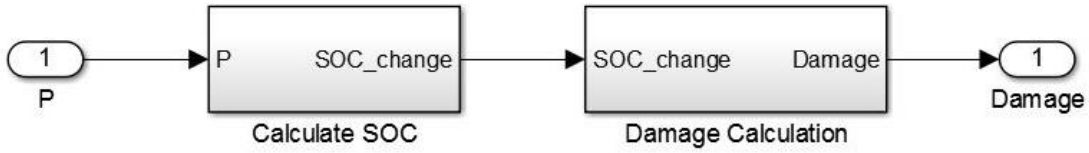

Fig. 4.10. Flywheel damage incurrence model

It is apparent that the damage incurred by the flywheel system in this model is a function of the change in state of charge, which corresponds to a portion of the system's rated cycle life.

In order to perform a simulation for this system, the same method utilized for the flow-cell battery RDI simulation is used here. The change in power data used for the LEC system is scaled and used as an input to the flywheel storage system. The rating for the flywheel storage system in this simulation is 2 MW, so the power output was limited between 2 MW charging and 2 MW discharging.

Fig. 4.11 below shows the results of this simulation over an approximately two hour time frame. Note that the damage incurred is a direct result of the SOC, and therefore of power output as well. The damage curve is shifted due to the method of calculating damage based on change in SOC, which requires that the resulting SOC be determined before damage incurrence is calculated.

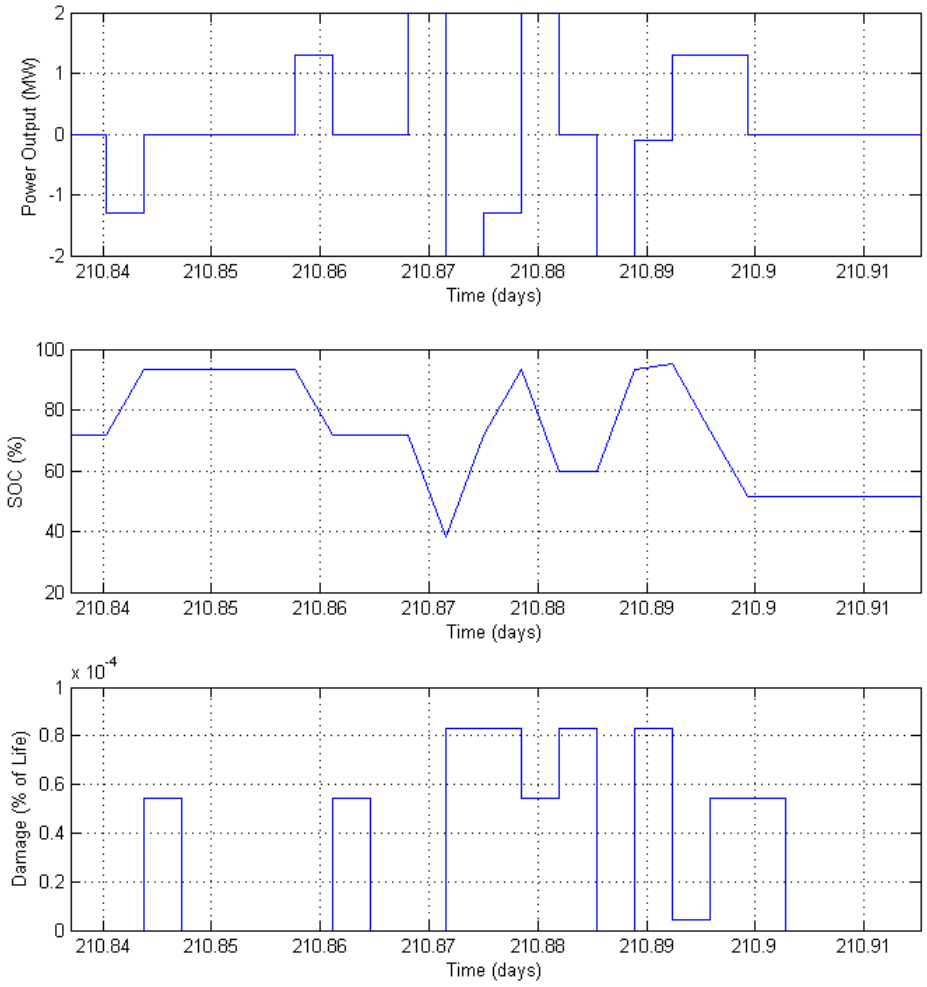

Fig. 4.11. Flywheel RDI Simulation – Two hours

As would be expected, larger power (either charging or discharging) results in a larger amount of damage incurred by the system.

The long term damage and cost accumulation of the flywheel storage system are given in the plots that follow for a simulation spanning over two years.

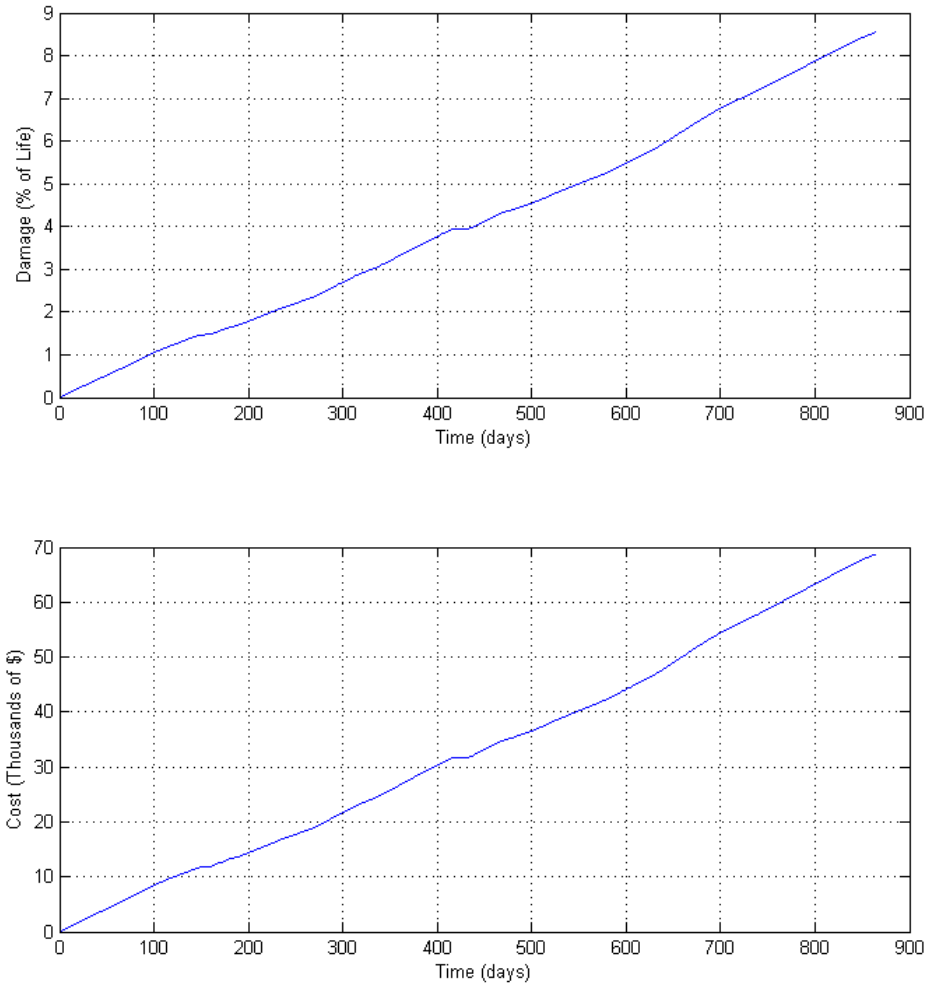

Fig. 4.12. Flywheel RDI Simulation – Two years

Over two years, a trend similar to that of the Zinc/Bromine flow-cell battery system is evident.

5 Development of Life Extending Control (LEC) System

After developing real time damage models for all of the units that are in consideration for the LEC system, this control system may be developed in order to reduce the cost of operation due to wear and tear.

5.1 Introduction to LEC System

In order to understand the principle motivation behind Life Extending Control, consider the following description by Lorenzo and Merrill (1991):

> The fundamental concept of life extending control is to control rates of change and levels of some performance variables to minimize damage (or damage rates) [of] critical components while simultaneously maximizing dynamic performance of the Plant.

This definition of Life Extending Control details the basis for LEC, what it does, and how it operates.

Implementation of LEC for this system may be performed by intelligently adjusting the power output of each component of the overall system (hydroelectric generating units, Zinc/Bromine flow-cell battery, and flywheels) in such a way that meets the required power output of the plant and results in lower cost incurred based upon the wear and tear of the various systems utilized. The overall system being developed may be visualized as is shown in Fig. 5.1. The LEC system receives the power that the overall system is required to generate, and it then allocates each unit (hydroelectric as well as ESS) in such a way to meet the power demand and reduce the amount of damage incurred by each component. The output power from each unit is then added together to generate the output power from the system.

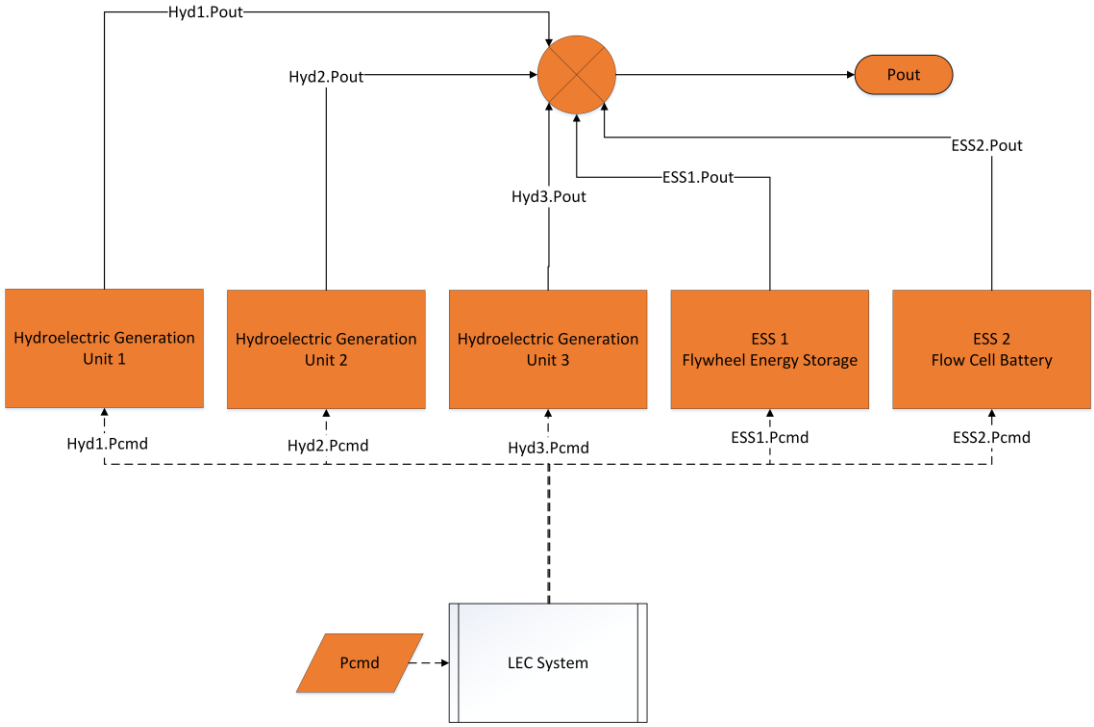

Fig. 5.1. LEC system overview

First, the benefits of such a system will be discussed. The main and most evident benefit of the implementation of a LEC system is a reduction of operating costs due to damage that is incurred by the various components of the system. In this case, the reduction of damage that leads to the largest cost is the greatest concern, but it is also possible to adjust the control to extend the life of specific components that are reaching the end of their projected lifespan through tracking of estimated damage accruement. This may allow a generating unit to operate for a longer time using the currently operating components, allowing time for other units to be brought back online or for replacement parts to be acquired.

In addition, by shifting some of the accrued damage away from the actual hydropower generating units themselves and instead to energy storage systems, it is possible that the repair frequency for the hydroelectric generating units may be decreased as some of the damage that would have been incurred is mitigated by ESS units. What this means is that the main units that provide the significant majority of the capacity of the plant are available for a greater portion of the time. Thus, the capacity of the plant may be closer to the maximum capacity, with all units available for operation, more often.

Also, note that simply by controlling the hydroelectric units in a way to lessen damage accruement can be beneficial from the perspective of extending the life of the various components, even without the addition of energy storage systems. However, with inclusion of energy storage systems the damage incurred by the hydroelectric generating units is further decreased.

The goals of the LEC system are as follows:

1.) Decrease damage to hydroelectric generating units, such that cost of operation due to damage accruement is less than in typical utilization.
2.) Utilize energy storage devices in order to lessen damage on hydroelectric generating units.
3.) Allocate energy storage units such that their cost of damage combined with the hydroelectric unit cost of damage under LEC does not exceed the cost due to damage of the original hydroelectric unit utilization.

There are many different ways to achieve these goals using different types of control systems. Sophisticated control systems that incorporate cost minimization given many operational constraints, and potentially model predictive control, are a potential candidate here. Due to the complexity of these types of control systems combined with the broad focus and short time frame of this research, that type of control system was outside of the scope of this work. The control system that is implemented here is more straightforward and simple in that it is easy to understand the reasons that different control actions are taken in order to reduce cost.

In order to achieve the goals mentioned previously, there were a number of considerations that were made and integrated into the control system. These considerations are detailed in the following section, as well as how they were integrated into the control system.

5.2 LEC System Development

In order to meet the goals of the life extending control system to both reduce damage and the cost due to damage, utilization of ESS units was limited such that the cost of damage accruement by these devices meets goal (3). They are still controlled such that they significantly assist in the reduction of damage accruement of hydroelectric generating units, but not utilized to the point of incurring excessive damage.

Based upon the power and energy characteristics of the devices, they are controlled differently. Flow-cells are slightly slower responding, and therefore the change in power was filtered in order to reduce the chances of rapidly alternating

between charging and discharging the system. Due to the damage model for Zinc/Bromine batteries, the charging power is also limited below 60% of rated power. Flywheel energy storage systems are very fast responding and are able to quickly switch between charging and discharging. Because of this, the flywheel system was allowed to change output between charging and discharging rapidly.

ESS units were controlled in such a way that their SOC remained as close to optimum levels as possible, in order to increase availability for charge and discharge. The flow-cell system was kept near 70% SOC because of the limitation in charging power and the flywheel system was kept near 50% SOC.

ESS units were first controlled to reduce the variation in power output demanded by hydroelectric units as much as possible, while considering goal (3) and keeping damage accruement cost reasonably low. However, they were only utilized if the change in power was greater than some threshold, termed the ESS "unit sensitivity." This threshold was enacted to prevent the ESS systems from cycling and incurring damage when the overall power change is relatively insignificant to hydroelectric generating unit damage incurrence.

The remaining power to be supplied, after ESS unit contributions were determined, was essentially divided equally between the hydroelectric units, within certain limits. Hydroelectric generating units were controlled such that they are only operated at power outputs between 50% and 115% of their nameplate values as given. This was found to be typical for unit utilization based on the acquired data, and matches well with the damage modeling for hydroelectric generators.

The steps for the LEC system are detailed as follows:

1. Determine commanded power (P_{cmd}).
2. Calculate change in power commanded ($P_{change} = P_{cmd} - P_{prev}$).
3. Filter the change in power using a simple box filter (P_{change_F}).
4. If $|P_{change\_F}|$ > flow-cell unit sensitivity, allocate flow-cell power (P_{FC}).
    - Flow-cell power should be the absolute minimum of the power constraints set, P_{change}, P_{change_F}, and the maximum possible power based on the flow-cell SOC.
5. Calculate the remaining change in power ($P_{change\_Rem} = P_{change} - P_{FC}$).
6. If $|P_{change\_Rem}|$ > flywheel unit sensitivity, allocate flywheel power (P_{FW}).
    - Flywheel power should be the absolute minimum of the flywheel power constraints set, P_{change_Rem}, and the maximum possible power based on the flywheel SOC.
7. Calculate remaining required power ($P_{rem} = P_{cmd} - P_{FC} - P_{FW}$).
8. Allocate hydroelectric units to cover the remaining power (P_{rem}).
    - The remaining power is divided equally among the hydroelectric units, utilizing the number of units necessary such that each unit remains within operational constraints previously defined.

The LEC system was implemented in MATLAB utilizing the steps listed above in order to meet the aforementioned goals. The overall flow of the LEC system is shown in the flowchart of Fig. 5.2.

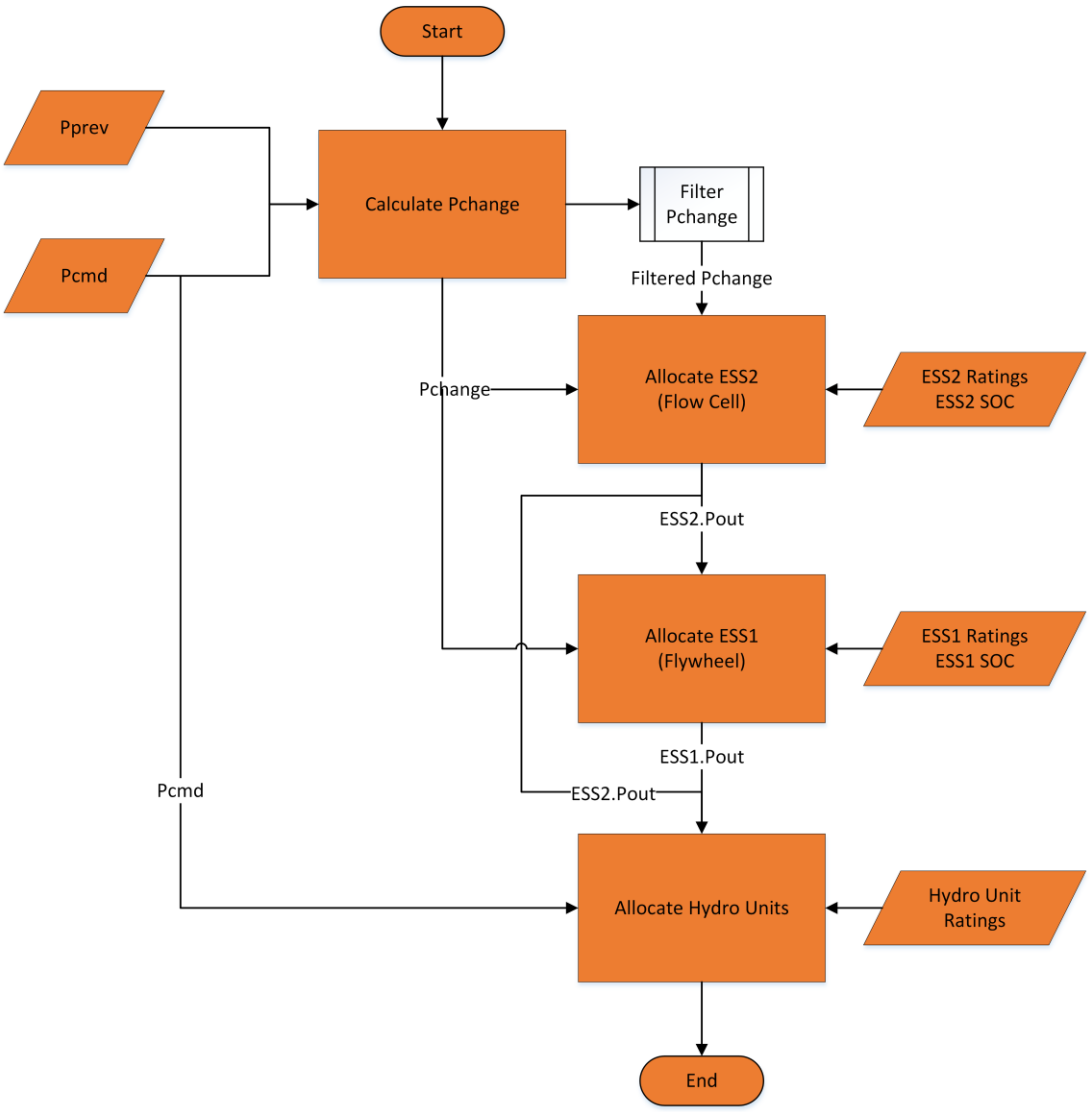

Fig. 5.2. LEC system flowchart

6 Simulation of LEC

In simulating the LEC system that was developed, it is necessary to have numerous system details in place. The number of hydroelectric units, the rating of the units, and original output data for the units must be known. The ratings and replacement costs of the ESS units to be included in the system must also be known. These system configuration parameters are given in the following table:

Table 6.1. LEC system parameters

Number of Hydro Units	3
Rating of Hydro Units	135 MW
Flow-cell Power Rating	6 MW
Flow-cell Energy Rating	12 MWh
Flow-cell Replacement Cost	$4,320,000
Flywheel Power Rating	2 MW
Flywheel Energy Rating	500 kWh
Flywheel Replacement Cost	$1,200,000

The system that is being simulated is a smaller-sized system compared to larger dams in order to see the effects of the LEC system on a smaller and more easily observed system. The ratings for the hydroelectric units are the same as those for the actual units from which the utilization data was acquired. The flow-cell and flywheel energy storage systems were sized large enough that their power outputs would be sufficient to provide some support to the system, but not so large that it would be unreasonable to implement a system like this for hydroelectric dam support based upon physical size of the installation. However, it should be noted that if this type of installation of ESS systems were to be implemented at a large hydroelectric dam with a large capacity, the total ESS power rating would have to be much higher

to provide significant benefit. The physical size of the ESS installations would also be substantially larger, requiring siting at an area near the dam. For the flow-cell battery system, sources give the replacement costs to be approximately 20% of the initial cost (Lex & Jonshagen, 1999), but for this simulation 30% was assumed in order to account for possible underestimation. Similarly, for the flywheel energy storage system the replacement cost has been assumed to be 40% of the installation cost. Installation costs are approximately $1200/kWh installed capacity for flow-cell installations and $1500/kW capacity installed for flywheel installations, per industry contacts.

Combined power output data for three units rated at 135 MW from John Day dam were used as the commanded power input for the LEC system, and this commanded power is shown in Fig. 6.1. Large increases or decreases in generated power are indicative of one or more units going online or offline.

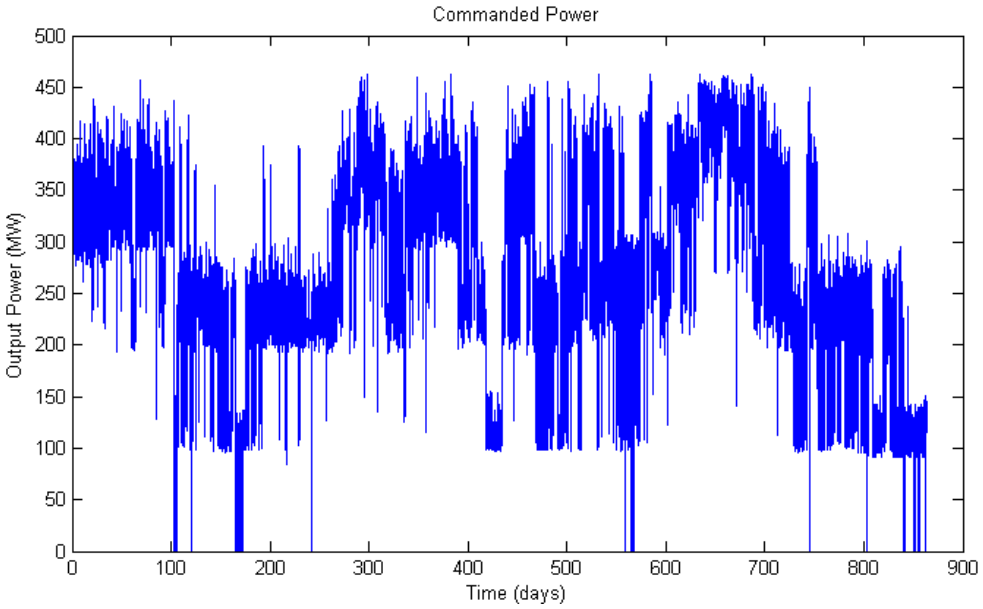

Fig. 6.1. Commanded Power input to LEC system

With this commanded power, the following figure shows the resulting output power from the LEC system as well as the commanded power. Note that because they are exactly equal only the LEC system output plot is visible (as it is directly on top of the commanded power plot). The output of the LEC system was enforced to be exactly equal to the original power output of the units in order to ensure that the LEC system can produce a power output that is the same as typical hydroelectric unit utilization.

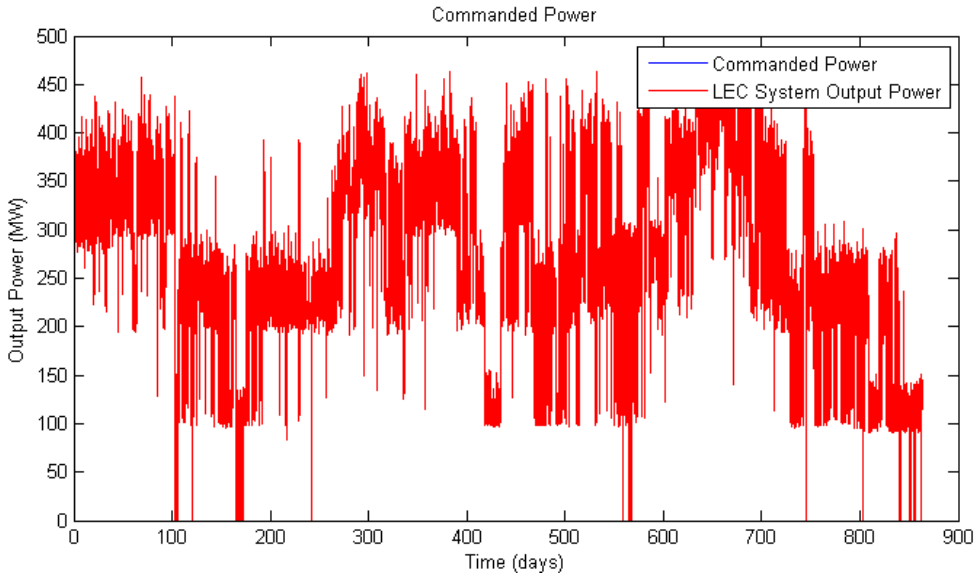

Fig. 6.2. Commanded power compared with LEC delivered power

Because of the length of the simulation, it is much more useful to view unit output data and other system characteristics on a much smaller time frame in order to observe how the LEC system functions. Shown below is a comparison of commanded power with LEC system output power on a time frame of approximately four and a half hours.

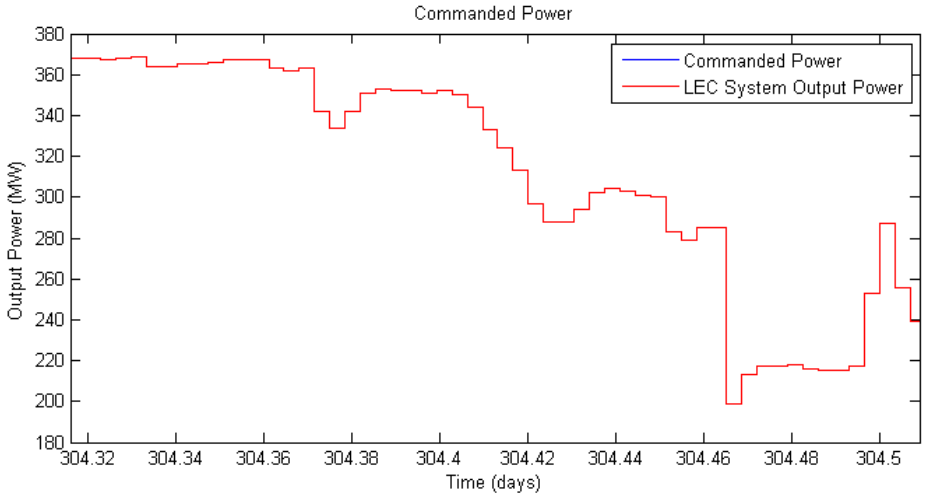

Fig. 6.3. Commanded power compared with LEC system output power – 4.5 Hours

Here it is again evident that the LEC system is indeed generating the correct amount of power, based upon the commanded power.

With this input commanded power, the first thing that the LEC system does is utilize the ESS units in order to reduce the amount of change in power that the hydroelectric generators have to endure. Fig. 6.4 shows the resulting power output that is commanded by each ESS unit over this same time period.

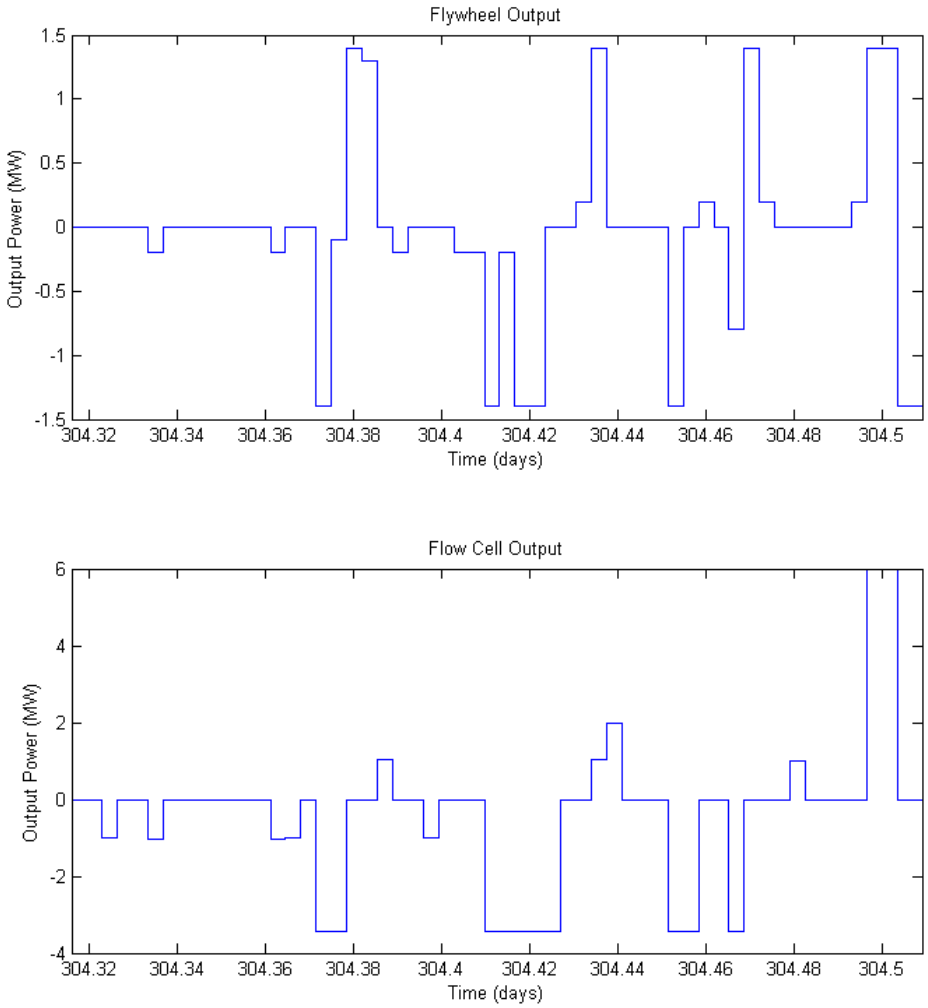

Fig. 6.4. ESS Units power output – 4.5 Hours

Viewing these power output values in relation to the change in power that the system is experiencing is very informative in showing why the ESS units were allocated as they were. Fig. 6.5 shows the change in power of the system, the allocated ESS unit output, and the remaining change in power after ESS unit allocation for each ESS unit at each time step.

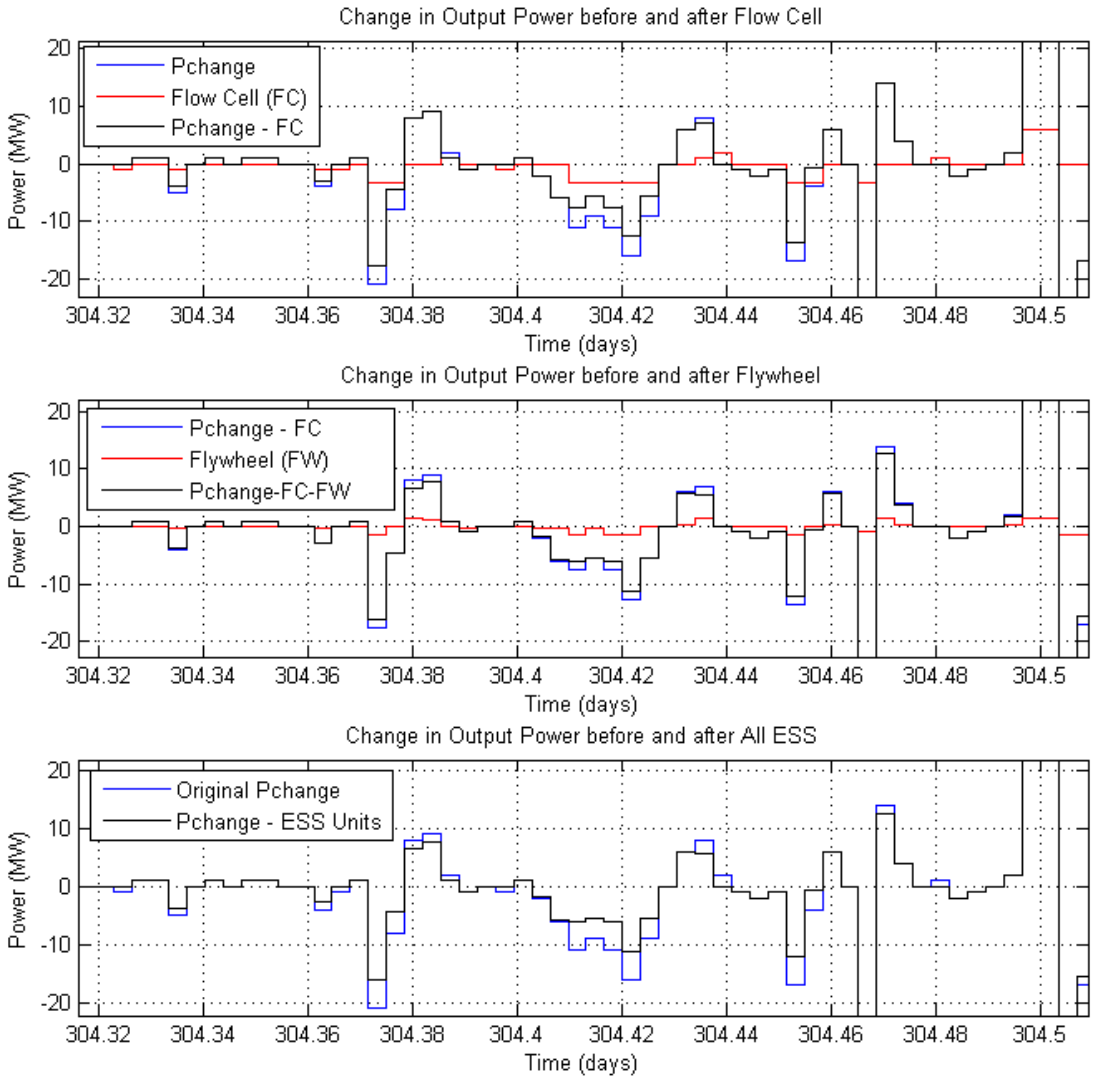

Fig. 6.5. Change in power before and after each ESS unit – 4.5 Hours

Here it is evident that each ESS unit is utilized to help reduce the change in power that the hydroelectric generation units must endure. The last plot in specific shows the effect that the energy storage devices have on the change in power that must be accounted for.

Shown in Fig. 6.6 are the SOC plots for each ESS unit. Note that in the second plot it is evident that the SOC for the flow-cell system was kept near 70% whenever possible, as was designed by the LEC system. While the SOC plot for the flywheel system varies far more rapidly (as the power rating for this storage technology is superior to its energy rating), it is still evident that in general this plot varies around 50% as designed.

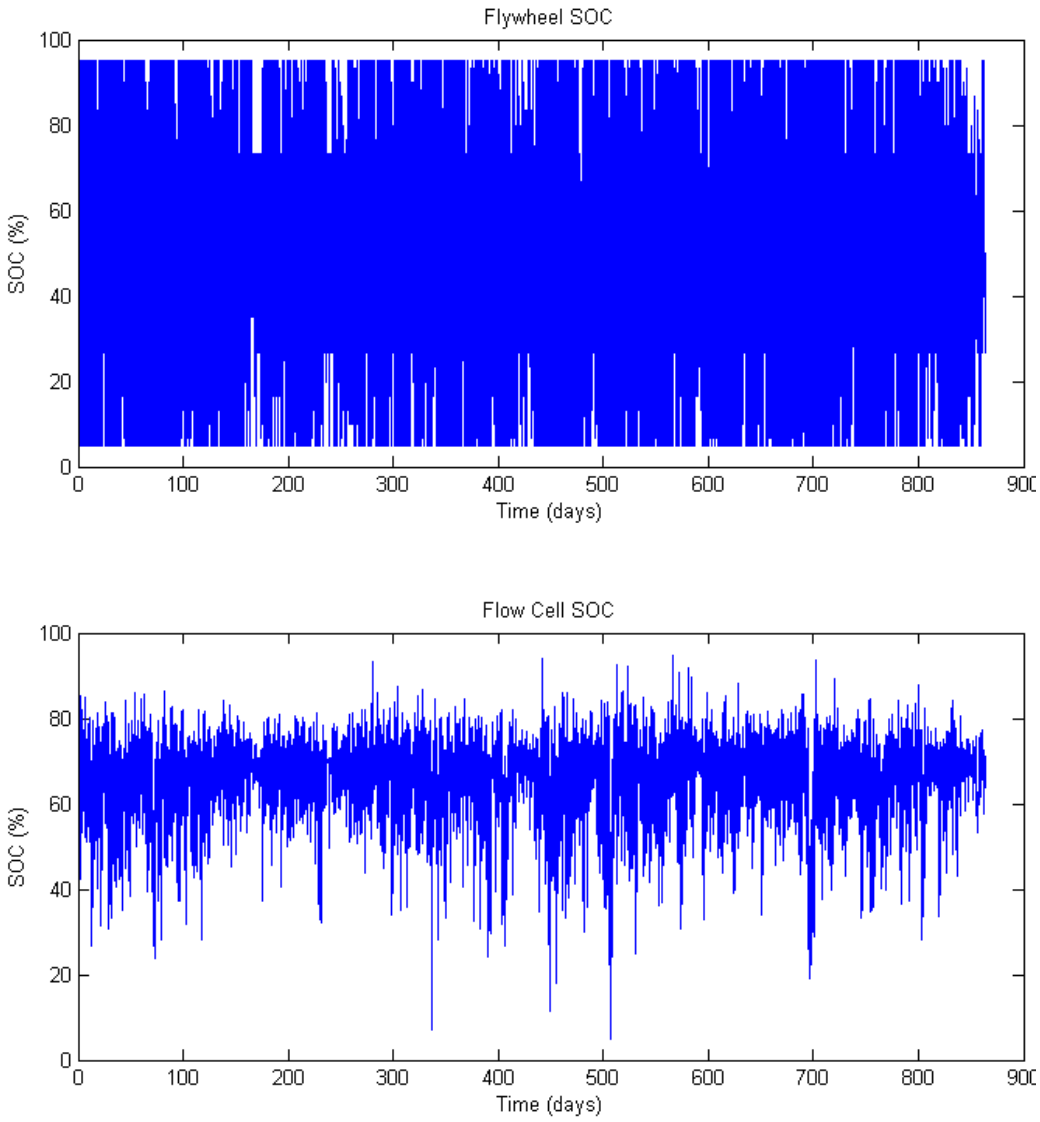

Fig. 6.6. ESS units' state of charge plots under LEC

In Fig. 6.7 it is clear that the remaining commanded power after allocation of ESS units has less variation than the original commanded power, as the hydroelectric units are not required to completely reach the peaks and valleys that they would have originally. The change in overall shape of the figure is not entirely changed, but moment to moment variations have been decreased in many instances. This decrease in variation is what allows for savings in damage accruement over time when compared with original unit utilization.

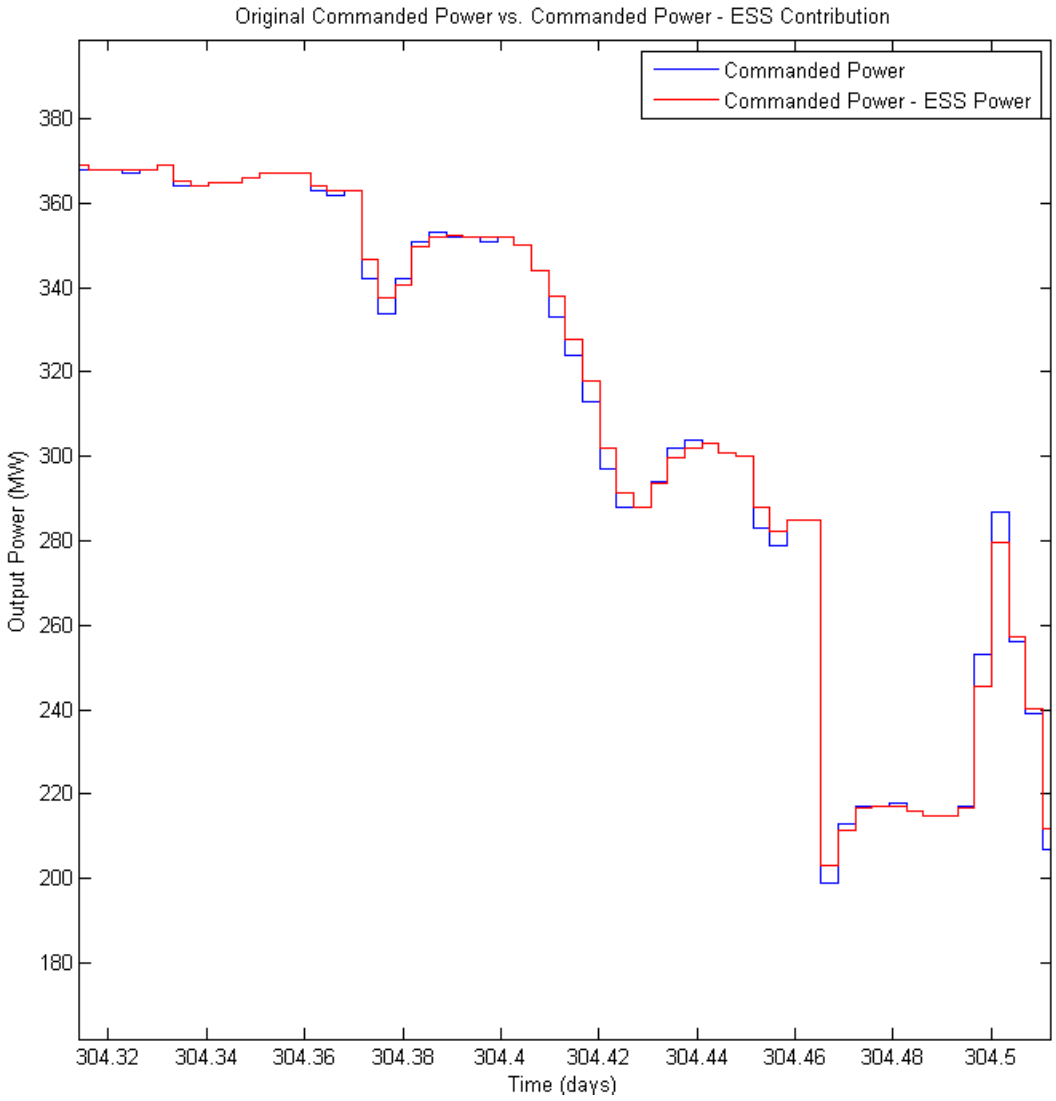

Fig. 6.7. Original commanded power minus ESS contribution – 4.5 Hours

Based upon this simulation, the RDI for each component of the LEC system may be calculated at each time step, as well as the RDI for the original hydroelectric units' utilization without LEC. The resulting costs due to the accrued damages may be accumulated in order to compare the cost due to damage incurrence for the LEC system implementation to the cost based on the original hydroelectric generation units' utilization, as is shown in Fig. 6.8.

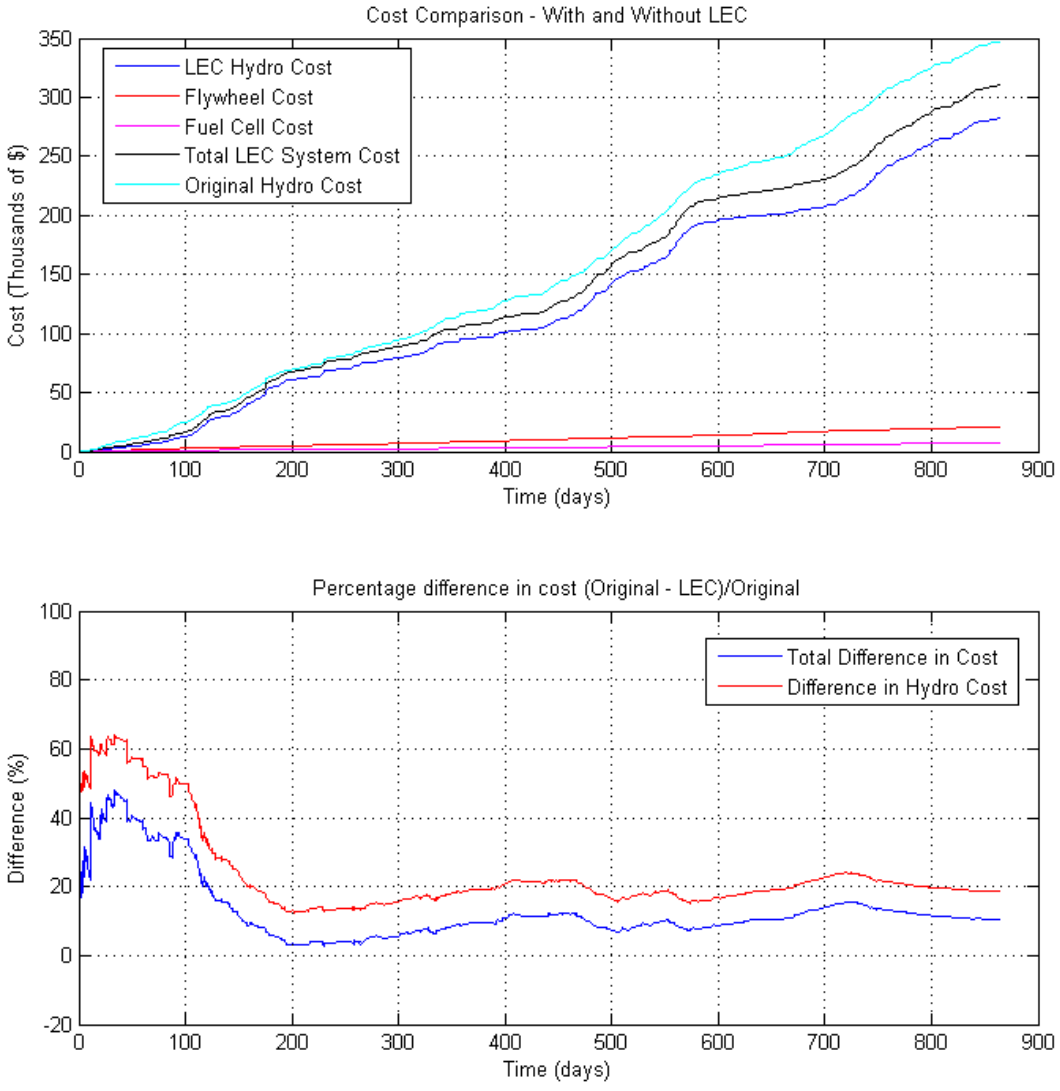

Fig. 6.8. Cost Analysis for LEC system compared to original hydroelectric utilization

The cost comparison in the preceding figure indicates that for the entirety of the simulation, the LEC system resulted in a reduction in the amount of cost that was accrued based upon the damage incurred. The final percentage of cost savings at the end of the simulation was 10.51%, with an 18.53% reduction in hydroelectric generation unit damage cost. These are very promising results, as there are cost savings even with incorporation of ESS RDI costs. The reason for the reduction in hydroelectric damage cost is that the LEC system, by reducing the amount of change in output that the hydroelectric units must experience, reduces the damage incurred on these units. The ESS units are also controlled in such a way that the amount of damage that they accrue is reduced, based upon their respective damage models, thus resulting in overall damage cost savings as well.

In order to see the effect that the ESS units have on decreasing the RDI costs of the system, the simulation was run again with ESS units turned off. It was found that there was still a 12.59% reduction in the cost of damage accrued by the hydroelectric units even without integration of ESS units, which matches with previous conjectures in Chapter 5. This is another promising result which indicates that solely by controlling the hydroelectric generation units in such a way to limit damage incurrence, savings in damage cost may be realized. The reduction in damage is, however, markedly less than in the case with ESS utilization.

Upon determining these results, it was of interest to determine what amount of cost reduction in ESS technologies would cause the total cost savings for LEC with ESS and without ESS to be the same. It was found that with a 26% reduction in ESS costs (through reduction in installation and/or replacement/repair costs), total

cost savings with and without ESS are essentially the same. This is the point at which the implementation of energy storage results in significant enough savings in hydroelectric RDI cost that the savings make up for the cost of the energy storage units. These results are given in Table 6.2. The cost reduction values vary over time, as depending upon conditions there may be larger or smaller cost savings at each instant (see Fig. 6.8). Because of this, the maximum and minimum values of total damage cost reduction and hydroelectric damage cost reduction over the simulation time, after stabilization at ~150 days, is given in Table 6.2 as well.

Table 6.2. LEC simulation cost reduction analysis

	LEC w/ESS - Original Cost	LEC w/o ESS	LEC w/ESS - 26% Less Cost
Final Cost Reduction - Total	10.51%	12.59%	12.60%
Final Cost Reduction - Hydro Damage	18.53%	12.59%	18.53%
Minimum Total Cost Reduction	2.77%	6.00%	5.33%
Maximum Total Cost Reduction	15.68%	18.11%	17.91%
Minimum Hydro Cost Reduction	12.52%	6.00%	12.52%
Maximum Hydro Cost Reduction	24.24%	18.11%	24.24%

Note also that even if the total final cost reduction is 0% (meaning that the total cost of damage incurred is the same, with and without LEC), as long as there is a savings in hydroelectric damage it means that damage was diverted from hydroelectric generating units to the ESS units. This is the result that was discussed earlier in Chapter 5 of having potentially increased availability of all hydroelectric units without adding to the overall damage incurrence cost.

6.1 Discussion

The results of the LEC simulation indicate that there are benefits to be gained from life extending control of hydroelectric generation units in conjunction with ESS units. How significant these benefits are depends upon the system in question, the initial variability of the system, the actual costs of all of the system components, and how the system is controlled. As was discussed previously, far more sophisticated control systems may be developed for this purpose. However, even with this initial and relatively simple control scheme there were significant cost savings compared to the original hydroelectric unit utilization.

It is important to note also that all costs considered for this work were replacement/repair costs at the end of life for each unit and/or subcomponent. This means that the initial installation costs for the ESS units are not directly accounted for in this analysis. Certainly, it would take a period of time for the savings in damage accruement to match the initial investment. This is more detailed financial analysis than is within the scope of this work however, as the goal of this research was to determine if such a system would have an impact and would result in cost savings over the long term.

7 Conclusion

This work has researched the relationship between wind power and hydroelectric power generation and developed real time damage models for hydroelectric generation units as well as multiple energy storage technologies. A life extending control system was also developed to reduce the amount of damage and cost due to damage that is accrued by hydroelectric generation units.

Results from the analysis of the relationship between wind power and hydroelectric power generation indicate that wind power is having an impact on hydroelectric generation of varying severity. Some dams show a markedly higher correlation than others based upon multiple methods of analysis. This implies that further increases in wind power penetration will continue to increase this impact, leading to a more significant need for additional methods of balancing wind power to ensure grid stability.

Real-time Damage Incurrence models have been developed for hydroelectric generation units at the component level, and for Zinc/Bromine flow-cell batteries as well as flywheel energy storage devices. Based upon different limitations in the available data for each, the damage models were developed accordingly. These damage models serve to give an indication of the damaging effects that different operational characteristics have on the various components, as well the total cost due to these actions. This type of modeling can be useful when implementing a control system to reduce the amount of damage that different systems incur.

The life extending control system that was developed indicates the possibility of decreasing the amount of damage incurrence that the various components of a hydroelectric generation unit experience. This is done through LEC of the hydroelectric units as well as ESS units. The results of the simulation of this system show that there may be benefit to be gained from such a system being implemented, just from the perspective of the cost of damage accruement. This does not consider the additional benefits that energy storage integration can have on the power system, including increased reserve capacity and improved reliability.

It is important to note again that these savings are based upon repair/replacement costs of the ESS units, which are the recurring costs after installation. Installation costs have not been included in this analysis. Because of this, it will certainly take time for the realized cost savings due to reduced damage incurrence to make up for the installation cost of the ESS units. For large hydroelectric dams, the physical size of ESS installations, with ratings that would be of significance to the LEC system, would generally be too large to be located on site at hydroelectric dams. This is an issue that may be overcome by siting the installations near hydroelectric dams or by simply by using remote installations of ESS units for balancing purposes. Future developments in ESS technologies may also alleviate this concern.

7.1 Future Work

Future work that may build upon or branch off of this research includes further analysis of the relationship between wind power and hydroelectric generation, more detailed determination of RDI models for hydroelectric components and ESS technologies, and more sophisticated control for the LEC system. This breadth of subject matter clearly covers many different areas of work within electrical engineering as well as many other disciplines.

Further investigating the relationship between wind and hydroelectric generation would entail a detailed correlation study that looks into all possible relationships between the two generation sources. This area of research could be very productive with advanced analysis on larger and higher resolution data sets. There may be many relationships that are in action that are difficult to detect without the right data. Specifically, the possibility of a regional relationship between wind generation and hydroelectric generation is one that could be investigated with wind and hydroelectric generation data from various projects. Analysis of the effect that the variability of wind power has on hydroelectric generation, as well as on grid stability, is a very important area of research. As penetration of renewable resources (especially wind and solar) increases, it is necessary to understand the effect that it will have on the grid in order to ensure dependability.

More detailed determination of RDI models for hydroelectric unit components and ESS technologies would also be extremely valuable in this area of research. These models may be derived from detailed mechanical and electrical operation data and analysis or by utilizing very thorough maintenance records. One

challenge with the use of maintenance records is the fact that, generally, a large portion of maintenance activities are scheduled, rather than based on necessity due to the condition of the component. This makes it difficult to determine damage incurrence based upon maintenance records.

A LEC system could be developed that is more sophisticated and better at potentially minimizing damage incurrence as well. This could be through the use of cost minimization techniques, model predictive control, or other similar methods. Other techniques may also be added to the LEC system to add further functionality as well. This may include monitoring of damage accruement and optimization of unit control based upon the amount of damage accrued by individual components of each unit. Hydroelectric generation units could then be controlled such that their operational lifespan is increased by specifically focusing on extending the life of key components that are reaching the end of their estimated life.

Bibliography

About hydropower generation. (2013). US Army Corps of Engineers - Portland District. Retrieved from http://www.nwp.usace.army.mil/HDC.aspx

Atwa, Y. M., El-Saadany, E. F., Salama, M. M. A., & Seethapathy, R. (2010). Optimal Renewable Resources Mix for Distribution System Energy Loss Minimization. *IEEE Transactions on Power Systems*, *25*(1), 360–370. doi:10.1109/TPWRS.2009.2030276

Bistrika, A. (2013, March 27). *Degradation of Graphite Electrodes in Acidic Bromine Electrolytes*. Oregon State University.

Bolund, B., Bernhoff, H., & Leijon, M. (2007). Flywheel energy and power storage systems. *Renewable and Sustainable Energy Reviews*, *11*(2), 235–258. doi:10.1016/j.rser.2005.01.004

BPA Balancing Authority Total Wind Generation, Near-Real-Time. (2013, May 29). BPA. Retrieved from http://transmission.bpa.gov/Business/Operations/Wind/twndbspt.aspx

FACT SHEET - Frequency Regulation and Flywheels. (2013). Beacon Power, LLC. Retrieved from http://www.beaconpower.com/files/Flywheel_FR-Fact-Sheet.pdf

Faries, R. (2012). Zinc-Bromine Flow Battery Technology for Energy Security. *RAYTHEON Technology Today*, (1), 35.

Flywheel Energy Storage System. (2013). Beacon Power, LLC. Retrieved from http://www.beaconpower.com/files/FESS_Tech_Data_Sheet.pdf

Halamay, D. A., Brekken, T. K. A., Simmons, A., & McArthur, S. (2011). Reserve Requirement Impacts of Large-Scale Integration of Wind, Solar, and Ocean Wave Power Generation. *IEEE Transactions on Sustainable Energy*, *2*(3), 321–328. doi:10.1109/TSTE.2011.2114902

Harano, M., Tani, K., & Nomoto, S. (2006). Practical Application of High-performance Francis-turbine Runner Fitted with Splitter Blades at Ontake and Shinkurobegawa No. 3 Power Stations of THE KANSAI ELECTRIC POWER CO., INC.

Höök, M., & Tang, X. (2013). Depletion of fossil fuels and anthropogenic climate change—A review. *Energy Policy*, *52*, 797–809. doi:10.1016/j.enpol.2012.10.046

Judkins, R. R., Fulkerson, W., & Sanghvi, M. K. (1993). The dilemma of fossil fuel use and global climate change. *Energy & Fuels*, *7*(1), 14–22. doi:10.1021/ef00037a004

Kariya, T., & Kurata, H. (2004). *Generalized Least Squares*. John Wiley & Sons.

Kasabov, N. K. (1996). *Foundations of Neural Networks, Fuzzy Systems and Knowledge Engineering*. Marcel Alencar.

Lex, P., & Jonshagen, B. (1999). The zinc/bromine battery system for utility and remote area applications. *Power Engineering Journal*, *13*(3), 142–148. doi:10.1049/pe:19990307

Lorenzo, C. F., & Merrill, W. C. (1991). Life Extending Control - A Concept Paper. In *American Control Conference, 1991* (pp. 1081–1095). Presented at the American Control Conference, 1991.

Maggio, G., & Cacciola, G. (2012). When will oil, natural gas, and coal peak? *Fuel*, *98*, 111–123. doi:10.1016/j.fuel.2012.03.021

Saade, J. J., & Diab, H. B. (2000). Defuzzification techniques for fuzzy controllers. *IEEE Transactions on Systems, Man, and Cybernetics, Part B: Cybernetics*, *30*(1), 223–229. doi:10.1109/3477.826965

Shieh, G. (2010). Estimation of the simple correlation coefficient. *Behavior Research Methods*, *42*(4), 906–917. doi:10.3758/BRM.42.4.906

U.S. Energy Information Administration. (2013). *Electric Power Annual - With Data for 2011*. Retrieved from http://www.eia.gov/electricity/annual/

Wind Generation Capacity in the BPA Balancing Authority Area. (2013, April 10). BPA. Retrieved from http://transmission.bpa.gov/business/operations/Wind/WIND_InstalledCapacity_PLOT.pdf

Zhao, K., Ling, F., Lev-Ari, H., & Proakis, J. G. (1994). Sliding window order-recursive least-squares algorithms. *IEEE Transactions on Signal Processing*, *42*(8), 1961–1972. doi:10.1109/78.301835

Appendices

Appendix 1: Correlation Analysis Code

```
%% Setup for Correlation Calculations
% Housekeeping
clc
clear

%Load all necessary data
load('rawWindData-Dates.mat')
load('BPA_TotalWindGen_Data.mat')
load('NameplateAnalysis.mat')

%Fix Wind Data (Remove NAN data and replace with mean of
%   surrounding values)
for j = 1:size(BPA_TotalWindGen_Data,2)
    nans = find(isnan(BPA_TotalWindGen_Data(:,j)));
    for i=1:length(nans)
        BPA_TotalWindGen_Data(nans(i),j) = mean([...
            BPA_TotalWindGen_Data(nans(i)-1,j) ...
            BPA_TotalWindGen_Data(nans(i)+1,j)]);
    end
end

%References
fcst = 2; gen = 3; err = 8; ld = 4; intchange = 7;
therm = 6; hydro = 5;
names = {'TDALLES','LWRGRAN','MCNARY','LWRMON','LILGOOS',...
    'JD','ICEHAR','GRANDC','CHIEF','BONNE'};

%Initialize all correlation matrices
DamWindGen = []; DamWindGenDiff=[]; DamWindErr=[];
DamWindErrDiff = []; DamLoad = []; DamDiffWindGen = [];
DamDiffWindGenDiff = [];  DamDiffWindErr = [];
DamDiffWindErrDiff=[]; DamDiffLoad=[];UnitWindGen = [];
UnitWindGenDiff=[]; UnitWindErr=[]; UnitWindErrDiff = [];
UnitLoad = [];UnitDiffWindGen = []; UnitDiffWindGenDiff = [];
UnitDiffWindErr = []; UnitDiffWindErrDiff=[]; UnitDiffLoad=[];
DamAdjWindGen=[]; DamAdjWindGenDiff=[]; DamAdjWindErr=[];
DamAdjWindErrDiff=[];UnitAdjWindGen=[]; UnitAdjWindGenDiff=[];
UnitAdjWindErr=[]; UnitAdjWindErrDiff=[];xCorrsDamWindGen = [];
DamRes = []; UnitRes=[]; xCorrsDamWindGenLags =[];
DamWindErrLAG = []; damLags = []; DamWindGenLAG = [];
damLagsG = []; damLagsE = [];unit = {}; ind =0;

%% Calculate Correlations for Each Dam, cycle through dams
for k = 1:length(names)
    %Import Appropriate Dam Data
    damData = importdata(strcat('BPA_',names{1,k},...
        '_Data.mat'));

    %Fix Dam Data (remove NAN's if necessary)
```

```
for j=1:size(damData,2)
    nans = find(isnan(damData(:,j)));
    for i=1:length(nans)
        damData(nans(i),j) = damData(nans(i)-1,j);
    end
end

%Total Generation of Dam
damTotal=sum(damData,2);

% Calculate Correlations at the Dam Level
a = corrcoef([damTotal BPA_TotalWindGen_Data(:,gen)]);
DamWindGen = [DamWindGen ; a(1,2)];

a = corrcoef([damTotal(2:end) ...
    diff(BPA_TotalWindGen_Data(:,gen))]);
DamWindGenDiff = [DamWindGenDiff ; a(1,2)];

a = corrcoef([damTotal BPA_TotalWindGen_Data(:,err)]);
DamWindErr = [DamWindErr ; a(1,2)];

a = corrcoef([damTotal(2:end) ...
    diff(BPA_TotalWindGen_Data(:,err))]);
DamWindErrDiff = [DamWindErrDiff ; a(1,2)];

a = corrcoef([diff(damTotal) ...
    BPA_TotalWindGen_Data(2:end,gen)]);
DamDiffWindGen = [DamDiffWindGen ; a(1,2)];

a = corrcoef([diff(damTotal) ...
    diff(BPA_TotalWindGen_Data(:,gen))]);
DamDiffWindGenDiff = [DamDiffWindGenDiff ; a(1,2)];

a = corrcoef([diff(damTotal) ...
    BPA_TotalWindGen_Data(2:end,err)]);
DamDiffWindErr = [DamDiffWindErr ; a(1,2)];

a = corrcoef([diff(damTotal) ...
    diff(BPA_TotalWindGen_Data(:,err))]);
DamDiffWindErrDiff = [DamDiffWindErrDiff ; a(1,2)];

%% Calculate Correlations for Each Unit of Each Dam
for l=1:size(damData,2)
    %Identify the unit (for writing to Excel Sheet)
    ind = ind+1;
    unit{ind,1} = strcat(names{1,k},[' ' num2str(l)]);

    % Calculate Correlations at the Unit Level
    a = corrcoef([damData(:,l) ...
        BPA_TotalWindGen_Data(:,gen)]);
    UnitWindGen = [UnitWindGen ; a(1,2)];
```

```
        a = corrcoef([damData(2:end,l) ...
            diff(BPA_TotalWindGen_Data(:,gen))]);
        UnitWindGenDiff = [UnitWindGenDiff ; a(1,2)];

        a = corrcoef([damData(:,l) ...
            BPA_TotalWindGen_Data(:,err)]);
        UnitWindErr = [UnitWindErr ; a(1,2)];

        a = corrcoef([damData(2:end,l) ...
            diff(BPA_TotalWindGen_Data(:,err))]);
        UnitWindErrDiff = [UnitWindErrDiff ; a(1,2)];

        a = corrcoef([diff(damData(:,l)) ...
            BPA_TotalWindGen_Data(2:end,gen)]);
        UnitDiffWindGen = [UnitDiffWindGen ; a(1,2)];

        a = corrcoef([diff(damData(:,l)) ...
            diff(BPA_TotalWindGen_Data(:,gen))]);
        UnitDiffWindGenDiff = [UnitDiffWindGenDiff ; a(1,2)];

        a = corrcoef([diff(damData(:,l)) ...
            BPA_TotalWindGen_Data(2:end,err)]);
        UnitDiffWindErr = [UnitDiffWindErr ; a(1,2)];

        a = corrcoef([diff(damData(:,l)) ...
            diff(BPA_TotalWindGen_Data(:,err))]);
        UnitDiffWindErrDiff = [UnitDiffWindErrDiff ; a(1,2)];
    end
end

%% PRINT OUTPUT TO .csv FILES
fid = fopen('DamCorrelations.csv','w');
titles = {'Dam Name' 'DamWindGen' 'DamWindGenDiff' ...
    'DamWindErr' 'DamWindErrDiff' 'DamDiffWindGen' ...
    'DamDiffWindGenDiff'...
    'DamDiffWindErr' 'DamDiffWindErrDiff'};
fprintf(fid,'%s ,',titles{:});
fprintf(fid,'\n');

for i = 1:length(names)
    fprintf(fid,'%s, %7.5f, %7.5f, %7.5f, %7.5f, %7.5f, %7.5f,
%7.5f, %7.5f\n',...
        names{1,i},DamWindGen(i),DamWindGenDiff(i),...
        DamWindErr(i),DamWindErrDiff(i),DamDiffWindGen(i),...
        DamDiffWindGenDiff(i),DamDiffWindErr(i),...
        DamDiffWindErrDiff(i));
end
fclose(fid);

fid = fopen('UnitCorrelations.csv','w');
titles = {'Unit' 'UnitWindGen' 'UnitWindGenDiff'...
    'UnitWindErr' 'UnitWindErrDiff' 'UnitDiffWindGen' ...
    'UnitDiffWindGenDiff','UnitDiffWindErr' ...
```

```
    'UnitDiffWindErrDiff'};
fprintf(fid,'%s ,',titles{:});
fprintf(fid,'\n');

for i = 1:length(unit)
    fprintf(fid,'%s, %7.5f, %7.5f, %7.5f, %7.5f, %7.5f, %7.5f,
%7.5f, %7.5f\n',...
        unit{i,1},UnitWindGen(i),UnitWindGenDiff(i),...
        UnitWindErr(i),UnitWindErrDiff(i),UnitDiffWindGen(i)...
        ,UnitDiffWindGenDiff(i),UnitDiffWindErr(i),...
        UnitDiffWindErrDiff(i));
end
fclose(fid);
```

Appendix 2: Linear Least Squares Analysis Code

```
%% Setup for Least Squares Analysis
%Housekeeping
clc
clear

% Import Relevant Data
WindData = importdata('BPA_TotalWindGen_Data.mat');
AllHydro = importdata('BPA_Total_All_Hydro.mat');
load('NameplateAnalysis.mat')
fcst = 2; gen = 3; err = 8; loadD = 4; intchange = 7;
therm = 6; hydro = 5;

% Determine maximum values of each parameter for
%calculation of LS Coefficients
maxfcst = max(WindData(:,fcst));
maxtherm = max(WindData(:,therm));
maxgen = max(WindData(:,gen));
maxerr = max(WindData(:,err));
maxloadD = max(WindData(:,loadD));
maxintchange = max(WindData(:,intchange));
maxhydro = max(WindData(:,hydro));
maxAllHydro = max(AllHydro);

%% Perfrorm LS Analysis for Each Dam's Output
%(Using Sliding Window Method)
% FOR EACH DAM
% n -> Number of data samples
% m -> Number of model Parameters (ie,  C1T, C1W, ...)
%(C1T = Coefficient for Hydro 1 Thermal,etc.)

%Basic format: Y = H*Param. where H is a matrix n*m
%and Param. is a column
%vector of the parameteres
%The LS Estimation of the Parameters is then found by:
%Param_est = pinv(H'*H)*H'*Y.

windowSamples = 1*24*12;    %Sliding window of 1 day
winSampIndx = windowSamples-1;

names = {'TDALLES','LWRGRAN','MCNARY','LWRMON','LILGOOS'...
    ,'JD','ICEHAR','GRANDC','CHIEF','BONNE'};
for k = 1:length(names)
    damData = importdata(strcat('BPA_',names{1,k},...
        '_Data.mat'));
    damDataTotal = sum(damData,2);
    DamParameters.(names{k}).LSvalues = zeros(5,...
        (length(AllHydro)-windowSamples));
    for i = 1:length(WindData)-windowSamples
        Y = damDataTotal(i:i+winSampIndx)./Nameplate{2,k};
```

```
        H = [WindData(i:i+winSampIndx,therm)./maxtherm ...
            WindData(i:i+winSampIndx,fcst)./maxfcst...
            WindData(i:i+winSampIndx,err)./maxerr  ...
            WindData(i:i+winSampIndx,loadD)./maxloadD...
            WindData(i:i+winSampIndx,intchange)./maxintchange];
        DamParameters.(names{k}).LSvalues(:,i) =(H'*H)\H'*Y;
    end
end

%% Plot Dam Parameters
close all
meanFcoeff = []; meanEcoeff =[]; meanLcoeff=[];
meanTcoeff=[]; stdFcoeff =[]; stdEcoeff=[];  stdTcoeff =[];
stdLcoeff=[];
for k = 1:length(names)
    parameters = DamParameters.(names{k}).LSvalues;

    %Determine mean and variation parameters for each
    ForecastKs = parameters(2,:);
    ErrorKs = parameters(3,:);
    ForecastKs = ForecastKs(abs(ForecastKs)<0.8);
    ErrorKs = ErrorKs(abs(ErrorKs)<0.8);
    meanFcoeff = [meanFcoeff mean(ForecastKs)];
    meanEcoeff = [meanEcoeff mean(ErrorKs)];
    stdFcoeff = [stdFcoeff std(parameters(2,:))];
    stdEcoeff = [stdEcoeff std(parameters(3,:))];

    % Plot Histogram of Forecast and Error Coefficients
    figure('Name',names{k},'units','normalized',...
        'outerposition',[0 0 1/2 1])
    subplot(2,1,1)
    hist(parameters(2,[1:1.21e5]),[ min(parameters(2,...
        [1:1.21e5])) :.003: max(parameters(2,[1:1.21e5]))])
    title([names{k} ' Histogram Of FORECAST Coefficient'])
    xlabel('Parameter Value')
    xlim([-1 .3]);
    hold on
    grid on
    ylabel('Occurrences')

    subplot(2,1,2)
    hist(parameters(3,[1:1.21e5]),[ min(parameters(3,...
        [1:1.21e5])) : .003 : max(parameters(3,[1:1.21e5]))])
    title([names{k} ' Histogram Of ERROR Coefficient'])
    xlabel('Parameter Value')
    xlim([-1 .3]);
    ylabel('Occurrences ')
    grid on
end
```

```
% Plot All Average Parameter values
figure
x = 1:10;
labels = names;
Ferr = 1.96*stdFcoeff/sqrt(length(parameters));
Eerr = 1.96*stdEcoeff/sqrt(length(parameters));
plotVars = [meanFcoeff' meanEcoeff' Ferr' Eerr'];
[sPlotVars ind] = sortrows(plotVars,2);

labels = labels(ind);
errorbar(x, sPlotVars(:,1), sPlotVars(:,3),'*')
set(gca, 'XTick', 1:10, 'XTickLabel', labels);
hold on;
errorbar(x,sPlotVars(:,2),sPlotVars(:,4),'*r')
grid on
hold on
x = 0:.0001:20;
plot(x,0*x)
xlim([0 11]);
title('Mean Wind Forecast and Wind Error Parameters for Least
Squares Estimation by Dam')
xlabel('Dam')
ylabel('Coefficient Value')
legend({'Forecast Coefficient Values', 'Error Coefficient Values'})
```

Appendix 3: Hydroelectric Unit RDI Simulation Code

```
% Hydro RDI Simulation Code
%% Setup for Simulation
clear
global Dparams

% Read in Damage Coefficients
[DamageDerivations tex raw] = xlsread(...
    'DamageDerivations_allHydro.xls');
K_dmg_smallRamp = DamageDerivations(:,5);
K_dmg_medRamp = DamageDerivations(:,9);
K_dmg_largeRamp = DamageDerivations(:,13);
K_dmg_StartStop = DamageDerivations(:,17);
K_dmg_safePower = DamageDerivations(:,21);
K_dmg_dmgPower = DamageDerivations(:,25);
K_cost = DamageDerivations(:,27);
CompLabels=tex(3:end,1);

Dparams = [K_dmg_smallRamp K_dmg_medRamp ...
    K_dmg_largeRamp K_dmg_StartStop K_dmg_safePower...
    K_dmg_dmgPower K_cost];

%% Load Data for Simulation
dataRead = importdata('BPA_JD_Data.mat');
data = dataRead(:,1)+dataRead(:,2)+dataRead(:,5);
simEnd = round(length(data));
% simEnd = 100000;
data = data(1:simEnd,:);
data = sum(data,2);

% Hydro Unit Data for Each Unit
Hyd1.Act = dataRead(1:simEnd,1)';
Hyd2.Act = dataRead(1:simEnd,2)';
Hyd3.Act = dataRead(1:simEnd,5)';
HydRating = 135;

%% Begin Simulation
D1a = zeros(simEnd,15);
C1 = zeros(simEnd,1);
D2a = zeros(simEnd,15);
C2 = zeros(simEnd,1);
D3a = zeros(simEnd,15);
C3 = zeros(simEnd,1);
for i = 2:simEnd
    %Calculate RDI for Each unit
    [D1a(i,:),C1(i)] = FuzzyRDIRealTime_new(...
        Hyd1.Act(i)/HydRating,...
        (Hyd1.Act(i)-Hyd1.Act(i-1))/HydRating,Dparams);
    [D2a(i,:),C2(i)] = FuzzyRDIRealTime_new(...
        Hyd2.Act(i)/HydRating,...
        (Hyd2.Act(i)-Hyd2.Act(i-1))/HydRating,Dparams);
```

```
    [D3a(i,:),C3(i)] = FuzzyRDIRealTime_new(...
        Hyd3.Act(i)/HydRating,...
        (Hyd3.Act(i)-Hyd3.Act(i-1))/HydRating,Dparams);
end
%% Plot Results
close all
x = 1:simEnd;
x = x/12/24;

%Show Instantaneous Damage Incurred
close all
figure
hsim(1) = subplot(3,1,1);
stairs(x,Hyd2.Act);
xlabel('Time (Days)')
ylabel('Unit Output (MW)')
title('Hydroelectric Generation Unit Output')
hsim(2) = subplot(3,1,2);
plot(x,(D2a(:,1:8)*100))
legend(CompLabels(1:8))
xlabel('Time (days)')
ylabel('Damage (% of Life)')
title('Hydroelectric Unit Damage Incurred per Component')
grid on
hsim(3)= subplot(3,1,3);
plot(x,(D2a(:,9:end).*100))
legend(CompLabels(9:15))
xlabel('Time (days)')
ylabel('Damage (% of Life)')
grid on

%Show Cummulative Damage and Cost Accrued
hsim(1) = subplot(3,1,1);
stairs(x,Hyd2.Act);
xlabel('Time (Days)')
ylabel('Unit Output (MW)')
title('Hydroelectric Generation Unit Output')
hsim(2) = subplot(3,1,2);
plot(x,cumsum(D2a(:,1:8)*100))
legend(CompLabels(1:8))
xlabel('Time (days)')
ylabel('Damage (% of Life)')
title('Hydroelectric Unit Damage Incurred per Component')
grid on
hsim(3)= subplot(3,1,3);
plot(x,cumsum(D2a(:,9:end).*100))
legend(CompLabels(9:15))
xlabel('Time (days)')
ylabel('Damage (% of Life)')
figure
plot(x,cumsum(C2))
xlabel('Time (days)')
ylabel('Cost (Thousands of $)')
grid on
```

Fuzzy Damage Function:

```
function [D, C] =
FuzzyRDIRealTime_new(Pvalues,Pchanges,DamageDerivations)

% function [D] =
FuzzyRDIRealTime(Pvalues,Pchanges,DamageDerivations)
% Input is: Pvalues - Power output from the Hydro Unit
%           Pchanges - Change in Power Output from Previous
Operating Point
%           DamageDerivations - Matrix of Damage/Cost Components
% Output is: D - Matrix of Damage incurred for each component.
% Everything is in per unit


% Damage Rates:
K_dmg_smallRamp = DamageDerivations(:,1);
K_dmg_medRamp = DamageDerivations(:,2);
K_dmg_largeRamp = DamageDerivations(:,3);
K_dmg_StartStop = DamageDerivations(:,4);
K_dmg_safePower = DamageDerivations(:,5);
K_dmg_dmgPower = DamageDerivations(:,6);
K_Costs = DamageDerivations(:,7);


P.values = Pvalues;
Pchange.values = Pchanges;

if (P.values == 0 && Pchange.values ~=0) || (P.values ~=0 &&
Pchange.values == P.values)
    D = K_dmg_StartStop.*abs(Pchange.values);
    C = sum(D.*K_Costs);
else

    %% Power memberships

    P.small.low = -10000000;
    P.small.midL = .25;
    P.small.midR = .25;
    P.small.high = .35;

    P.damage.low = .25;
    P.damage.midL = .35;
    P.damage.midR = .45;
    P.damage.high = .55;

    P.safe.low = .45;
    P.safe.midL = .55;
    P.safe.midR = 0.55;
    P.safe.high = inf;
```

```
    %
%%%%%%%%%%%%%%%%%%%%%%%%%%%%%%%%%%%%%%%%%%%%%%%%%%%%%%%%%%%%%%%%%%%%%%%%
%%%%
    % %OPTIONAL CODE TO PLOT MEMBERSHIPS
    %
%%%%%%%%%%%%%%%%%%%%%%%%%%%%%%%%%%%%%%%%%%%%%%%%%%%%%%%%%%%%%%%%%%%%%%%%
%%%%
    % x = 0:.001:1;
    % for i = 1:length(x)
    % y(i) =
mTRImod(x(i),P.small.low,P.small.midL,P.small.midR,P.small.high);
    % z(i) =
mTRImod(x(i),P.damage.low,P.damage.midL,P.damage.midR,P.damage.high)
;
    % w(i) =
mTRImod(x(i),P.safe.low,P.safe.midL,P.safe.midR,P.safe.high);
    % end
    % figure
    % plot(x,y)
    % hold on
    % plot(x,z,'r')
    % plot(x,w,'k')
    % xlabel('PU Power Level')
    % ylabel('Membership Value')
    % legend({'Low','Damaging','Safe'})
    % title('Power Output Membership Functions')
    % ylim([-.1 1.1])
    %
%%%%%%%%%%%%%%%%%%%%%%%%%%%%%%%%%%%%%%%%%%%%%%%%%%%%%%%%%%%%%%%%%%%%%%%%
%%%%

    % memberships
    P.small.m =
mTRImod(P.values,P.small.low,P.small.midL,P.small.midR,P.small.high)
;
    P.damage.m =
mTRImod(P.values,P.damage.low,P.damage.midL,P.damage.midR,P.damage.h
igh);
    P.safe.m =
mTRImod(P.values,P.safe.low,P.safe.midL,P.safe.midR,P.safe.high);

    %% Error derivative memberships

    Pchange.small.low = -10000000;
    Pchange.small.midL = .05;
    Pchange.small.midR = .05;
    Pchange.small.high = .15;

    Pchange.med.low = .05;
    Pchange.med.midL = .15;
    Pchange.med.midR = .15;
    Pchange.med.high = .25;

    Pchange.large.low = .15;
```

```
    Pchange.large.midL = 0.25;
    Pchange.large.midR = 0.25;
    Pchange.large.high = inf;

    %
%%%%%%%%%%%%%%%%%%%%%%%%%%%%%%%%%%%%%%%%%%%%%%%%%%%%%%%%%%%%%%%%%%%%
%%%%%
    % %OPTIONAL CODE TO PLOT MEMBERSHIPS
    %
%%%%%%%%%%%%%%%%%%%%%%%%%%%%%%%%%%%%%%%%%%%%%%%%%%%%%%%%%%%%%%%%%%%%
%%%%%
    % x = 0:.001:1;
    % for i = 1:length(x)
    % y(i) =
mTRImod(x(i),Pchange.small.low,Pchange.small.midL,Pchange.small.midR
,Pchange.small.high);
    % z(i) =
mTRImod(x(i),Pchange.med.low,Pchange.med.midL,Pchange.med.midR,Pchan
ge.med.high);
    % w(i) =
mTRImod(x(i),Pchange.large.low,Pchange.large.midL,Pchange.large.midR
,Pchange.large.high);
    % end
    % figure
    % plot(x,y)
    % hold on
    % plot(x,z,'r')
    % plot(x,w,'k')
    % xlabel('Change in PU Power')
    % ylabel('Membership Value')
    % legend({'Small','Medium','Large'})
    % title('Chane in Power Output Membership Functions')
    % ylim([-.1 1.1])
    %
%%%%%%%%%%%%%%%%%%%%%%%%%%%%%%%%%%%%%%%%%%%%%%%%%%%%%%%%%%%%%%%%%%%%
%%%%%

    % memberships
    Pchange.small.m =
mTRImod(abs(Pchange.values),Pchange.small.low,Pchange.small.midL,Pch
ange.small.midR,Pchange.small.high);
    Pchange.med.m =
mTRImod(abs(Pchange.values),Pchange.med.low,Pchange.med.midL,Pchange
.med.midR,Pchange.med.high);
    Pchange.large.m =
mTRImod(abs(Pchange.values),Pchange.large.low,Pchange.large.midL,Pch
ange.large.midR,Pchange.large.high);


    %% Rules
    w = [(Pchange.small.m*P.small.m)';
        (Pchange.small.m*P.damage.m)';
        (Pchange.small.m* P.safe.m)';
        (Pchange.med.m* P.small.m)';
```

```
        (Pchange.med.m* P.damage.m)';
        (Pchange.med.m* P.safe.m)';
        (Pchange.large.m* P.small.m)';
        (Pchange.large.m* P.damage.m)';
        (Pchange.large.m* P.safe.m)']';

    R = abs([Pchange.values*K_dmg_smallRamp' +
P.values*K_dmg_safePower' ;
        Pchange.values*K_dmg_smallRamp' + P.values*K_dmg_dmgPower' ;
        Pchange.values*K_dmg_smallRamp' +P.values*K_dmg_safePower' ;
        Pchange.values*K_dmg_medRamp' + P.values*K_dmg_safePower' ;
        Pchange.values*K_dmg_medRamp' + P.values*K_dmg_dmgPower' ;
        Pchange.values*K_dmg_medRamp' +P.values*K_dmg_safePower' ;
        Pchange.values*K_dmg_largeRamp' +P.values*K_dmg_safePower' ;
        Pchange.values*K_dmg_largeRamp' + P.values*K_dmg_dmgPower' ;
        Pchange.values*K_dmg_largeRamp' +
P.values*K_dmg_safePower']);

    % Weight action with rule
    D = w*R;

    %% DIVIDE BY WEIGHTS
    D = D/sum(w);
    C = sum(D.*K_Costs');
end
```

Memberships Calculation Function:

```
function [m] = mTRImod(data,a,b,c,d)

if b > c
    c = b;
end

if b < a
    b = a;
end

if c > d
    d = c;
end

m = (data>a) .* (data<d) .* ...
    ((data < b).*((data-a)>0).*(data-a)...
    .* 1/(b-a) + ((data-c)>0) .* (1-(data-c)...
    .* 1/(d-c))) + (data >= b & data <= c);
```

Appendix 4: ESS RDI Simulation Code

```
% ESS RDI Simulation Code
clear

%% Load Data for Simulation
dataRead = importdata('BPA_JD_Data.mat');
dataRead = dataRead .* (dataRead >0);
data = dataRead(:,1)+dataRead(:,2)+dataRead(:,4);
simEnd = round(length(data));
% simEnd = 100000;
data = data(1:simEnd,:);
data = sum(data,2);

%Calculate Change in Power to generate it in
%same way as with LEC system
Pchange = [0 ; diff(data)]';

%% Initialize System
%First Energy Storage System (Flywheels)
ESS1.Prated = 2;
ESS1.Erated = ESS1.Prated/4;
ESS1.SOC = zeros(1,simEnd);
ESS1.SOC(1) = .5;
ESS1.Cost = 1500*ESS1.Prated*.4*0.67;

%Second Energy Storage System (ZBB)
ESS2.Prated = 6;
ESS2.Erated = ESS2.Prated*2;
ESS2.SOC = zeros(1,simEnd);
ESS2.SOC(1) = .5;
ESS2.Cost = 1200*ESS2.Erated*0.4*0.67;

%% Run Simulations of ESS RDI
%Generate scaled Pchange vectors for each ESS Unit
ESS1.scaledChanges = min(2, max(-2, Pchange.*13./10));
ESS2.scaledChanges = min(6, max(-5, Pchange.*13./10));
ESS1.Pout = zeros(length(ESS1.scaledChanges),1);
ESS2.Pout = zeros(length(ESS2.scaledChanges),1);

%Original SOC is 0.5 for each
ESS1.SOCsim = ESS1.SOC*0+0.5;
ESS2.SOCsim = ESS2.SOC*0+0.5;

%Variables for tracking damage and cost
D4sim = zeros(simEnd,1);
D5sim = D4sim;
C4sim = D4sim;
C5sim = D4sim;
```

```
for i = 2:length(ESS1.scaledChanges)
    % Calculate SOC
    ESS1.SOCsim(i) = ESS1.SOCsim(i-1) - ...
        ESS1.Pout(i-1)/(ESS1.Erated*12);
    ESS2.SOCsim(i) = ESS2.SOCsim(i-1) - ...
        ESS2.Pout(i-1)/(ESS2.Erated*12);

    % Assign ESS Units depending upon SOC and scaledChanges
    if ESS1.scaledChanges(i) > 0
        ESS1.Pout(i) = min([...
            (12*ESS1.Erated*(ESS1.SOCsim(i)-0.05)),...
            ESS1.Prated,ESS1.scaledChanges(i)]);
    elseif ESS1.scaledChanges(i) < 0
        ESS1.Pout(i) = max([...
            (12*ESS1.Erated*(ESS1.SOCsim(i)-0.95)),...
            -ESS1.Prated,ESS1.scaledChanges(i)]);
    else
        ESS1.Pout(i) = 0;
    end
    if ESS2.scaledChanges(i) > 0
        ESS2.Pout(i) = min([...
            (12*ESS2.Erated*(ESS2.SOCsim(i)-0.05)),...
            ESS2.Prated,ESS2.scaledChanges(i)]);
    elseif ESS2.scaledChanges(i) < 0
        ESS2.Pout(i) = max([...
            (12*ESS2.Erated*(ESS2.SOCsim(i)-0.95)),...
            -ESS2.Prated,ESS2.scaledChanges(i)]);
    else
        ESS2.Pout(i) = 0;
    end

    % Calculate Damage Incurrence
    [D4sim(i),C4sim(i)] = FlywheelDamage(...
        abs(ESS1.SOCsim(i) - ESS1.SOCsim(i-1)),ESS1.Cost);
    [D5sim(i),C5sim(i)] = FlowCellDamage(...
        ESS2.Pout(i),ESS2.Prated,ESS2.Erated,ESS2.Cost);
end
```

```
%% Plot Results
close all
x = 1:simEnd;
x = x/12/24;

%Flywheel Plotting
%Instantaneous
figure('Name','Flywheel Damage Simulation',...
    'units','normalized','outerposition',[0 0 1/2 1])
axa(1) = subplot(3,1,1);
stairs(x,ESS1.Pout)
xlabel('Time (days)')
ylabel('Power Output (MW)')
grid on
axa(2)=subplot(3,1,2);
plot(x,ESS1.SOCsim*100)
xlabel('Time (days)')
ylabel('SOC (%)')
grid on
axa(3)=subplot(3,1,3);
stairs(x,D4sim*100)
xlabel('Time (days)')
ylabel('Damage (% of Life)')
grid on
linkaxes(axa,'x')

%Cummulative
figure('Name','Flywheel Damage Accumulation',...
    'units','normalized','outerposition',[1/2 0 1/2 1])
axb(1) = subplot(2,1,1);
stairs(x,cumsum(D4sim)*100)
xlabel('Time (days)')
ylabel('Damage (% of Life)')
grid on
axb(2)=subplot(2,1,2);
stairs(x,cumsum(C4sim))
xlabel('Time (days)')
ylabel('Cost (Thousands of $)')
grid on
linkaxes(axb,'x')
```

```
%ZBB Plotting
%Instantaneous
figure('Name','ZBB Damage Simulation',...
    'units','normalized','outerposition',[0 0 1/2 1])
axa(1) = subplot(3,1,1);
stairs(x,ESS2.Pout)
xlabel('Time (days)')
ylabel('Power Output (MW)')
grid on
axa(2)=subplot(3,1,2);
plot(x,ESS2.SOCsim*100)
xlabel('Time (days)')
ylabel('SOC (%)')
grid on
axa(3)=subplot(3,1,3);
stairs(x,D5sim*100)
xlabel('Time (days)')
ylabel('Damage (% of Life)')
grid on
linkaxes(axa,'x')

%Cummulative
figure('Name','ZBB Damage Accumulation',...
    'units','normalized','outerposition',[1/2 0 1/2 1])
axb(1) = subplot(2,1,1);
stairs(x,cumsum(D5sim)*100)
xlabel('Time (days)')
ylabel('Damage (% of Life)')
grid on
axb(2)=subplot(2,1,2);
stairs(x,cumsum(C5sim))
xlabel('Time (days)')
ylabel('Cost (Thousands of $)')
grid on
linkaxes(axb,'x')
```

Appendix 5: LEC System Simulation Code

```
% LEC System Simulation Code
%Performs LEC system and Runs simulation

%% Setup for Simulation
clear
global Dparams

% Read in Damage Coefficients
[DamageDerivations tex raw] = xlsread(...
    'DamageDerivations_allHydro.xls');
K_dmg_smallRamp = DamageDerivations(:,5);
K_dmg_medRamp = DamageDerivations(:,9);
K_dmg_largeRamp = DamageDerivations(:,13);
K_dmg_StartStop = DamageDerivations(:,17);
K_dmg_safePower = DamageDerivations(:,21);
K_dmg_dmgPower = DamageDerivations(:,25);
K_cost = DamageDerivations(:,27);
CompLabels=tex(3:end,1);

Dparams = [K_dmg_smallRamp K_dmg_medRamp K_dmg_largeRamp ...
    K_dmg_StartStop K_dmg_safePower K_dmg_dmgPower K_cost];

%% Load Data for Simulation
dataRead = importdata('BPA_JD_Data.mat');
dataRead = dataRead .* (dataRead >0);
data = dataRead(:,1)+dataRead(:,2)+dataRead(:,5);
simEnd = round(length(data));   %Set Simulation end point
data = data(1:simEnd,:);
data = sum(data,2);

%Set up variables for tracking of system characteristics
Pchange = zeros(1,simEnd);
changesTracking = zeros(12,1);
filteredChange = zeros(1,simEnd);
PchangeRem = zeros(1,simEnd);
HydroDifference= zeros(1,simEnd);
Difference= zeros(1,simEnd);
totalHydroCost = zeros(1,simEnd);
totalESS1Cost = zeros(1,simEnd);
totalESS2Cost = zeros(1,simEnd);
totalDamageCostAct = zeros(1,simEnd);
D2 = zeros(simEnd,15);
D2a = zeros(simEnd,15);
D4 = zeros(simEnd,1);
D5 = zeros(simEnd,1);

%Actual/Original Hydroelectric units' generation
Hyd1.Act = dataRead(1:simEnd,1)';
Hyd2.Act = dataRead(1:simEnd,2)';
Hyd3.Act = dataRead(1:simEnd,5)';
```

```
%% Initialize System
%First Energy Storage System (Flywheels)
ESS1.Prated = 2;
ESS1.Erated = ESS1.Prated/4;
ESS1.SOC = zeros(1,simEnd);
ESS1.SOC(1) = .5;
ESS1.deltaSOC = zeros(1,simEnd);
ESS1.cycles = 0;
ESS1.Cost = 1500*ESS1.Prated*.4*1;
ESS1.Pout = zeros(1,simEnd);

%Second Energy Storage System (ZBB)
ESS2.Prated = 6;
ESS2.Erated = ESS2.Prated*2;
ESS2.SOC = zeros(1,simEnd);
ESS2.SOC(1) = .5;
ESS2.deltaSOC = zeros(1,simEnd);
ESS2.cycles = 0;
ESS2.Cost = 1200*ESS2.Erated*0.3*1;
ESS2.Pout = zeros(1,simEnd);

%Hydro Units
HydRating = 135;
Hyd1.Pout = zeros(1,simEnd);
Hyd2.Pout = zeros(1,simEnd);
Hyd3.Pout = zeros(1,simEnd);
numUnits = 3;

%LEC system parameters
Psens = 6;
PsensZBB = 3;
ZBBlim = 0.57;
ZBBslowLim = 0.3;

%% Begin Control Scheme

%Determine number of units to turn on initially
if data(1)/(HydRating*numUnits) > 0.7
    numOn = numUnits;
elseif data(1)/(HydRating*(numUnits-1)) > 0.7
    numOn = numUnits-1;
else
    numOn = numUnits -2;
end

% Initial Power Outputs (Start with Hydro Split evenly)
Pcmd = data(1);
Pavg = Pcmd/numOn;
Hyd3.Pout(1) = Pavg * (numOn > 2);
Hyd2.Pout(1) = Pavg * (numOn > 1);
Hyd1.Pout(1) = Pavg;
```

```
% Use LEC to determine power output for all time samples
for i = 2:simEnd
    % Calcuate SOC and Cycles for each ESS
    ESS1.SOC(i) = ESS1.SOC(i-1) - ...
        ESS1.Pout(i-1)/(ESS1.Erated*12);
    ESS2.SOC(i) = ESS2.SOC(i-1) - ...
        ESS2.Pout(i-1)/(ESS2.Erated*12);
    ESS1.deltaSOC(i) = abs(ESS1.SOC(i)-...
        ESS1.SOC(i-1));
    ESS2.deltaSOC(i) = abs(ESS2.SOC(i)-...
        ESS2.SOC(i-1));
    ESS1.cycles = ESS1.cycles + ESS1.deltaSOC(i);
    ESS2.cycles = ESS2.cycles + ESS2.deltaSOC(i);

    % Commanded Power and Change in Power Determination
    Pprev = data(i-1);
    Pcmd = data(i);
    Pchange(i) = Pcmd-Pprev;
    % Perform simple box filtering on Pchange
    changesTracking = [changesTracking(2:12) ;...
        Pchange(i)];
    filteredChange(i) = sum(changesTracking(9:12))./4;

    %Assign Flow-cell Power Output based on
    %Filtered change, change, SOC, and system ratings
    if filteredChange(i) > PsensZBB
        ESS2.Pout(i) = min([...
            (12*ESS2.Erated*(ESS2.SOC(i)-0.05)),...
            ESS2.Prated,filteredChange(i),Pchange(i)]);
    elseif filteredChange(i) < -PsensZBB
        ESS2.Pout(i) = max([...
            (12*ESS2.Erated*(ESS2.SOC(i)-0.95)),...
            -ESS2.Prated*ZBBlim,filteredChange(i),...
            Pchange(i)]);
    else
        %Keep SOC close to 70% if possible
        if (ESS2.SOC(i)-0.7)*(Pchange(i))>0
            ESS2.Pout(i) = sign(Pchange(i))*min(...
                abs([(12*ESS2.Erated*(ESS2.SOC(i)-0.5))...
                ,ESS2.Prated*ZBBlim*ZBBslowLim,...
                Pchange(i)]));
        else
            ESS2.Pout(i) = 0;
        end
    end
    %Ensure that Flow-cell System never adds to Pchange
    if Pchange(i)*filteredChange(i) < 0
        ESS2.Pout(i) = 0;
    end
    %Calculate remaining Pchange for the rest of system
    PchangeRem(i) = Pchange(i) - ESS2.Pout(i);

    %Assign Flywheel Power Output based on
    %Pchange, SOC, and system ratings
```

```
    if PchangeRem(i) > Psens
        ESS1.Pout(i) = min([...
            (12*ESS1.Erated*(ESS1.SOC(i)-0.05)),...
            ESS1.Prated*.7,PchangeRem(i)]);
    elseif PchangeRem(i) < -Psens
        ESS1.Pout(i) = max([...
            (12*ESS1.Erated*(ESS1.SOC(i)-0.95)),...
            -ESS1.Prated*.7,PchangeRem(i)]);
    else
        if (ESS1.SOC(i)-0.5)*(PchangeRem(i))>0
            ESS1.Pout(i) = sign(PchangeRem(i))*min(...
                abs([(12*ESS1.Erated*(ESS1.SOC(i)-0.5))...
                ,ESS1.Prated*0.1,PchangeRem(i)]));
        else
            ESS1.Pout(i) = 0;
        end
    end
    PchangeRemain = PchangeRem(i) - ESS1.Pout(i);

%     %Set ESS Outputs to 0 to see w/o ESS (FOR TESTING)
%     ESS1.Pout(i) = 0;
%     ESS2.Pout(i) = 0;

    % Allocate Hydro evenly with consideration for
    %unit operating points
    loop = 1;
    while loop == 1
        Pcmd = Pcmd-ESS1.Pout(i)-ESS2.Pout(i);
        Hyd3.Pout(i) = ((Pcmd)/numOn)*(numOn > 2);
        Hyd2.Pout(i) = ((Pcmd)/numOn)*(numOn > 1);
        Hyd1.Pout(i) = ((Pcmd)/numOn);
        % If a hydro unit does not fit within designated
        %operating range turn one on/off  as needed
        if Hyd1.Pout(i) > 1.15*HydRating || ((numOn > 1)...
                && (Hyd2.Pout(i) > 1.15*HydRating)) ||...
                ((numOn >2) && (Hyd3.Pout(i) > 1.15*HydRating))
            numOn = numOn + 1;
            ESS1.Pout(i)=0;
            ESS2.Pout(i)=0;
        elseif Hyd1.Pout(i) < 0.5*HydRating ||...
                ((numOn > 1) && ...
                (Hyd2.Pout(i) < 0.5*HydRating)) ||...
                ((numOn >2) && (Hyd3.Pout(i) < 0.5*HydRating))
            numOn = numOn - 1;
            ESS1.Pout(i)=0;
            ESS2.Pout(i)=0;
        else
            loop = 0;
        end
        if numOn < 1
            Hyd1.Pout(i) = 0;
            Hyd2.Pout(i) = 0;
            Hyd3.Pout(i) = 0;
            loop = 0;
```

```
        end
    end
    Hyd1.Pout(i) = Hyd1.Pout(i) + ...
        (data(i)-(Hyd1.Pout(i)+Hyd2.Pout(i)+...
        Hyd3.Pout(i)+ESS1.Pout(i)+ESS2.Pout(i)));

    %Calculate damage incurred by Hydro Units under LEC
    [D1,C1] = FuzzyRDIRealTime_new(Hyd1.Pout(i)/HydRating,...
        (Hyd1.Pout(i)-Hyd1.Pout(i-1))/HydRating,Dparams);
    [D2(i,:),C2] = FuzzyRDIRealTime_new(Hyd2.Pout(i)/HydRating,...
        (Hyd2.Pout(i)-Hyd2.Pout(i-1))/HydRating,Dparams);
    [D3,C3] = FuzzyRDIRealTime_new(Hyd3.Pout(i)/HydRating,...
        (Hyd3.Pout(i)-Hyd3.Pout(i-1))/HydRating,Dparams);
    totalHydroCost(i) = totalHydroCost(i-1) + C1 + C2 + C3;
    %Calculate damage incurred by ESS under LEC
    [D4(i),C4] = FlywheelDamage(ESS1.deltaSOC(i),ESS1.Cost);
    [D5(i),C5] = FlowCellDamage(ESS2.Pout(i),ESS2.Prated,...
        ESS2.Erated,ESS2.Cost);
    totalESS1Cost(i) = totalESS1Cost(i-1) + C4;
    totalESS2Cost(i) = totalESS2Cost(i-1) + C5;

    %Calculate damage incurred by original Hydro Units
    [D1a,C1] = FuzzyRDIRealTime_new(Hyd1.Act(i)/HydRating,...
    (Hyd1.Act(i)-Hyd1.Act(i-1))/HydRating,Dparams);
    [D2a(i,:),C2] = FuzzyRDIRealTime_new(Hyd2.Act(i)/HydRating,...
        (Hyd2.Act(i)-Hyd2.Act(i-1))/HydRating,Dparams);
    [D3a,C3] = FuzzyRDIRealTime_new(Hyd3.Act(i)/HydRating,...
        (Hyd3.Act(i)-Hyd3.Act(i-1))/HydRating,Dparams);
    totalDamageCostAct(i) = totalDamageCostAct(i-1) ...
        + C1 + C2 + C3;

    %Calculate the difference between original and LEC costs
    Difference(i) = 1-(totalHydroCost(i)+totalESS1Cost(i)...
        +totalESS2Cost(i))/totalDamageCostAct(i);
    HydroDifference(i) = 1-(totalHydroCost(i)/...
        totalDamageCostAct(i));
end

%% Plot Results
clc
close all
x = 1:simEnd;
x = x/12/24;

% Figure 1 - LEC Hydro Outputs
figure('Name','Hydro Unit Outputs',...
    'units','normalized','outerposition',[0 0 1/2 1])
ha(1) = subplot(3,1,1);
stairs(x,Hyd1.Pout)
xlabel('Time (days)')
ylabel('Output Power (MW)')
title('Unit 1 - LEC Output')
ha(2) = subplot(3,1,2);
stairs(x,Hyd2.Pout)
```

```
xlabel('Time (days)')
ylabel('Output Power (MW)')
title('Unit 2 - LEC Output')
ha(3) = subplot(3,1,3);
stairs(x,Hyd3.Pout)
xlabel('Time (days)')
ylabel('Output Power (MW)')
title('Unit 3 - LEC Output')

% Figure 2 - Original Hydro Outputs
figure('Name','Actual Hydro Unit Outputs',...
    'units','normalized','outerposition',[1/2 0 1/2 1])
ha(9) = subplot(3,1,1);
stairs(x,Hyd1.Act)
xlabel('Time (days)')
ylabel('Output Power (MW)')
title('Unit 1 - Actual Output')
ha(10) = subplot(3,1,2);
stairs(x,Hyd2.Act)
xlabel('Time (days)')
ylabel('Output Power (MW)')
title('Unit 2 - Actual Output')
ha(11) = subplot(3,1,3);
stairs(x,Hyd3.Act)
xlabel('Time (days)')
ylabel('Output Power (MW)')
title('Unit 3 - Actual Output')

% Figure 3 - ESS SOC figures
figure('Name','ESS SOC','units',...
    'normalized','outerposition',[0 0 1/2 1])
ha(4) = subplot(2,1,1);
plot(x,ESS1.SOC*100)
xlabel('Time (days)')
ylabel('SOC (%)')
title('Flywheel SOC')
ha(5) = subplot(2,1,2);
plot(x,ESS2.SOC*100)
xlabel('Time (days)')
ylabel('SOC (%)')
title('Flow-cell SOC')

% Figure 4 - Commanded Power
figure
ha(6) = subplot(1,1,1);
stairs(x,data)
xlabel('Time (days)')
ylabel('Output Power (MW)')
title('Commanded Power')

% Figure 5 - Commanded Power vs Actual LEC Power
figure
ha(6) = subplot(1,1,1);
stairs(x,data)
```

```
hold on
stairs(x,Hyd1.Pout + Hyd2.Pout + ...
    Hyd3.Pout + ESS1.Pout + ESS2.Pout,'r')
hold off
xlabel('Time (days)')
ylabel('Output Power (MW)')
title('Commanded Power')
legend('Commanded Power','LEC System Output Power')

% Figure 6 - ESS Outputs
figure('Name','ESS Unit Outputs','units',...
    'normalized','outerposition',[1/2 0 1/2 1])
ha(7) = subplot(2,1,1);
stairs(x,ESS1.Pout)
xlabel('Time (days)')
ylabel('Output Power (MW)')
title('Flywheel Output')
ha(8) = subplot(2,1,2);
stairs(x,ESS2.Pout)
xlabel('Time (days)')
ylabel('Output Power (MW)')
title('Flow-cell Output')

% Figure 7 - Effects of ESS on Pchange
figure
ha(12) = subplot(3,1,1);
stairs(x,Pchange)
hold on
stairs(x,ESS2.Pout,'r')
stairs(x,Pchange-ESS2.Pout,'k')
grid on
xlabel('Time (days)')
ylabel('Power (MW)')
title('Change in Output Power before and after Flow-cell')
ha(13) = subplot(3,1,2);
stairs(x,Pchange-ESS2.Pout)
hold on
stairs(x,ESS1.Pout,'r')
stairs(x,Pchange-ESS2.Pout-ESS1.Pout,'k')
grid on
xlabel('Time (days)')
ylabel('Power (MW)')
title('Change in Output Power before and after Flywheel')
ha(14) = subplot(3,1,3);
stairs(x,Pchange)
hold on
stairs(x,Pchange-ESS1.Pout-ESS2.Pout,'k')
grid on
xlabel('Time (days)')
ylabel('Power (MW)')
title('Change in Output Power before and after All ESS')
linkaxes(ha,'x')

% Figure 8 - Cost Comparisons
```

```
figure('Name','Cost Comparison','units',...
    'normalized','outerposition',[0 0 1 1])
hb(1) = subplot(2,1,1);
stairs(x,totalHydroCost)
title('Cost Comparison - With and Without LEC')
hold on
stairs(x,totalESS1Cost,'r')
stairs(x,totalESS2Cost,'m')
stairs(x,totalHydroCost+totalESS1Cost+totalESS2Cost,'k')
stairs(x,totalDamageCostAct,'c')
hold off
grid on
xlabel('Time (days)')
ylabel('Cost (Thousands of $)')
legend('LEC Hydro Cost','Flywheel Cost',...
    'Fuel Cell Cost','Total LEC System Cost',...
    'Original Hydro Cost')
hb(2)=subplot(2,1,2);
stairs(x, Difference*100)
hold on
stairs(x, HydroDifference*100,'r')
xlabel('Time (days)')
ylabel('Difference (%)')
title('Percentage difference in cost (Original - LEC)/Original')
grid on
legend('Total Difference in Cost','Difference in Hydro Cost')
linkaxes(hb,'x')

% Figure 9 - Damage of Actual Unit
figure
hsim(1) = subplot(3,1,1);
stairs(x,Hyd2.Act);
xlabel('Time (Days)')
ylabel('Unit Output (MW)')
title('Hydroelectric Generation Unit Output')
hsim(2) = subplot(3,1,2);
plot(x,cumsum(D2a(:,1:8)*100))
legend(CompLabels(1:8))
xlabel('Time (days)')
ylabel('Damage (% of Life)')
title('Hydroelectric Unit Damage Incurred per Component')
grid on
hsim(3)= subplot(3,1,3);
plot(x,cumsum(D2a(:,9:end).*100))
legend(CompLabels(9:15))
xlabel('Time (days)')
ylabel('Damage (% of Life)')
grid on

%Figure 10 - Damage accured with LEC
figure
hsim(4) = subplot(3,1,1);
stairs(x,Hyd2.Pout);
xlabel('Time (Days)')
```

```
ylabel('Unit Output (MW)')
title('Hydroelectric Generation Unit Output')
hsim(5) = subplot(3,1,2);
plot(x,cumsum(D2(:,1:8)*100))
legend(CompLabels(1:8))
xlabel('Time (days)')
ylabel('Damage (% of Life)')
title('Hydroelectric Unit Damage Incurred per Component')
grid on
hsim(6)= subplot(3,1,3);
plot(x,cumsum(D2(:,9:end).*100))
legend(CompLabels(9:15))
xlabel('Time (days)')
ylabel('Damage (% of Life)')
grid on
linkaxes(hsim,'x')

% Figure 11 - Flow-cell Damage Accrued
figure
subplot(2,1,1)
plot(x,ESS2.Pout)
xlabel('Time (days)')
ylabel('Power Output (MW)')
subplot(2,1,2)
plot(x,cumsum(D5)*100)
xlabel('Time (days)')
ylabel('Damage (% of Life)')

% Figure 12 - Flywheel Damage Accrued
figure
subplot(2,1,1)
plot(x,ESS1.Pout)
xlabel('Time (days)')
ylabel('Power Output (MW)')
subplot(2,1,2)
plot(x,cumsum(D4)*100)
xlabel('Time (days)')
ylabel('Damage (% of Life)')

% Figure 13 - Commanded Power vs. Commanded Power - ESS
figure
subplot(1,1,1);
plot(x,data)
hold on
plot(x,data'-(ESS1.Pout + ESS2.Pout),'r')
hold off
xlabel('Time (days)')
ylabel('Output Power (MW)')
title('Commanded Power vs. Commanded Power - ESS Contribution')
legend('Commanded Power','Commanded Power - ESS Power')
```